

CZECH UNIVERSITY OF LIFE SCIENCE IN PRAGUE  
FACULTY OF FORESTRY AND WOOD SCIENCE

GLUING AND SURFACE TREATMENT PRIMING PROPERTIES OF LASER-  
CUT WOOD

CZECH UNIVERSITY OF LIFE SCIENCE IN PRAGUE  
FACULTY OF FORESTRY AND WOOD SCIENCE

GLUING AND SURFACE TREATMENT PRIMING  
PROPERTIES OF LASER-CUT WOOD

**DISSERTATION**

Study program:	Wood Processing and Forest Machinery
Department (department / institute):	Department of Wood Processing and Biomaterials
Dissertation supervisor:	doc. Ing. Milan Gaff, PhD.
Dissertation advisor:	Prof. Dr. Peter Niemz

Prague 2022

**Fatemeh Rezaei**

## **ACKNOWLEDGEMENT**

I would like to extend thanks to the many people who so generously contributed to the work presented in this thesis. Special mention goes to my enthusiastic advisor, Prof. Peter Niemz. My Ph.D. has been an amazing experience and I thank my supervisor, Assoc. Prof. Milan Gaff, not only for his tremendous academic support, but also for giving me so many wonderful opportunities.

Similar, profound gratitude goes to Dr. Anil Sethy Kumar who has been a truly dedicated person. I am particularly indebted to Dr. Sethy for his advice, feedback, arrangement and suggestion, and for his support when I was really in stressful moments.

Special mention goes to Prof. Rupert Wimmer and Prof. Robert Nemeth for going far beyond the call of duty. To Dr. Claudia Gusenbauer, Dr. Milos Bak, Dr. Radim Rousek for their training in microscopy device and for nurturing my enthusiasm for wood biology. I am also hugely appreciative to my colleagues, Gourav Kamboj, Sumanta Dass, Roberto Corleto, Salvio Marino, Gianluca Ditommaso especially for sharing their experiences so willingly, and also for fantastic scientific courage. Finally, but by no means least, thanks go to my family for almost unbelievable support. They are the most important people in my world and I dedicate this thesis to them.

# CZECH UNIVERSITY OF LIFE SCIENCES PRAGUE

Faculty of Forestry and Wood Sciences

## Ph.D. THESIS ASSIGNMENT

Fatemeh Rezaei

Forestry Engineering  
Wood Processing and Forest Machinery

Thesis title

**Gluing and surface treatment priming properties of laser cut wood**

---

### Objectives of thesis

Laser technology, considered as a new technology, is able to cut a wood material by focusing a beam on the material and then, when the energy of beam distributes through the whole material, the material breaks apart by absorbing the energy. The main advantage of using laser over saw is to provide highly precise cut, narrow kerf width, extremely smooth surface, and flexibility on starting and finishing at any point on material. The quality of Laser-cut wood is important for further manufacturing processing such as gluing and finishing [7].

There is not much studies which investigate the gluing properties of a bondline constituted laser cut wood. In 1993, Rabiej et al., investigated the shear strength of samples cut by laser. A significant reduction of shear strength of the bond line was resulted. The reduction in the glued-layers can be explained by some underlying assumption. The first assumption probably is surface inactivation, reducing extremely the bond strength of glue line. This can be explained by a reduction in the wettability of wood. The second one most likely is the degradation of chemical bond, interrupting the wood adhesion. Modifications in cellulose, hemicellulose and lignin as a consequences of laser beam can be leads to changes in gluing property. Also, Carbon formation on the wood surface, as a result of burning from laser energy, block almost all cell's lumen and thus strongly prevent adhesive penetration. The adhesive penetration in combination with other factors (adhesive's type, wood species, etc.) plays an important role in wood bonding strength [9,10]. It is important to mention that no research was conducted to prove or reject the assumptions.

The research objectives of the work can be divided into few points:

1. Analyses of CO<sub>2</sub> laser parameters (cutting speed, feed speed, focal point position) on the tensile shear strength of laser-cut wood.
2. Microscopy analyses on the anatomical and morphological-structure of wood cut by CO<sub>2</sub> laser.
3. Investigations of the adhesive penetration into porosity structure of laser-cut wood, assessment of bondline failure after shear glue test, analyses of the wetting properties of the wood cut by CO<sub>2</sub> laser.
4. The investigation of the surface

### Methodology

According the aim, the methodology of the work can be divided into few points:

1. A primary step for this study is literate review. The previous research scientific works give us numerous broad hints about the selection of proper methods and materials.
  - 1.1. Literate review regarding processing parameters of CO2 laser, bonding phenomenon, properties of wood affected by the laser cutting
2. The research plan is prepared according to hypotheses. Characteristics on samples are determined. Test samples are defined
  - 2.1. Variation in the processing parameters of CO2 laser (cutting speed, gas pressure, focal point position),
  - 2.2. wood species and its properties (Beech and oak species, moisture content)
3. Test method are defined. Data collection is performed according to the plan in the laboratory scale.
  - 3.1. Universal testing machine
  - 3.2. Scanning electron Microscopy
  - 3.3. Microscopy (laser or Digital microscopy)
4. The data which collected are modeling and analyzed.
  - 4.1 Statistical software

**The proposed extent of the thesis**

100

**Keywords**

CO2 laser machine, tensile shear test, beech and oak wood species

**Recommended information sources**

- Barnekov, V. G.; McMillin, C.; Huber, H. A. J. F. P. J.-. Factors influencing laser cutting of wood. 1986.
- Belforte, D. J. I. L. R., Non-metal cutting. 1998, 13 (9), 11-13
- Hernandez-Castaneda, J. C.; Sezer, H. K.; Li, L. J. T. I. J. o. A. M. T., Dual gas jet-assisted fibre laser blind cutting of dry pine wood by statistical modelling. 2010, 50 (1-4), 195-206
- Kúdela, J.; Mrenica, L.; Javorek, L. J. A. F. X. Z. r. P. S., THE INFLUENCE OF MILLING AND SANDING ON WOOD SURFACE MORPHOLOGY. 2018, 60 (1), 71-83
- Malkoçoğlu, A. J. B.; Environment, Machining properties and surface roughness of various wood species planed in different conditions. 2007, 42 (7), 2562-2567
- Neese, J.; Reeb, J.; Funck, J. J. F. p. j., Relating traditional surface roughness measures to gluebond quality in plywood. 2004, 54 (1
- Pizzi, A.; Mittal, K. L., Handbook of adhesive technology. CRC press: 201
- Rabiej, R. J.; Ramrattan, S. N.; Droll, W. J. J. F. p. j., Glueline shear strength of laser-cut wood. 1993, 43 (2), 45.
- Ülker, O., Wood Adhesives and Bonding Theory. In Adhesives-Applications and Properties, InTech: 2016
- YUSOFF, Nukman, et al. Selected Malaysian wood CO2-laser cutting parameters and cut quality. American Journal of Applied Sciences, 2008, 5:8: 990-996.

**Expected date**

2020/21 SS – FFWS – State Doctoral Examinations

**The Dissertation Thesis Supervisor**

doc. Ing. Milan Gaff, PhD.

**Supervising department**

Department of Wood Processing and Biomaterials

Electronic approval: 18. 6. 2021

**doc. Ing. Roman Fojtík, Ph.D.**

Head of Institute

Electronic approval: 18. 6. 2021

**doc. Ing. Milan Gaff, PhD.**

Chairperson of Field of Study Board

Electronic approval: 31. 8. 2022

**prof. Ing. Róbert Marušák, PhD.**

Dean

Prague on 26. 09. 2022

## **Abstract**

This study aims to identify the tensile shear strength of glued beech (*Fagus sylvatica L.*) and oak (*Quercus robur L.*) samples cut by CO<sub>2</sub> laser. The main focus is on the characteristics of the bondline made of laser-cut wood. The laser beam was cut the samples in the perpendicular direction to the grain. The surface quality of the laser cut samples was measured by using a contact and contactless (laser) methods. A scanning electron microscope was used to show the anatomical structure, the penetration depth of PVAc resin and O/C ratio of the laser cut surface. Contact angle measurement and chemical analysis were implemented by using Fourier transform infrared spectroscopy and a contact angle goniometer. The tensile shear test on the laser cut samples bonded with polyvinyl acetate were carried out using universal testing machine. We gained knowledge about the glued strength of laser cut wood. The work brings new information about the physical and chemical properties of laser-cut surface prior to gluing. The main characteristics of the bondline made of laser-cut wood were successfully determined.

Key words: CO<sub>2</sub> laser, glued tensile shear strength, CO<sub>2</sub> processing parameters.

---

## **Hypothesis and Objectives**

### **Hypothesis**

1. Glued tensile shear strength of beech and oak wood could be decreased when cutting with a CO<sub>2</sub> laser, due to chemical and physical changes occurred on the laser-cut surface.
2. Laser-cut surface may lead to a better surface quality, due to the melting process, compared to a surface obtained by a contact tool (milling, planing, sawing).
3. It is assumed that the wetting properties of the laser-cut surface decreases, because of heat affected zone of laser-cut surfaces. The anatomical structure of laser-cut surface could be affected by CO<sub>2</sub> laser, due to variation in thermal degradation of wood. There would be the degradation of wood chemical compound, and the degradation rate is highly correlated to speed and power of CO<sub>2</sub> laser.

### **Objectives**

1. Analysis of CO<sub>2</sub> laser parameters (cutting speed, feed speed, focal point position) on the tensile shear strength of the laser-cut wood.
2. Microscopy analysis on the anatomical and morphological-structure of wood cut by CO<sub>2</sub> laser.
3. Investigations of the adhesive penetration into porosity structure of laser-cut wood, assessment of bondline failure after shear glue test, analysis of the wetting properties of the wood cut by CO<sub>2</sub> laser.

---

## Contents

<b>1 Introduction</b> .....	<b>14</b>
1.1 Laser cutting process .....	14
1.2 CO <sub>2</sub> laser versus conventional cutting process.....	18
1.3 Wood as a workpiece material .....	19
1.4 Process indicators .....	21
1.4.1 Wood properties on bonding performance .....	21
1.4.2 Contact angle measurement and wettability .....	23
1.4.3 Wood bond formation and performance .....	24
1.4.4 Adhesive penetration into the cellular structure of wood .....	29
1.5 Monitored factors on process indicators.....	31
1.5.1 Cutting speed .....	31
1.5.2 Gas pressure .....	31
1.5.3 Focal-point position .....	32
<b>2 Materials and methods</b> .....	<b>34</b>
2.1 Materials .....	34
2.1.1 Wood species .....	34
2.1.2 Adhesive .....	35
2.2 Methods .....	35
2.2.1 CO <sub>2</sub> laser cutting .....	35
2.2.2 Analysis of Laser-cut surface before gluing .....	36
2.2.3 Analysis of the glued laser cut surface .....	38
<b>3 Synthesis of acquired knowledge</b> .....	<b>41</b>
3.1 Discussion.....	43
<b>4 Conclusion and future works</b> .....	<b>47</b>
<b>5 List of used literature</b> .....	<b>49</b>
<b>6 Separate articles and manuscripts</b> .....	<b>54</b>
6.1 Interactions of monitored factors upon tensile glue shear strength on laser cut wood .....	54
6.2 Surface quality measurement by contact and laser methods on thermally modified spruce wood after plain milling .....	65
6.3 Anatomical and morphological characteristics of beech wood after CO <sub>2</sub> laser cutting .....	76
6.4 CO <sub>2</sub> laser cutting on the bondline characteristics of beech wood .....	88

---

6.5	The effect of alternating freezing and high temperatures on the tensile-shear strength of glued Norway spruce ( <i>Picea abies</i> (L.) H. Karst.) and European larch ( <i>Larix decidua</i> Mill.) wood .....	109
-----	--	-----

---

## List of Figures

Figure 1. Configuration of CO <sub>2</sub> laser.....	15
Figure 2. Concentric bands of a tree stump .....	20
Figure 3. Links between adhesive and wood bond using the schematic from Mara (1980). Link 1: Adhesive layer, Link 2 and 3: adhesive interphase layer, Link 4 and 5: adhesive wood interface, Link 6 and 7: wood interface layer, Link 8 and 9: wood layers.....	27
Figure 4. X-ray computed tomography (XCT) slice showing a bondline made using latewood loblolly pine and the 135-min BrPF resin a before and b after segmentation. (Jakes et al. 2019).....	30
Figure 5. Focal point positions on the workpiece .....	32
Figure 6. Contact angles of PVAc resin .....	37
Figure 7. Two methods of surface profile measurement; a) contactless method, b) contact method .....	38
Figure 8. Tensile shear test of the laser-cut samples performed by a universal testing machine equipped with a video extensometer (left) and without a video extensometer (right) .....	38

---

**List of Tables**

Table 1. The average properties of three wood species (Konnerth et al. 2016). ...	34
Table 2. Technical parameters of the selected adhesives .....	35
Table 3. Applied processing parameters of CO <sub>2</sub> laser on the wood species.....	36

---

## List of published articles

### I. A list of all output during the Ph.D. study

#### a) A list of all articles registered on Web of Science

1. Milan Gaff, **Fatemeh Rezaei**, Adam Sikora, Štěpán Hýsek, Miroslav Sedlecký, Gianluca Ditommaso, Roberto Corleto et al. "Interactions of monitored factors upon tensile glue shear strength on laser cut wood." *Composite Structures* 234 (2020): 111679. DIO: [10.1016/j.compstruct.2019.111679](https://doi.org/10.1016/j.compstruct.2019.111679)
2. **Fatemeh Rezaei**, Milan Gaff, Anil Kumar Sethy, Peter Niemz, Gourav Kamboj, Gianluca Ditommaso, Roberto Corleto, Sumanta Das, and Miroslav Gašparík. "Surface quality measurement by contact and laser methods on thermally modified spruce wood after plain milling." *The International Journal of Advanced Manufacturing Technology* 110, no. 5 (2020): 1653-1663. DOI:[10.1007/s00170-020-05983-7](https://doi.org/10.1007/s00170-020-05983-7)
3. **Fatemeh Rezaei**, Rupert Wimmer, Milan Gaff, Claudia Gusenbauer, Stephan Frömel-Frybort, Anil Kumar Sethy, Roberto Corleto, Gianluca Ditommaso, and Peter Niemz. "Anatomical and morphological characteristics of beech wood after CO<sub>2</sub>-laser cutting." *Wood Material Science & Engineering* (2022): 1-10.
4. **Fatemeh Rezaei**, Milan Gaff, Robert Nemeth, Jerzy Smardzewski, Anil Kumar sethy, Peter Niemz, Luigi Todaro, Gourav Kamboj, Sumanta Dass, Roberto Corleto, Gianluca Ditommaso, Mikos Bak. "Effect of CO<sub>2</sub> laser parameters on tensile-shear strength of laser-cut wood" (under review, 2022).
1. Miroslav Gašparík, **Fatemeh Rezaei**, Elham Karami, Sumanta Das, Tomáš Kytka, Lukáš Vlk, Roberto Corleto, and Gianluca Ditommaso. "The effect of alternating freezing and high temperatures on the tensile-shear strength of glued Norway spruce (*Picea abies* (L.) H. Karst.) and European larch (*Larix decidua* Mill.) wood." *European Journal of Wood and Wood Products* (2022): 1-8.
5. Gianluca Ditommaso, Milan Gaff, František Kačík, Adam Sikora, Anil Sethy, Roberto Corleto, **Fatemeh Rezaei** et al. "Interaction of technical and technological factors on qualitative and energy/ecological/economic indicators in the production and processing of thermally modified merbau wood." *Journal of Cleaner Production* 252 (2020): 119793.
6. Gourav Kamboj, Miroslav Gašparík, Milan Gaff, František Kačík, Anil Kumar Sethy, Roberto Corleto, **Fatemeh Rezaei** et al. "Surface quality and cutting power requirement after edge milling of thermally modified meranti (*Shorea* spp.) wood." *Journal of Building Engineering* 29 (2020): 101213.
7. Gourav Kamboj, Milan Gaff, Jerzy Smardzewski, Eva Haviarová, David Hui, **Fatemeh Rezaei**, and Anil Kumar Sethy. "Effect of cellulose nanofiber and cellulose nanocrystals reinforcement on the strength and stiffness of PVAc bonded joints." *Composite Structures* (2022): 115821.
8. Gourav Kamboj, Milan Gaff, Jerzy Smardzewski, Eva Haviarová, David Hui, Radim Rousek, Sumanta Das, **Fatemeh Rezaei**, and Anil Kumar Sethy. "Comparative study on the properties of cellulose nanofiber (CNF) and cellulose

---

nanocrystals (CNC) reinforced 1C-PUR adhesive bonded wooden joints." *Construction and Building Materials* 344 (2022): 128262.

## **b) A List of lectures and conferences**

1. 29th International Conference on Wood Modification and Technology 2018, at Zagreb  
Oral presentation by **Fatemeh Rezaei** with the title of;  
“Evaluation of Laser and Mechanical Methods for Measuring Roughness and Waviness of Milled Surface of Spruce and Oak”
2. 5th International Conference on Mechanics of Composites Lisbon, Portugal, 1 - 4 July 2019.  
Oral Presentation by **Fatemeh Rezaei** with the title of;  
Gluing properties of wood after CO<sub>2</sub> laser

## **II. A list of articles from which the final thesis is composed.**

2. Milan Gaff, **Fatemeh Rezaei**, Adam Sikora, Štěpán Hýsek, Miroslav Sedlecký, Gianluca Ditommaso, Roberto Corleto et al. "Interactions of monitored factors upon tensile glue shear strength on laser cut wood." *Composite Structures* 234 (2020): 111679. DIO: 10.1016/j.compstruct.2019.111679.
3. **Fatemeh Rezaei**, Milan Gaff, Anil Kumar Sethy, Peter Niemz, Gourav Kamboj, Gianluca Ditommaso, Roberto Corleto, Sumanta Das, and Miroslav Gašparík. "Surface quality measurement by contact and laser methods on thermally modified spruce wood after plain milling." *The International Journal of Advanced Manufacturing Technology* 110, no. 5 (2020): 1653-1663. DOI:10.1007/s00170-020-05983-7.
4. **Fatemeh Rezaei**, Rupert Wimmer, Milan Gaff, Claudia Gusenbauer, Stephan Frömel-Frybort, Anil Kumar Sethy, Roberto Corleto, Gianluca Ditommaso, and Peter Niemz. "Anatomical and morphological characteristics of beech wood after CO<sub>2</sub>-laser cutting." *Wood Material Science & Engineering* (2022): 1-10.
5. **Fatemeh Rezaei**, Milan Gaff, Robert Nemeth, Jerzy Smardzewski, Anil Kumar sethy, Peter Niemz, Luigi Todaro, Gourav Kamboj, Sumanta Dass, Roberto Corleto, Gianluca Ditommaso, Mikos Bak. “Effect of CO<sub>2</sub> laser parameters on tensile-shear strength of laser-cut wood” (under review).
6. Miroslav Gašparík, **Fatemeh Rezaei**, Elham Karami, Sumanta Das, Tomáš Kytka, Lukáš Vlk, Roberto Corleto, and Gianluca Ditommaso. "The effect of alternating freezing and high temperatures on the tensile-shear strength of glued Norway spruce (*Picea abies* (L.) H. Karst.) and European larch (*Larix decidua* Mill.) wood." *European Journal of Wood and Wood Products* (2022): 1-8.

---

# 1 Introduction

## 1.1 Laser cutting process

The term “LASER” is stand for “Light Amplification by the Stimulated Emission of Radiation”. The process called “stimulated emission” was introduced by Albert Einstein in 1917. Later on. In 1958, producing light with a wavelength in the visible range was reported by Charles Townes and Arthur Schawlow. Different materials such as ruby laser (short pulses of laser light) and Helium-neon gas laser or liquid dye lasers (continuous beam of light) can be used as lasting materials. The advent of the first gas laser was recorded in 196. Afterward, newer types of lasers have been developed which are more advanced and reliable. Actually, Lasers are Coherent, monochromatic, and highly directional beams of light which are able to melt and vaporize the material by focusing and delivering high energy-densities to small areas of a material (Modest et al. 2001). All lasers build from three main parts; an active medium (lasing material that produce the light), a power supply (a source of energy to excite the active medium) and resonant cavity (an optical resonator consisting of two parallel mirrors which amplify the light) (Kannatey-Asibu 2009).

Lasers are categorized based on their lasing mediums. the lasing mediums of laser can be in the state of gas, liquid, or solid. Moreover, the operation of all laser’s types occurs in one or two temporal modes, continuous wave and pulsed modes. The continuous wave mode occurs when the laser beam emits continually, without any interruption. Whereas, in pulse mode, the laser beam emits periodically (Chryssolouris 1991). Currently, for material processing, lasers with lasing media in the form of a solid or gas are used. The ruby laser, neodymium glass laser. and the neodymium yttrium aluminum garnet (Nd-YAG) laser are three types of solid-state laser. The Nd-YAG laser is able to maintain higher power for longer periods, as compared to the other two types. The output wave length of the Nd-YAG laser is 1.06  $\mu\text{m}$  while for carbon dioxide ( $\text{CO}_2$ ) laser (gas laser), used in the material processing, the length is far greater, roughly 10.06  $\mu\text{m}$  (Dawes 1992). The other types of laser which allocated for material processing are carbon monoxide (CO) and the Excimer laser etc. However, among all types of laser, the Nd-YAG laser and  $\text{CO}_2$  laser are the best for laser cutting of different materials. the processing capability of the Nd-YAG laser is poor for wood materials while the  $\text{CO}_2$  laser is representing the excellent capability (Havrilla and Anthony 2003). In the present study, a  $\text{CO}_2$  laser was

selected to cut the wood. So, a detailed review of its performance is provided in the following paragraph.

CO<sub>2</sub> laser is widely applicable as a source in the laser processing of materials. The highest efficiencies for the conversion of electrical to optical energy can be the first reason. Another reason can be the ease of operation at high power levels in both continuous wave and pulsed configurations rotational lines in the 9.4 μm and 10.4 μm bands of the CO<sub>2</sub> molecules generate laser emission (Duley and Williams 1983) (Figure 1).

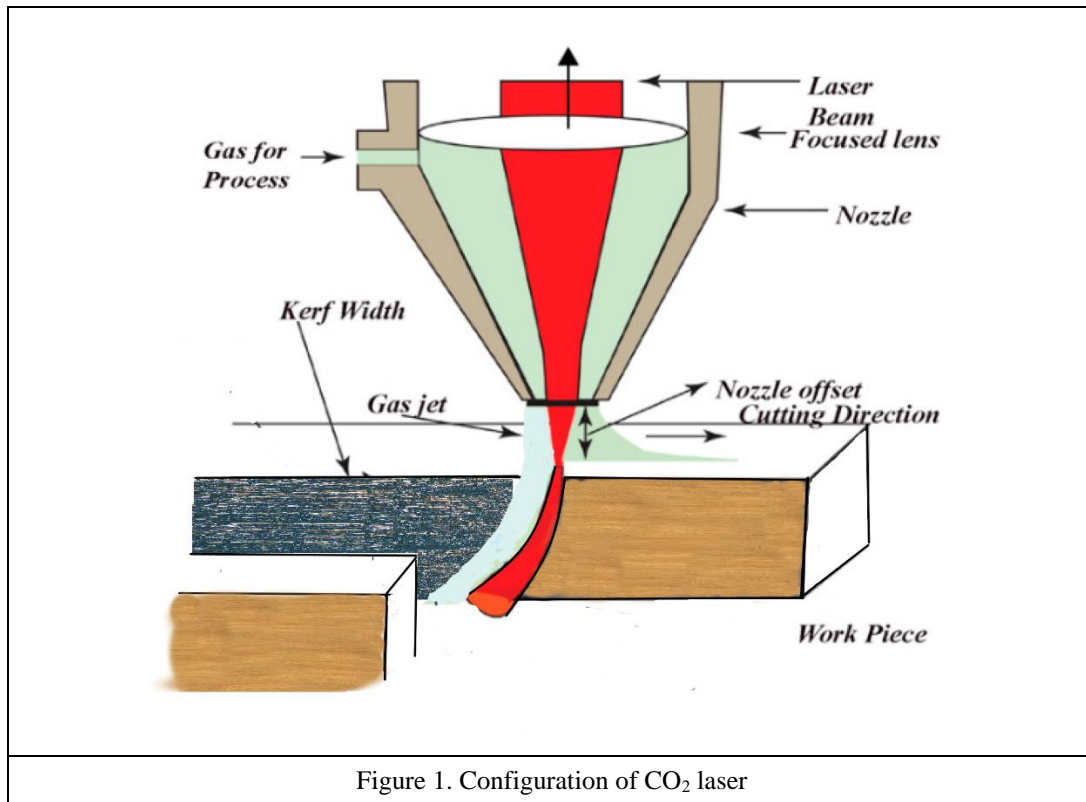


Figure 1. Configuration of CO<sub>2</sub> laser

---

The active medium of CO<sub>2</sub> laser is a mixture of gases including carbon dioxide gas (1-9%), Helium (60-85%), nitrogen (13-35%), and other gases. The combination of each amount of the gas depends on the design of optimal cavity, the gas flow rate, and the output coupler used. A high electrical potential is produced by power supplied (a high electrical potential) to keep the gas mixture in the excited state (Chryssolouris 1991).

The resonant cavity composed of a discharge tube holding the excited gas mixture between two end mirrors. One mirror is allocated to reflect the beam totally while other mirror is partially transparent in order to give a permission for beam output. Numerous effective changes in resonant cavity such as an acceptable beam divergence and high efficiency, a variety of mirror configuration can be carried out in order to achieve the required beam stability.

The optical resonator described above is responsible for the amplification of light. The parallel mirrors in the resonant cavity direct the light back into the lasing medium. Such back and forth activity of photons through lasing medium induces more and more emissions. photons which are not in the alignment of resonator are not able to be redirected by mirrors, resulting no more stimulation for emission. As photons are amplified by mirrors, the coherent beam develops quickly (Chryssolouris 1991, Kannatey-Asibu 2009)

Five basic configurations of commercial CO<sub>2</sub> laser are available; sealed, transversely excited atmospheric pressure (TEA), slow axial flow, fast axial flow and transverse flow. The differences of each type are characterized by the geometry of gas flow in the optical cavity.

Cutting mechanisms of laser beam: Lasers have several features, particularly monochromatic, coherent, and low divergence as compared with normal light. With such features, it can be able to produce high power densities. When the laser beam focuses on a small area of material, the power of laser beam is transferring to the material, resulting in heating, melting, and finally removing of the material. the melting material is removed by using assist gas (Powell J., 1998) (Kannatey-Asibu 2009) (Havrilla and and Anthony 2003).

Five different mechanisms of laser cutting are defined; 1. inert gas melt shearing cutting, 2. active gas melt shearing, 3. vaporization, 4. chemical degradation and 5. scribing.

Inert gas melt shearing: a base material is melting and removing by using a high-pressure inert assist gas. This mechanism requires lower energy of laser beam, as compared to

---

other methods. The melting energy is totally provided by laser beam. The formation of striations (valleys and peaks that creates along the thickness) on the cut surface and dross (molten materials which solidify on the cut edge) is a major problem of this cutting method (Kannatey-Asibu 2009).

Active gas melt shearing: this cutting method is resembling the inert gas melt shearing with a few differences. An exothermic chemical reaction probably generated additional energy, resulting in increasing cutting speed, as comparison with inert gas melt shearing method. Higher temperature of this method compared to inert gas melt shearing induces edge charring in carbon-based materials. Oxygen or air is considered as an active gas. However. The active gas melt shearing method shows the same major problem as mentioned in inert gas melt shearing method (Kannatey-Asibu 2009, Ion 2005).

Vaporization: The material reaches its vaporization temperature by heating before extensive melting with thermal conduction. Subsequently, the removal of material is occurred by vaporization and also an inert gas jet ejecting liquid. The mechanism is used to cut plastics such as Poly (methyl methacrylate) and polyacetal. The vaporization mechanism is provided the excellent quality and narrow kerf width. However, the thin section of material is useful for cut, due to extensive energy required to cut a unit volume of material, as comparison to melt shear cutting (Powell 1998, Ion 2005, He et al. 2005).

Chemical degradation: the laser beam breaks the chemical bonds of material, which deeply changes the material's integrity. This method is used for wood, wood-based products, most thermoset polymers, rubber products, and epoxy resins. The flat and smooth surface of cut edge is resulted from this method. However, a fine layer of residual carbon dust remains on the cut edge, which may require cleaning (Powell 1998, Ion 2005, He et al. 2005).

Scribing: by making a hole and groove in the material, the structure of the material is getting poor. Therefore, the mechanical property of the material is getting weak also. The hole is sometime provided by laser to the other side of the material and the hole is not so deep. Vaporization with a small Heat Affected Zone (HAZ) can be formed by low energy and high-power density pulses. This mechanism can be effective to cut alumina, some glasses and composites (Green et al. 1991, Wenham and Green 1988, Green et al.1996, Steen 2003, Ion 2005, Abbott 2006,).

The fundamental aspects of modification of wood by using a laser beam and related different parameters such as intensity, time, laser type, and focus to the surface

---

morphology was stated by Haller et al. (2001). The ablation and melting process could be observed by using scanning electron microscopy. The penetration of water into laser treated surfaces is significantly stopped. By controlling the energy input, the laser beam can be used to remove microscopical amounts in order to clean or to prepare the surface for coatings. This can be useful in the preservation of historic monuments. The possibility of using laser ablation on wood without carbonization can be performed for certain parameter sets. Because of the absorption properties of the wood, UV and IR-pulse lasers are appropriate for this purpose. For these laser types, melting of the cellulose in the  $\mu\text{m}$  range was detected, which fulfills the hypothesis of mainly thermal ablation at laser wavelengths above 300 nm. when CO<sub>2</sub> laser and pulse width in the range of 1 ms was used, the melting of wood surfaces without carbonizing is observed. The depth of the molten layer was discovered to be in the range from 2  $\mu\text{m}$  up to 7  $\mu\text{m}$ . Hence, the depth of thermal/ structural modifications was evaluated in the range from 5  $\mu\text{m}$  up to 15  $\mu\text{m}$ . Short time measurements have shown that the moisture absorption of the laser irradiated wood surface slowed remarkably low.

## **1.2 CO<sub>2</sub> laser versus conventional cutting process**

Laser cutting method on wood and wood-based materials provides following advantages over conventional cutting process:

Contact-free process: Sharpening, replacing, repairing tools are not required, due to the absent of reaction forces exerted on the workpiece. The deformation of the cut part is not occurred during process, even material is flexible. However, other components such as lenses are required to maintain (McMillin and Harry 1971, Peters and Marshall 1975, Szymani and Dickinson 1975, Barnekov et al. 1989, Powell 1998, Powell and Kaplan 2004).

Narrow Kerf width: The lower the material removed, the less the waste material resulted. Conventional process provides wider width kerf and higher waste material compared to laser method. (McMillin and Harry 1971, Peters and Marshall 1975, Szymani and Dickinson 1975, Huber et al. 1982, Barnekov et al. 1989, Mukherjee et al. 1990, Powell 1998, Powell and Kaplan 2004).

Fully CNC controlled: It indicates that the complex shapes or patterns can be achieved by laser. The cutting process can be started from any point, followed by line, circles, curves, and terminated to any desire point. Laser shows a greater potential when it comes to design a complex geometry (McMillin and Harry 1971, Szymani and Dickinson 1975,

---

Huber et al. 1982, Barnekov et al. 1989, Mukherjee et al. 1990, Powell 1998, Powell and Kaplan 2004). Extremely hard and brittle wood materials can be cut by laser. However, the laser cutting of composite and compounds is not as comfortable as conventional method (Peters and Marshall 1975, Szymani and Dickinson 1975). Laser cutting of composites and compounds is not always easier compared to conventional methods. Laser is advantageous only when precision, controllability and flexibility are needed; however, the requirements vary among cut operations.

Cutting accuracy is improved: the smoother surface of wood obtained from laser method rather than conventional method. Post-processing, like cleaning or sanding are not required. A Charring mark on the wood surface as a result of laser cutting can be used as a decorative purpose (McMillin and Harry 1971, Peters and Marshall 1975, Szymani and Dickinson 1975, Powell 1998, Powell and Kaplan 2004).

A low running cost: A running cost are extremely lower in comparison with conventional method. The conventional method requires high energy (Huber et al. 1982, Powell 1998, Powell and Kaplan 2004).

Low noise: laser cutting generated very slight noise, and the process is extremely quiet. (Peters and Marshall 1975, Huber et al. 1982, Powell 1998, Powell and Kaplan 2004).

Fully automated: lase cutting is more secure than conventional method (Huber et al. 1982, Powell 1998, Powell and Kaplan 2004).

### **1.3 Wood as a workpiece material**

Throughout human history, wood was used as a major source for the construction of boats, shelters, weapons and also for cooking food. Earlier society used wood in Egyptian pyramids, Chinese temples and tombs, and ancient ships. The earlier society was found very early the great advantages of wood, including widely distributed, multifunctional, strong, easy to work, aesthetic, sustainable, and renewable. For centuries, wood has been used as a major source for construction purposes, cooking and heating, even the fact that wood has instability toward moisture, and degradations due to microorganisms, termites, fire, and ultraviolet radiation (Pizzi and Mittal 2003, Niemz 2006, Handbook 2010).

Wood is an inhomogeneous and anisotropic material constituted of varying types of cells, and chemical compounds, accompanying together to provide the needs of living plant. The three main functions of wood in living plant is water conduction, mechanical support, storage, synthetic of biochemical. To fulfill these functions, wood cells must design well

and interconnected. Through these functions, 20,000 different species of woody plants were evolved, with their unique properties.

Looking at a tree stump, several concentric bands were observed. A quick observation from outside to the inside of the stump is demonstrating several certain bands nominated as outer bark, inner bark, vascular cambium, sapwood, heartwood, and pith (Figure 2).

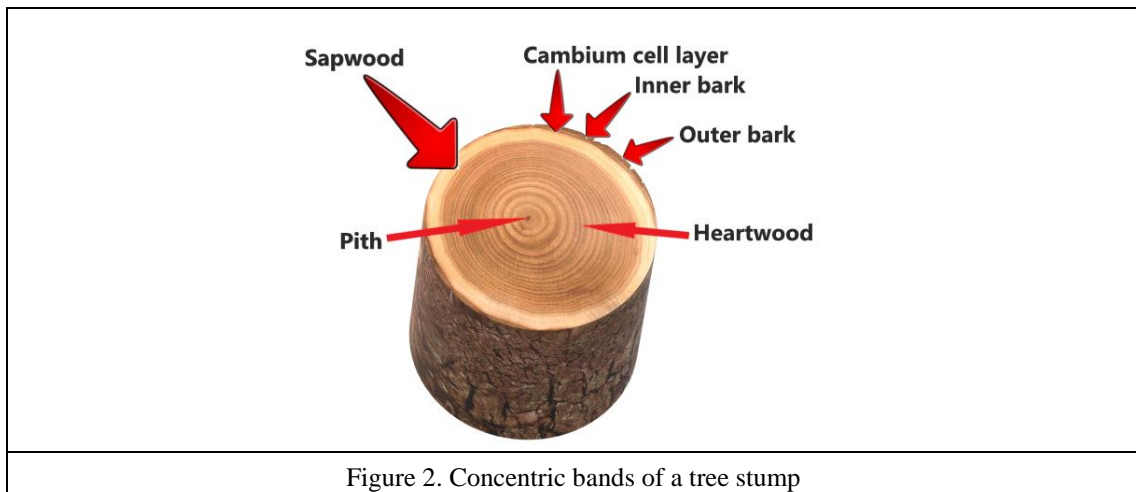


Figure 2. Concentric bands of a tree stump

Outer bark acts like fence, protecting mechanically the inner bark and restricting the water loss. Inner bark acts like transit, transporting sugar formed by photosynthesis within the tree. The boarder between bark and wood is defined as vascular cambium, containing meristic characteristics to produce the both wood and bark tissues. Sapwood is a living tissue which able to carry water or sap from the roots to the leaves. Inactive and nonconducting tissue, located in the middle of most trees, for many species noticed as darker color (due to accumulation of mainly colourful chemicals), is called heartwood. Pith tissue is the remaining part of early growth before the wood formation. Annual rings are a consequence of seasonal growth in temperate zones. The growth rate is highest in early spring, forming early wood, while, it is lowest during summer and autumn, forming late wood. Early wood is characterized as cells with thin walls and wide lumen while late wood is labeled as cells with thick walls and small lumen. In a trunk, there are longitudinal (L) axis in the parallel direction to the grain, radial axis in the direction from pith to the bark and tangential axis in the perpendicular direction to the grain and tangential to the radial axis. Wood is divided into two groups, hardwood and softwood, based on their origin and anatomical structure (Bowyer et al 2003).

---

Hardwood is botanically originated from angiosperm (flowering plants) and softwood is originated from gymnosperm (mostly conifers). The broadleaf, deciduous trees are considered as hardwood, including beech, oak, maple and etc. In contrast, the needle-leave evergreen trees are considered as softwood, particularly pine, spruce and etc. The anatomical structure of hardwood is more complex. The present of vessel elements in hardwood is the most important distinction between softwood and hardwood.

Other differences can be explained as; a) density is one of the most important physical properties of wood and determined by the wood anatomical structure (Handbook 2010). The density increases when the proportion of cells with thick cells walls rises. Therefore, hardwood often has a higher density, but also the amount of void spaces by vessels needs to be considered. The density is always related to the wood moisture content, which is another crucial property of wood. Due to the woods high number of pores (in average 50-60% of the wood material), it has a high inner surface area (International Agency for Research on Cancer. 2006). This cavity system absorbs humidity from the air as well as other liquids such as adhesives. Wood obtains a three-dimensional network of cells with different tasks such as conducting, storing and strengthening cells. The orientation and composition of these cells varies greatly for soft- and hardwood and further for individual species. Softwood contains a much simpler anatomical structure and has mainly tracheids ( $\geq 95\%$ ) (Niemz and Sonderegger 2017) and parenchyma, but further wood rays, resin channels and pits.

## **1.4 Process indicators**

### **1.4.1 Wood properties on bonding performance**

It has long been known that the bond performance properties are influenced by the quality of the wood surface.

Surface roughness: the wood surface roughness of the wood bond elements is another critical factor that affects wood bond quality. Even if suitable technological solutions are available for measuring surface roughness, the direct measurement and the determination of surface topography are rarely performed in a systematic manner (Sandak et al. 2020). Wood industries rely upon the frequent scheduling of tool changes, the superior quality of the cutting tools and the adjustment to the feed speed as an alternative of monitoring surface roughness. Thus, there is limitation in the quality of glued surfaces, which is significant for statistical process control, especially in small production plants.

---

Wood moisture: the cyclic sorption and desorption of moisture in wood attribute to variations in the relative humidity (RH) of the air. A reduction of RH in the winter leads to the rapid drying of wood. The wood moisture at the surface reach the same level of the surrounding moisture within minutes, while the moisture exchange in the bulk interior occurred via diffusion which is not occurred fast (Niemz and Gereke 2009).

This resulted in technical problems in wood gluing when 1C-PUR resin used. PUR resin demands water for hardening, which is insufficient when wood is dry. Sometimes, extra water is spraying onto the glued wood surface to compensate for the reduction of RH during winter. The internal stress in the wood causes the wood deformation, due to moisture gradients. the thicker the glued wood. the higher pressure required to compensate for the sample deviation.

Grain angle: The effect of grain angle on the penetration behaviour of adhesive into wood was investigated by Hass (2012). The mechanical strength was influenced by grain angles where the wood failure percentage of glued wood bond under stress was appeared.

Density: variation in density within annual rings or between early wood and late wood can be found, mainly in coniferous wood species (Lanvermann 2014). The bulk density can be different between species, even within a single tree. The morphological structure of ring-porous hardwoods, ash or oak, varies significantly from that of diffuse-porous hardwood species, beech and birch (Arnold et al. 2019). Therefore, the adhesive bond performance behaves differently based on the morphology differences. Generally, softwood has lower density than hardwood, as a result, lower mechanical strength and swelling/shrinkage. This results in lower shear stresses in the bond line during the service life. This is clearly proved when testing adhesive bond in dry condition or after immersing into water. In addition, the low mechanical resistant of softwood leads to a higher rate of wood failure when gluing these lower density species (Hänsel et al. 2022). Thole (2017) found that there was no direct correlation between wood failure ratio and lap shear strength in beech wood LVL. In addition, the expand of wood breakage did not provide any signal for expected strength of the adhesive bond. The performance requirements for hardwood species can not be easily applied on softwood, due to the higher native strength of hardwood. Wood surface characteristics include weak boundary layers, surface inactivation, chemical heterogeneity, and processing impacts, particularly aging, machining, drying (Gardner 2006). Studies of the bond quality (Christiansen 1990, John 1980) show the importance of freshly prepared, clearly cut wood surfaces, leading to form uniformly thin bondline

---

#### **1.4.1.1 Mechanical damage at the wood surface**

The damaged wood adjacent to the bondline forms the mechanical weak boundary layer (NWBL) which can be repaired by resins (Bikerman 2013). Even with an attempt to make a “perfect” surface, planners or veneer peelers induces cells to be rushed or torn. For this reason, sanding must be used on the surfaces prior to gluing. The freshly prepared surface is more applicable on surfaces of particleboard and fiberboard to remove the surface layer that is overdried or over cured and with high wax content.

#### **1.4.1.2 Surface Chemistry Barriers to Bonding**

A chemical weak boundary layer (CWBL) restricts bond formation. Methods that are sensitive to chemical properties are required. Wood species contains a large amount of nonpolar extractive are generally hard to which improve the natural resistance of wood to biotic agents. However, the hydrophilic properties of wood surface decreases over time which limits the spread of water-based adhesives. Most tropical wood species and some domestic wood species containing high extractive are difficult to glue (Zeppenfeld and Grunwald 2005, Frihart et al. 2021). The quantity and chemical structure of the extractive in heart and sapwood are different, resulting in different bond performance. Oak (*Quercus* sp.), black locust (*Robinia* sp.), and ash (*Fraxinus* sp.) are identified in gluability Variation, due to the variation in extractive contents (Lüdke et al. 2015, Konnerth et al. 2016, Bockel et al. 2019, Bockel 2020). A fresh planned surface reduces contact angle (between wood and waterborne resin) and provides better wettability. If wood contains a large amount of extractive, an adhesive application immediately after fresh planned surface is required.

#### **1.4.2 Contact angle measurement and wettability**

The standard analytical method of assessing surface wettability is contact angle with water, polar liquids, or the resin. A low contact angle implies that surface tension of the solid is higher in relation to the liquid. The low angle is also showing the liquid will make molecular scale contact with the wood. The perfect interfacial strength takes place when the surface energies of the wood and adhesive are the same. The rate that adhesive penetrate into a capillary such as lumen is influenced by contact angle. If a contact angle is too high, the proper wetting and spreading of liquid was not occurred. In a case of proper wetting, further reduction in contact angle induces overpenetration and/or distribution of the resin over too large an area.

---

Many factors that are probably influenced to the gradual loss of surface energy at the wood surface are determined. The first possible factor is that the movement of extractives such as resin and fatty acids and their esters, waxes, sterols and terpenes to the wood surface. Adhesives with a high pH were recommended to use for wood containing a high level of extractives on the surface. There could also be chemical changes to the molecules on the surface like oligosaccharides, phenols and tannins moving to the surface. There are not only lowering surface energy, but also hinder the cure of the resin, by dissolving in the resin. Very acidic woods like oak is not very critical to bond if the resin is strongly buffered. Moreover, a fresh and high energy surface absorb contaminants from the air which decrease surface energy. Overtrying of wood (veneer for plywood LVL oriented strandboard fakes) is the second possible factor in which surface inactivation occurs. Physical effects along with the degradation of the mechanical properties of the surface layer, and blocking of surface cracks, thus decreasing surface area. Chemical changes are the movement of hydrophobic wood ingredients to the surface. Oxidation, molecular rearrangement of various functional groups on the surface and elimination of hydroxyl groups are as a result of chemical modification. The third possible factor is a time of year that a tree is harvested. Freshly cut wood harvested in winter provides difficulty for bonding, due to high contact angles from high levels of extractive.

### **1.4.3 Wood bond formation and performance**

Adhesion technology is one of the most important surface phenomena in which glued solid surfaces remain attached to each other. Understanding adhesion phenomena requires extensive studies because it's not belonging to single area or science but it comprises of many in particular macromolecular science, physical chemistry of surfaces and interfaces, materials science, mechanics and micromechanics of fracture, and rheology.

Four main theories which explain adhesion phenomenon are as follows:

1. Mechanical interlocking theory.
2. Diffusion theory.
3. Electronic theory.
4. Adsorption/specific adhesion theory (Pizzi 1994).

Mechanical interlocking theory was first introduced by MacBain & Hopkins (1925). The theory was emphasizing on mechanical performance of cured adhesive into enclosed

---

spaces (micro and macro scales) of substrate. This theory was not supported by many who had proved that satisfactory adhesion can be formed by smooth surface (without porous) (Israelachvili & Tabor 1972). For supporting this theory, lots of studies demonstrated that the bonding strength increased with an increase in surface roughness, that is to say, more penetration into substrate. These results primarily were not found to be matched completely when wood was involved as substrate. A large amount of adhesive was required when the surface roughness values was increased. This eventually led to weaknesses in bond strength. The starved edges, as a result of over-penetration of adhesive into wood cells, were the reason behind. As mentioned, the higher the level of surface roughness, the higher the adhesive utilization. However, with such a high price of adhesive nowadays, the quantity of adhesive on surface was of great importance for wood applications. Despite of the fact that the mechanical interlocking theory had provided strength in bonding, it was not only a crucial factor for bond strength (Pizzi 1994).

Diffusion theory: The second theory was presented by Voyutskij (1963) at the beginning of 1960s. The distribution of polymer molecules of both adherent and adhesive was occurred in interface area. The polymers were become close to each other with the purpose of solubility. The theory was called “diffusion”. For being dissolved, first of all, the rate of solubility parameters should be nearly the same. It’s crucial to note that the numbers of adhesives had different degree of solubility parameters close to wood polymers or far too much from them (Urea or phenol formaldehyde). Secondly, amorphous polymers were demanded for solubility.

Therefore, the crystalline portions of cellulose were not able to take part in solubility phenomenon. Hence, it’s apparent that all parts of wood components had not behaved the same concerning diffusion theory. The bonding joint strength was relied firstly on intimate contact in interface area and the weight of resin molecular. With regards to diffusion theory, ultimately, inter-diffusion was not possible in the situation where crosslinked polymers and extremely crystalline portions were found (Pizzi, 1994a).

Electronic theory: the third one was proposed by Derjaguin & Smilga (1967). When adhesive was kept in contact with substrate, an electron transfer was occurred. That was because of the opposite electrons which were setting in each material. However, the electronic forces built through interface were supposed to be a reason for adhesion. Disapproval was expressed by scientists who declared that the motion of electron from one surface to other was very fast and was not very slow process to able to create

---

adhesion. A questionable assumption was made by scientists who stated that these electronic forces maybe contributed to initial adhesion. For wood bonding, this theory is inapplicable. There was not empirical evidence to show electronic theory was responsible for an adhesion phenomenon when wood was used (Pizzi 1994).

Adsorption theory: Adsorption theory was defined as forces which actually exist between substrate and adhesive as a result of atomic and molecular attraction. The theory was generally approved and widely recognized in adhesion phenomenon. There were two types of forces; primary (ionic, covalent and metallic bonds) and secondary forces (hydrogen band and electrostatic forces). These forces were acceptable equally based on adsorption theory. But in wood bonding, nonetheless, an incorrect opinion was expressed for separation between primary and secondary forces. The separation was not actually proper. Both attractive forces were two features of adsorption theory (Pauling 1960, Patrick 1989).

The model of interaction secondary forces between resin (phenol and urea formaldehyde) and crystalline- amorphous region of cellulose in interface region was designed and theoretical forces were measured. It was revealed that by altering parameters in resin preparation to desire degree, an adhesion improvement between resin and cellulose was resulted (Pizzi & Eaton 1987, Pizzi 1990). This outcome and other parallel findings emphasized that the secondary forces in adsorption theory were significant factor in adhesion phenomenon.

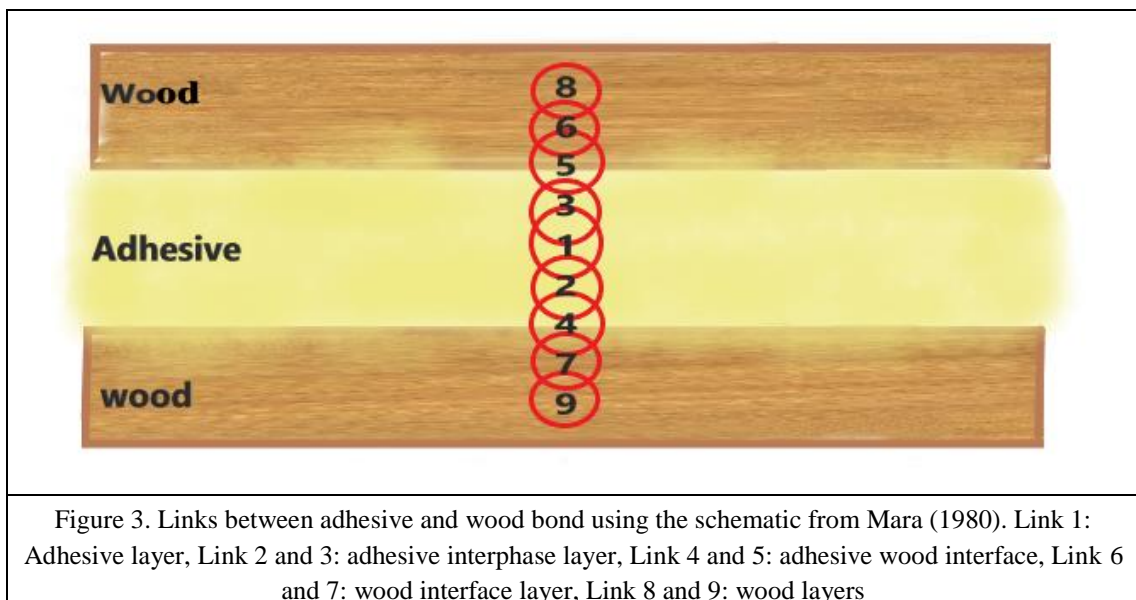
As mentioned before, primary forces were subdivision of adsorption theory. However, for being clear, the definition was mandatory. Forces were created by covalent chemical, ionic and metallic coordination bond in interface areas known as primary forces. Initial reactivity between resin and substrate was not easily obtained (Pizzi 1994).

It was significant to accept several numbers of modifications to get strong covalent bond like adding reactive groups to resin or substrate. In fact, the primary chemical reaction in interface areas was taken place intrinsically or under a certain condition (modification). Examples for those react naturally were polyurethane adhesive and epoxy-based primer which proved by Klein et al. (1983).

Primary chemical bonds did not exist in wood adhesion under normal circumstances as Johns (1989) was demonstrated in his research. Pizzi et al. (1993) and Frisch et al. (1983) indicated that there was not covalent bond under usual condition between isocyanate group and wood surface components when they were in contact with each other. It was

neglected the high reactivity rate between isocyanate and water. Thus, because of small amount of water in wood, the small proportion of covalent bond may be generated. Further examples can be provided to ensure the accuracy of John's findings. The first one was that the methylene groups in adhesive (urea, Melamine and phenol formaldehyde) was able to react rapidly with wood components (hydroxyl groups and aromatic nuclei) when they were in exposure to high temperature. The second one illustrated that the covalent bond was not formed in normal condition when urea formaldehyde was applied as adhesive to wood surface. Adjusting PH value of urea formaldehyde in particular condition leads to form covalent bonds. Covalent bond is mainly discussed in the text above. Ionic and metallic coordination bond were not involved. Wood treated with copper-chromium-arsenate (CCA) can be considered as example for metallic coordination bond. In reality, Copper reacts with chemical structures in lignin and form stable bond.

The strength and stiffness of wood products increases by effective adhesive transfer and distribute loads between components. The efficient load transfer is attributed to the strength of the chain links from one member to another across the wood adhesive bond (Figure 3). Therefore, the interaction of the complex factors that connected to the properties of the individual links can determined the performance of a bonded joint during product assembly (Frihart and Hunt 2010).



---

Adhesive classification: There are two classification methods; classification by curing method and adhesive origin. Classification by curing method contains parts; one-part adhesives is including epoxies, polyimides, acrylics, urethanes and cyanoacrylates which are able to cure by heat application, UV light and moisture or pressure. Moreover, two-part adhesives are curing when two or more components are mixed and constitute a chemical-cross link reaction of the polymer molecule.

Base on adhesive origin, wood adhesives are mainly grouped as naturel and synthetic. Pre-polymers or polymers obtained from petrochemical material are called synthetic. Wetting wood surface is possible only by the liquid shape of resins or as water solution. Curing is occurred by the support of heating or crosslinking. Setting is started to happen just with cooling the polymers melted or water evaporation (Ebnesajjad 2008).

Synthetic adhesives itself are categorized as thermosetting and thermoplastic based on their polymer behaviors after curing or setting. Thermoplastic adhesives are required cooling to room temperature after being in the exposure of heating through softening. In contrast, thermosetting adhesives are not softening by heating and they form crosslinking through curing (Conner 2001). Numerous important Examples for thermosetting adhesives are represented as follow: 1) Phenol formaldehyde (PF) is one the most important adhesives used for exterior wood applications including plywood mostly produced from softwood (White 1995, Knop & Pilato 1979). 2) Urea formaldehyde (UF) is annually manufactured around 1'000'000 ton and 5% of its application is belong to hardwood plywood utilized in interior atmosphere (White 1995). It has been used predominantly all over the world because of some advantages especially low cost, water solubility, great thermal properties, resistance to biological attack, hardness and easy to apply on wood surface. Alongside these advantages, there are disadvantages also. UF adhesive is not resistance to moisture like PF. This can be a great issue for using in exterior applications. Due to the moisture-resistant property of phenolic compounds, PF adhesives is used for exterior application (Rowell 2005).

In general, formaldehyde-based adhesives are releasing formaldehyde which is harmful and requires more consideration during production in wood industries (Meyer & Hermanns 1986). Another term for thermoplastic adhesives is hot melt, too. Examples for thermoplastic adhesives can be Polyvinyl Acetate (PVAc) and Ethylene Vinyl Acetate (EVA).

---

Natural adhesives are derived from natural sources. For a long time, in the past, the utilization of natural adhesive namely animal, soy, and casein and blood-based adhesives (known as proteinaceous adhesives) was common. However, with the advent of synthetic adhesive in the mid twentieth centuries their utilization was limited to some extent. Frequently usage of synthetic adhesives was resulted in an increase in cost. Hence, the tendency for using natural based components such as carbohydrate, tannin, Lignin and etc. was initiated again. There are several disadvantages resulted from the proteinaceous adhesives in contrast to synthetic adhesives. Proteinaceous adhesives are not resistance to microorganism attack and moisture (Ebnesajjad 2008).

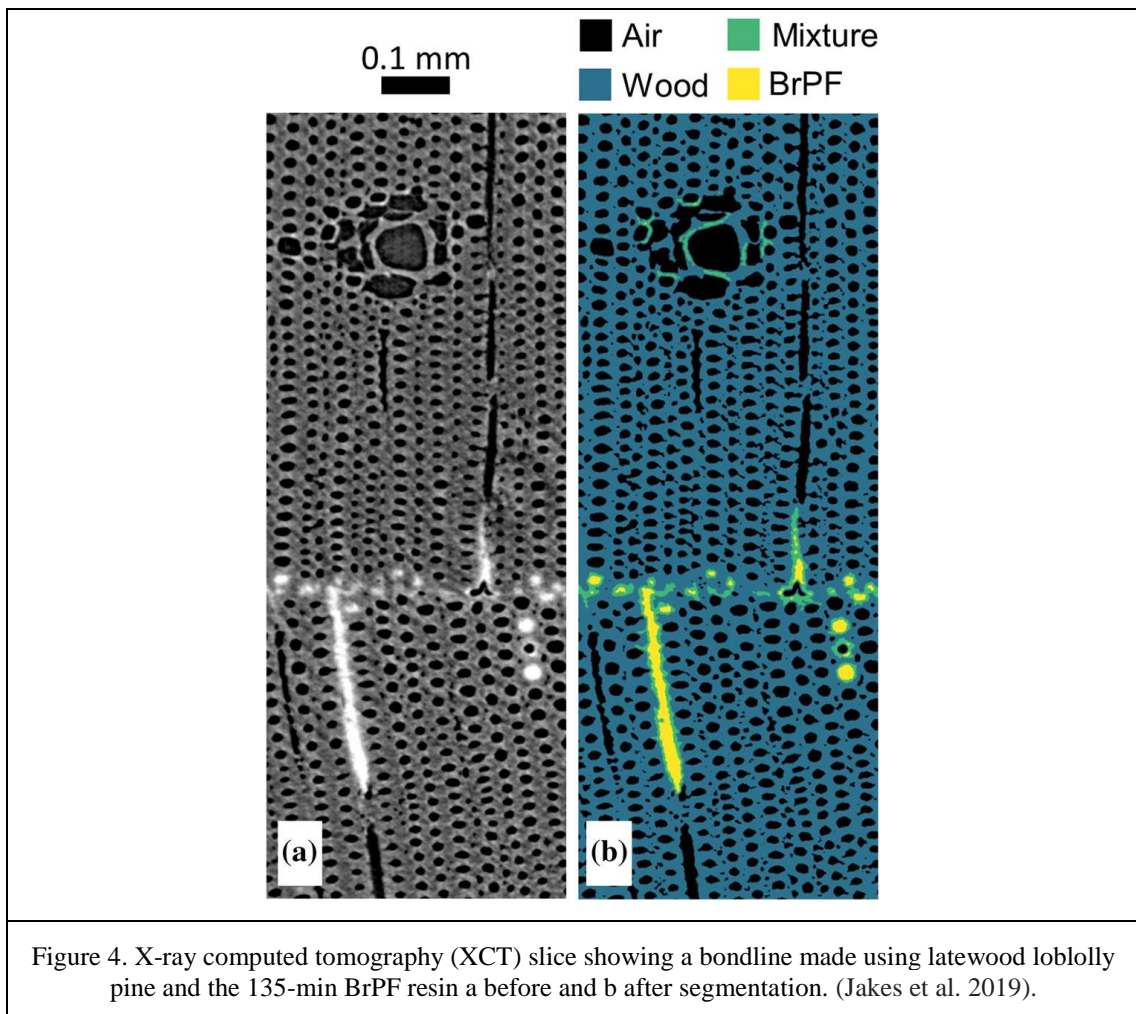
Poly vinyl acetate (PVAc): PVAc is linear and thermoplastic polymer which is an excellent alternative to replace some other adhesive containing formaldehyde. As a wood adhesive, utilization of PVAc is effortless as it is water soluble, biodegradable with excellent chemical resistance and has no toxic action on human body. The main advantages of this wood adhesive that it does not need high temperature for curing. But it has a drawback and poor performance toward humid condition at elevated temperature. So, to overcome these problems and increase the performance of PVAc two approaches have been used 1) Copolymerizing vinyl acetate with more hydrophobic monomers or functional monomer (Qiao et al. 2011) 2) blending PVAc with other adhesives and hardener (Qiao and Eastal 2001, Kaboorani and Riedl 2011)

Jiang et al (2018) conducted a study in which he used commercial polyvinyl acetate and starch adhesive were mixed with dicarboxylic acid with cellulose nanofiber. By adding optimum amount of CNF, the lap joint strength increased to 74.5%.

#### **1.4.4 Adhesive penetration into the cellular structure of wood**

The effect of penetration on bonding performance has been the object of important investigations for several decades (Figure 4). Penetration in combination with other factors such as cohesive strength, and covalent and secondary chemical bonding affects bonding performance in some adhesives. Indeed, stress can be distributed evenly through interface areas when the curing stage of adhesive was occurred (Nuryawan et al. 2014). It's still under discussion that the bonding strength performance is affected more by cell wall penetration or cell lumen. The ideal penetration depth for bonding strength is unidentified. The effect of different penetration depths on shear bonding strength was investigated by Suchsland (1985). The final results proved that there is no relationship

between penetration and shear bonding strength. Failure which is occurred in bonding strength maybe arises from over-penetration or under-penetration.



The percent of wood failure during shearing test was different in latewood and earlywood cells of Douglas fir. Because Tracheas were responsible for mechanical properties of wood. When only the earlywoods were involved in shear test, 100% wood failure was occurred. In reference to latewood, the failure was detected in bulk adhesive and the percent of wood failure was 10%.

In contrast, in Beech wood, various wood failures were not found in latewood and early wood cells (Gavrilovic et al. 2012). Another remarkable research was performed by Ivana demonstrated that there was the opposite relationship between the viscosity of UF adhesive and shear strength of beech wood. The more viscosity, the less penetration, and at the end the lower shear strength would be resulted. This can be explained by mechanical interlocking theory or reinforcing the interface areas of wood by penetration.

---

The Mechanical properties of wood-based panel have been influenced by the cell wall penetration of UF adhesive. As a matter of fact, higher elastic modulus and hardness were achieved by the existence of UF adhesive into cell wall (Stöckel et al. 2010, 2012). Cell wall penetration provided dimensional stability and also recovered damage cell walls during surface treatment (Lizhe et al. 2016). Penetration into cell walls was specialized for adhesives with low molecular weight as discussed before (Konnerth et al. 2008).

## **1.5 Monitored factors on process indicators**

### **1.5.1 Cutting speed**

Cutting speed can be defined as the rate at which the laser passes through materials per minute. The high speed decreases the laser exposure time to a material. When the cutting speed decreased, the material removal and cutting edges declined as well. If the thickness of a workpiece is high, the low cutting requires in cooperation with the laser power (Lum et al 2000, Barnekov et al 1986, Yusoff et al. 2008)

### **1.5.2 Gas pressure**

A coaxial gas-get nozzle system is responsible for three functions:

- 1) Vaporized products are removed from the cut area, for instance; carbon dust and exhaust smoke, resulting in protecting the lens.
- 2) Controlling excessing burning by remove ignition at which a high air speed induces to handle wood vaporization.
- 3) Increase the cutting located below the lens focus.

The gas-jet system is attributed to the characteristics of the nozzle, to the nozzle hole's diameter, to nozzle standoff distance, and to the type of gas (Peters and Marshall 1975, Szymani and Dickinson 1975, Barnekov et al. 1986).

The more common nozzles in laser cutting of wood is convergent nozzles (Li and Mazumder 1991). Mukherjee et al. (1990) reported that the use of a supersonic nozzle resulted an increase of 50% in cutting speed (4.6 m/min) when a basswood had a thickness of 25.4mm. The standard nozzle resulted in a low cutting speed, 3m/min. However, there were no changes in the surface quality of the cut surfaces, charring and kerf width.

The laser beam should be mainly placed exactly at the centre of the nozzle hole, which has a diameter of 1mm. MDF was cut successfully with a nozzle diameter of 1.5 mm and

paper was cut with a nozzle diameter of 0.2mm. Increasing the nozzle diameter declines the gas pressure (Li and Mazumder 1991, Eltawahni et al 2011, Hovikorpi et al. 2004) The standoff distance, known as standoff position, rarely affects the laser cutting process. In fact, using a standoff distance of 1mm can perform successfully wood and paper cutting (Quintero et al. 2011).

The type of gas and the pressure can influence on the penetration depth, feed speed and quality. The cheap clean compressed air already brings fairly satisfactory results (Peters and Marshall 1975, Powell 1998, Lum et al. 2000)

### 1.5.3 Focal-point position

The distance between the converging and the diverging laser beam is related to focal point position at which the energy of the bundled laser light is highly concentrated. The three focal point position are defined:

- a) Above the work piece surface.
- b) Slightly above the workpiece centre.
- c) On the workpiece surface (Barnekov et al 1986) (Figure 3).

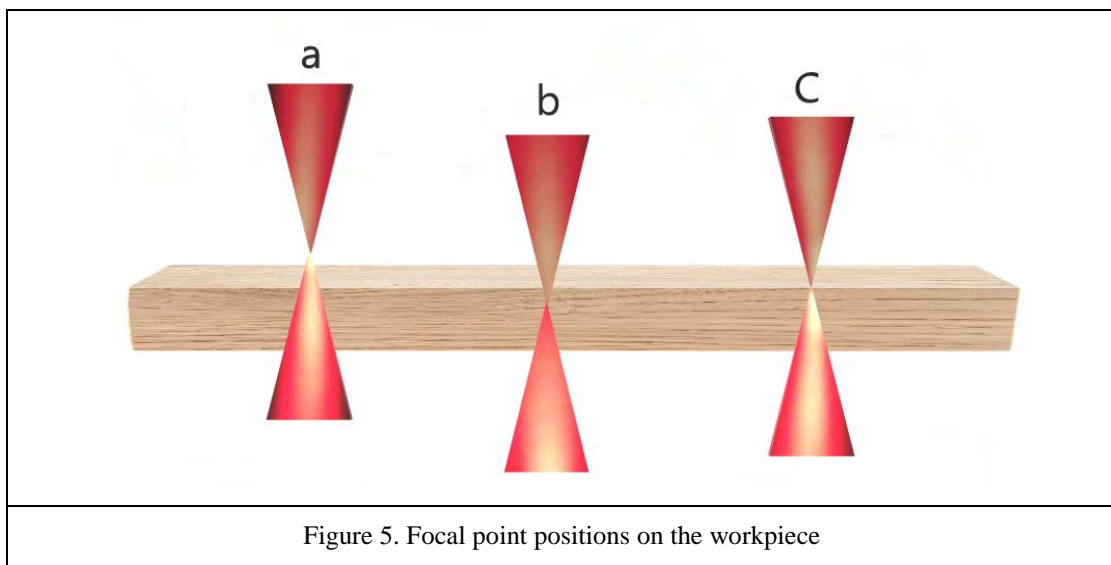


Figure 5. Focal point positions on the workpiece

When the focal point was above the workpiece surface, energy density declined. In this case, the wide kerf width and high charred surface resulted. By positioning the focal point on the surface, the maximum surface energy density achieved. The uniformity of energy density was occurred once the focal point is at or slightly above the workpiece centre, resulting in smooth surface with less charring (Barnekov et al 1986, Hovikorpi et al. 2004). Eltawahni et al. (2013) analyzed the possibility of focal point position at the

---

workpiece bottom. The kerf width at the upper side of the workpiece was higher than the rest part. The focal point positions are not an issue at which thin materials are used, except for precision. An A-shaped cutting kerf was resulted as a consequence of placing focal point above the workpiece surface. In contrast, placing the focal point below the workpiece surface generated a V-shaped. For paper materials, with a thin thickness, the focal point should be between - 0.2 mm and 0.2 mm to reach the narrowest kerf width (Malmberg et al 2006).

---

## 2 Materials and methods

This chapter discusses the selected wood species and adhesive type used in this study. Detailed information about the CO<sub>2</sub> laser process, the selected processing parameters (cutting speed, gas pressure, focal point position) is provided. The methods required for chemical and physical analysis of laser cut surface, including contact and contactless (laser) devices, contact angle measurement, Fourier-transform infrared spectroscopy (FTIR), Scanning Electron Microscope (SEM) are also described. In addition, the specific information on the glued laser-cut samples, glued shear test, bondline failure, adhesive penetration, numerical calculation of shear model based on the experimental result are provided.

### 2.1 Materials

#### 2.1.1 Wood species

Defect-free beech (*Fagus sylvatica* L), Oak (*Quercus robur* L), spruce (*Picea abies* L) and Larch (*Larix decidua* Mill.) wood was selected for the specimen test. The species were harvested from the Vysočina region in the Czech Republic and purchased from Wood Store ® company, Czech Republic. The properties of the species are provided in Table 1. The boards were cut into pieces with a dimension of 50 cm × 25 cm × 3 cm (length × width × thickness) and conditioned at 8%, 12% and 18% and above fiber saturation point.

Table 1. The average properties of three wood species (Konnerth et al. 2016).

<b>Wood species Properties</b>	<b>European beech (<i>Fagus sylvatica</i> L.)</b>	<b>European spruce (<i>Picea abies</i> (L.) Karst.)</b>	<b>European Oak (<i>Quercus robur</i> L)</b>	<b>Larch (<i>Larix decidua</i> Mill.)</b>
<b>Mean Density [g/cm<sup>3</sup>]</b>	0.743 (0.026)	0.445 (0.028)	0.698 (0.0230)	0.632 (0.06)
<b>Moisture content (%)</b>	12.52 (1.17)	12.74 (0.7)	11.39 (0.45)	11.55 (1.24)
<b>Tensile shear strength (N/mm<sup>2</sup>)</b>	8.5 - 12.1	6.5 - 7.7	7.9 - 10.3	7 - 8.3

---

## 2.1.2 Adhesive

Polyvinyl acetate (PVAc), Polyurethane (PUR), and two-component emulsion polymer isocyanate (EPI) were used for gluing of the the laser-cut samples. The technical specification of the resin adhesive is shown in Table 2. The adhesive was applied manually with a roller on the wood sample surfaces, with a range of 150 - 180 g/m<sup>2</sup> for PVAc.

**Table 2. Technical parameters of the selected adhesives**

<i>Resin</i> <i>Properties</i>	<b>PVAc</b>	<b>PUR</b>	<b>EPI</b>
<b>Viscosity (mPas)</b>	5000-7000 (at 23 ° C)	6000-19000	3500 (5000 with hardener)
<b>Working time (min)</b>	15-20	15-20	7-12
<b>Density (g/cm<sup>3</sup>)</b>	0.9-1.1 (at 23 ° C)	1.16	1.15
<b>Open time (min)</b>	15	15	12

## 2.2 Methods

### 2.2.1 CO<sub>2</sub> laser cutting

CO<sub>2</sub> laser machines from two companies, BLT WoodCut, and TRUMPF®, Czech Republic, were used to cut the wood pieces. The wood pieces were conditioned at 8%, 12%, 18% and above fibre saturated point before laser cutting process. Laser beam cut the pieces in the direction parallel to the grain, even there was a possibility to cut in the perpendicular direction. The aim of cutting along the grain is to assess the glued tensile shear strength. The resulted laser-cut samples have a semi-dark surface on the tangential section. The selected processing parameters of CO<sub>2</sub> laser are provided in Table 3.

Table 3. Applied processing parameters of CO<sub>2</sub> laser on the wood species

<i>Varied setting CO<sub>2</sub> parameters</i>	<b>BLT WoodCut Comany</b>	<b>TRUMPF® Company</b>	
<b>Cutting speed (m/min)</b>	3	3	3.5
<b>Focal point position</b>	At 1/3 of the workpiece from top surface	At the centre of the workpiece At the top of the workpiece	
<b>Laser power (W)</b>	5000	3200	
<b>Gas pressure (bar)</b>	-	17	21
<b>Nozzle diameter (mm)</b>	2.7	2.7	

## 2.2.2 Analysis of Laser-cut surface before gluing

### 2.2.2.1 Scanning Electron Microscopy (SEM)

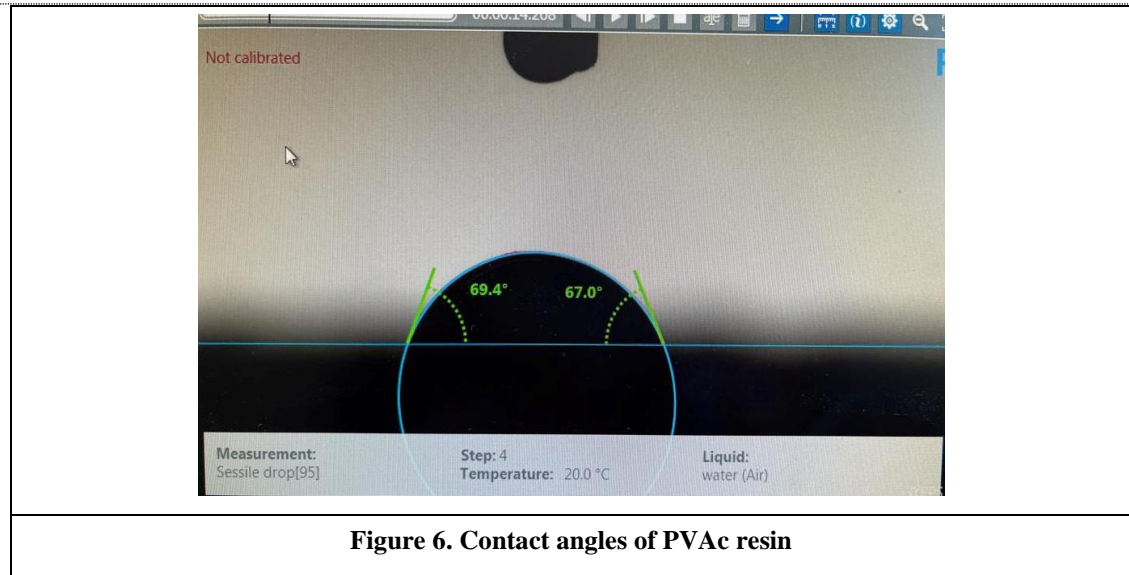
SEM, made in Germany (Leica SM 2000R, Leica Biosystems Nussloch GmbH), Czech Republic, Brno (Tescan Orsay Holding) and the USA (Thermo Fisher Scientific, Hillsboro), was used to investigate the anatomical structure of laser cut surface. The changes in O/C ratio on the laser cut surface and the layers below the surface were also investigated by SEM.

### 2.2.2.2 Fourier transform infrared spectroscopy (FTIR)

FTIR, made in Czech Republic (Nicolet, Křelovická), was used to investigate the chemical degradation occurred in the laser cut surface.

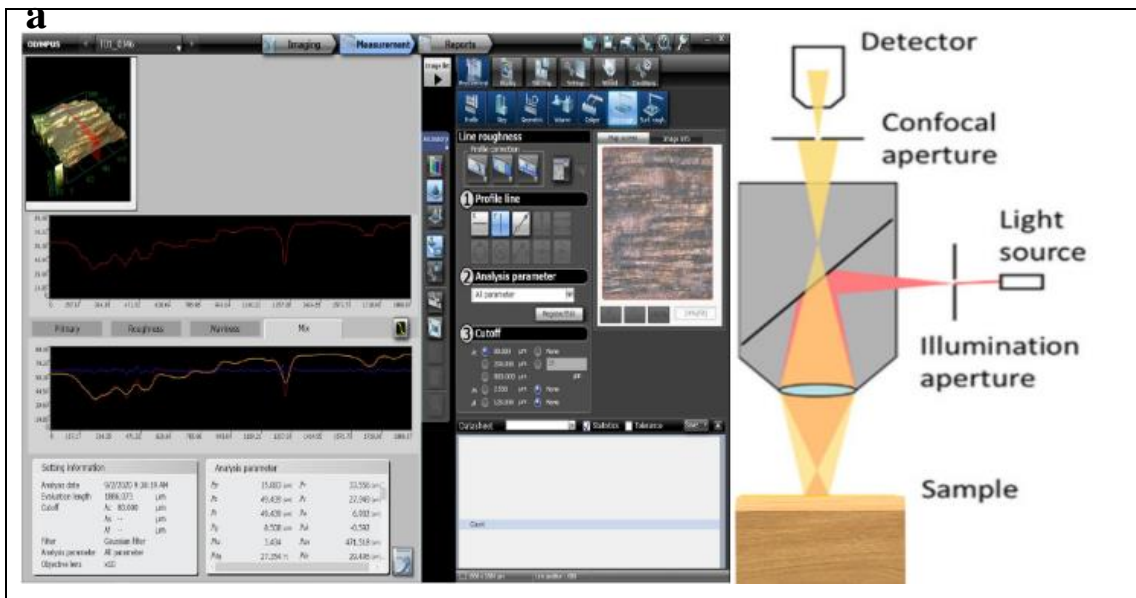
### 2.2.2.3 Contact angle measurement

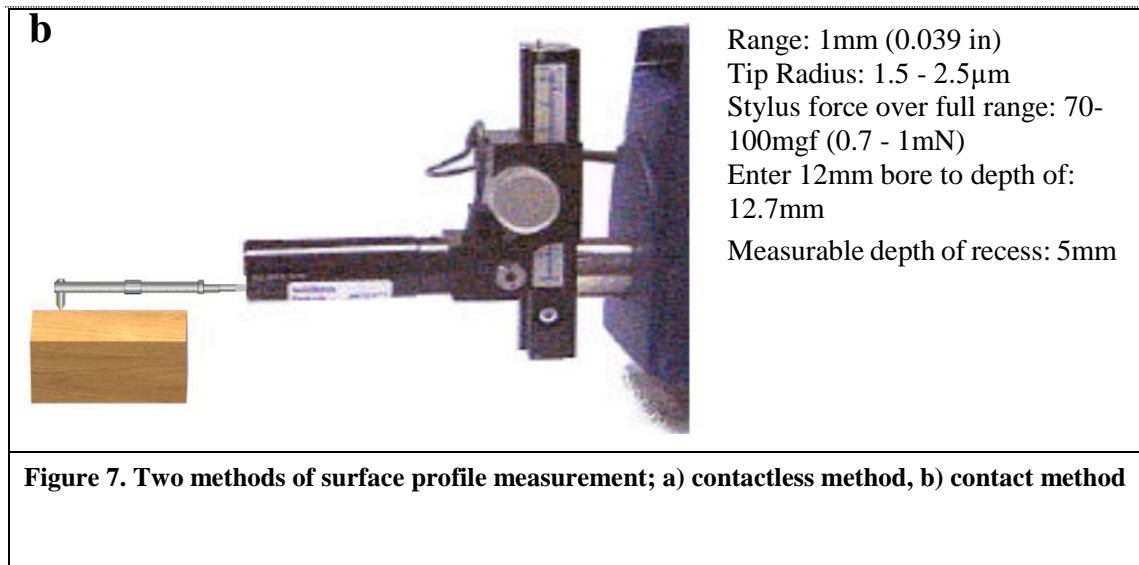
Contact angle device, made in Germany, Humburg (Krüss), was used to measure the degree of angle drop, PVAc resin, on the laser-cut samples (Figure 6).



#### 2.2.2.4 Surface profile measurement of the laser cut surface

The surface profile measurement was carried out by two different methods on the laser-cut samples; 1) a contact device using a contact tool (Form Talysurf 50 Intra, England) 2) A contactless device (Olympus, Japan) (Figure 7). The average waviness ( $W_a$ ) and the average roughness ( $R_a$ ) were obtained by filtering surface profile.

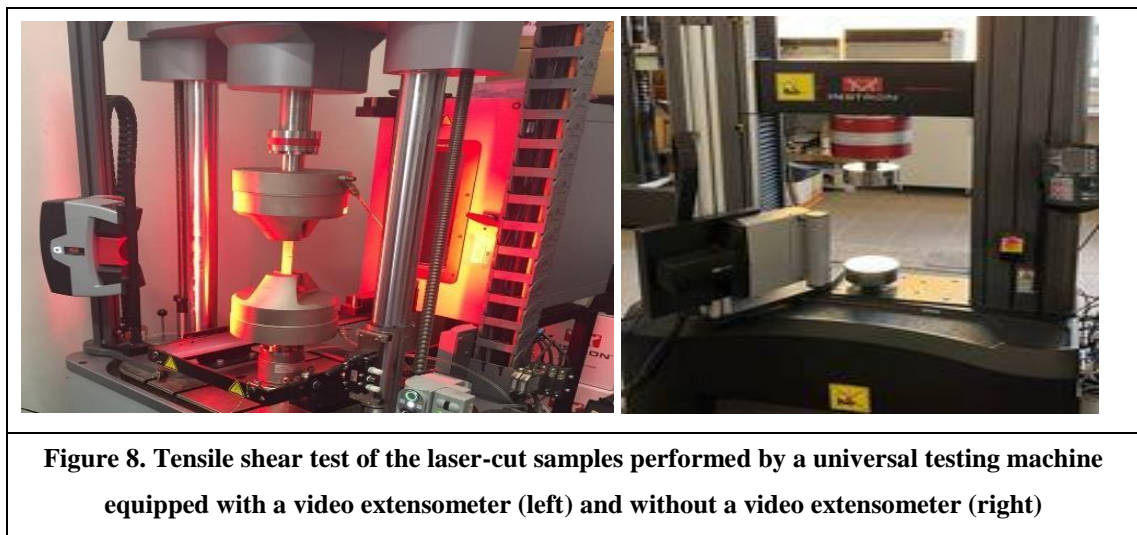




## 2.2.3 Analysis of the glued laser cut surface

### 2.2.3.1 Tensile shear strength of the glued laser-cut samples

After applying PVAc resin, the tensile shear test on the glued laser-cut samples was performed by using a universal testing machine equipped with a video extensometer (INSTRON® 5882, NORWOOD, USA) and other universal testing machine UTS 50 (TIRA, Germany) was also used (Figure 3).



### 2.2.3.2 Numerical calculation of the glued shear model

Based on the load and displacement of the data obtained from extensometer's software, the numerical analyses were carried out. The knowledge of Elongation model of overlap

---

joint was necessary to obtain the linear elasticity, the surface of the cross section, the internal load of the glue line. The assumption was that the module of linear elasticity, the surface of the cross section and internal loads of cladding were equal. By considering only loads in the cladding, and by calculating the elongation of the cladding, the module of linear elasticity of glue line  $E_g$  (MPa) was computed by assuming that the Poissons ratio is equal to 0.3. The results of analytical calculations were verified by the method of finite elements.

Wood material data was calibrated using standard Abaqus tools.  $E_g$  (MPa) adhesive weld modules for individual types of connections were calculated. A method of non-linear calculations was used. The given extension  $dL$  forced the load values (mm) obtained based on experimental tests. The sample was immobilized by assigning freedom levels adequate to the experimental tensile test. The weld and cladding were modelled with the use of C3D8R elements (an 8-node linear brick, reduced integration, hourglass control, the total number of nodes: 71778, total number of elements: 54120). Quicking was made on the commercial version of the Abaqus v. 6.13 (Dassault System Simulia Corp. Providence, RI, USA). The correctness of the model calibration is presented in the form of numerical calculations and their comparisons with the results of experimental research. The method of measuring the elongation of the connection appropriate for elongations in the mathematical model. The results of all measurements were collected and compiled in the form of stress and deformation accounts, as well as calculated modulus of glue lines.

### **2.2.3.3 Failures in the bondline after shear test**

Adhesive, cohesive and wood failure occurred in the bondline of the laser-cut samples after shear test were determined visually.

### **2.2.3.4 Scanning Electron Microscope (SEM)**

SEM, made in Germany (Leica SM 2000R, Leica Biosystems Nussloch GmbH), Czech Republic, Brno (Tescan Orsay Holding) and the USA (Thermo Fisher Scientific, Hillsboro), was used to investigate the penetration behavior of PVAc resin into porosity structure of the beech and oak wood. Elemental analysis of the bondline after shear test was also determined by energy dispersive X-ray (EDX) spectrometry.

---

### **2.2.3.5 Statistical evaluation**

Duncan's test, with a significance level of  $\alpha = 0.05$ , was chosen to evaluate the results and their interactions. Based on the significance level 'P', this test determines whether the observed factor is statistically significant. According to the value of P, the monitored factor is evaluated.

- $P = 0$  - the probability that the factor does not act is zero.
- $P < 0.05$  - the influence of the factor is statistically significant.
- $P = 0.05$  – the influence of the factor is on the border of statistical significance.
- $P > 0.05$  – the effect of the factor is not statistically significant.

---

### 3 Synthesis of acquired knowledge

This chapter shows the summary results of the dissertation published in a professional publication during the doctoral study. The PhD dissertation consists of five articles: three first-author article and two second author article. One first author article and two second author article have been published and two first author articles is submitted (under review). The first part of the results focuses on the glued tensile shear strength of the bondline made of the laser-cut wood (beech and oak species) (section 3.1). The second part compares the contact and contactless method for measuring surface quality on the thermally modified spruce wood (section 3.2). The third part is dealing with the morphology and anatomical structure of laser-cut samples (3.3). The forth part is investigating the characteristics of the bondline made of laser cut wood (beech) (section 3.4). The fifth part is investigating the shear bondline strength under the

The quality of the wood-adhesive bond is highly depended on the properties of wood and adhesive along with the production processes. If one of the bondline elements (adhesive or wood) become change, due to surface or adhesive preparation, the bondline strength become affected.

Article no. 1 (Milan Gaff, Fatemeh Rezaei et al. 2020) shows that the shear strength of the glued laser-cut samples (beech and oak) decreased, compared to those of milled samples. This research shows that the percentage of adhesive failure was higher than the percentage of wood and cohesive failures. This research demonstrates the degradation of laser-cut surface with lower moisture content was higher rather than that of with higher moisture content. The current study shows also that the surface quality ( $W_a$  and  $R_a$ ) of the laser-cut surface was lower (measured by contact method) rather than that of milled surface.

Article no. 2 (Fatemeh Rezaei, Milan Gaff et al. 2020) compares the two methods (contact and contactless) of surface quality measurement. In this research, the average surface roughness and waviness were obtained by two methods on the thermally treated spruce milled with different processing parameters (cutting speed, rate angle and feed speed). More accurate results obtained by contactless method was proven, compared with contact method.

---

Article no. 3 (Fateme Rezaei, Rupert Wimmer et al. 2022) shows the anatomical structure and surface quality of the laser-cut samples with different CO<sub>2</sub> processing parameters; cutting speed, gas pressure, focal point position. This research demonstrated that the average roughness values of the samples cut with high and low cutting speed did not change, however, the structural integrity of the laser-cut samples (cross section) with a high speed showed a better result. Replacing the focal point position from top to the centre of the workpiece provides rougher surface and reduce the structural integrity. This paper represents the higher gas pressure resulted in smoother surface rather than that with lower gas pressure.

Article no. 4 (Fateme Rezaei, Gaff Milan et al. 2022) shows the bondline characteristics made of laser-cut samples. This paper discusses that the contact angles between PVAc resin and laser cut surface is lower than those at sawn surface. The penetration behavior of PVAc resin into the porosity structure of laser and sawn cut was the same. The chemical degradation was occurred on the laser cut surface mainly in hemicellulose and lignin. The numerical calculation of the shear model was the same as the experimental shear model.

Article no. 5 (Miroslav Gašparík, Fateme Rezaei et al. 2022) showed that the glued tensile shear strength of the samples cut by a tool (larch and spruce) was not affected under alternating different freezing and high temperatures. This paper represents that although there were variations in moisture content of the glued samples when subjected to alternating freezing and high temperature, the glued tensile shear strength remained unchanged, compared to that without conditioning.

---

### 3.1 Discussion

The gluing properties of the bondline made of laser cut wood (non-contact) was lower than those cut by contact tools (milling, planing, saw, etc.). To find out the reasons, the physical and chemical analysis of the laser cut surface along with the characteristics of the bondline were investigated.

The surface quality cut by contact and non-contact tool: At the beginning, to investigate the surface quality of the laser-cut samples, a contact method (a stylus tip) was used. Later, following the arrival of non-contact method (confocal microscope), the research was conducted by using only confocal microscope. No studies have been found to prove which method provides more accurate and reliable data. A research study was carried out to compare the two methods. Confocal microscope was proven to have more accuracy than a stylus tip. Hence, the surface quality of the laser-cut samples was measured only using the confocal microscope.

The quality of a cut surface is depending on; a) machining tools and the cutting parameter used b) wood's anatomical structure and properties such as moisture content, density, and anatomical structure (vessels, fibres, ray cells). The accuracy of the measuring method is also quite important to provide an accurate wood surface profile.

Wood cutting tools and measuring methods of surface profile: It was assumed that the surface subjected to laser energy provides a smoother surface than surface cut by a contact tool. The assumption covers the idea that the wood surface structure melts down and induces smoothness. At the beginning, when using a stylus tip, the hypothesis was accepted, later, when using a confocal microscopy, the hypothesis was rejected. The average surface roughness ( $R_a$ ) of laser-cut samples measured by a stylus tip was lower than samples cut by the tools. In opposite, the  $R_a$  of the laser-cut samples measured by confocal microscope was higher than those cut by the tools. The confocal microscope can measure the deeper valleys and peaks with the lower radius than the stylus tip. Therefore, the results of the confocal microscope are more precise and reliable than those measured by the stylus tip. The higher  $R_a$  of the laser cut surface can be related to charring at which the distribution rate was not uniform. Even the wood samples were securely anchored before laser cutting, the traces of wood vibration on some samples were also observed. The processing parameters of the laser-cut samples measured by two different methods were different, as a result, leading to the formation of new surface profile.

---

Moisture content: The wood samples conditioned to different moisture content (MC) before cutting can influenced cutting parameters and leading to a new surface profile. The exact model of  $R_a$  was not possible to determine for the laser cut surfaces with high and low MC. The laser cut surface of beech was rougher at higher MC than the surface at low MC. In opposite, by changing the wood species, oak, the laser cut surface at high MC was smoother than the surface at low MC. The rougher laser cut surface of beech was resulted at almost high MC (18%) rather than the surface at low MC. The interaction of MC with processing parameters (gas pressure) could affect the  $R_a$ .

Processing parameters of laser cutting: The optimization of CO<sub>2</sub> processing parameters and the intimate interaction with material properties can be resulted in acceptable surface profile for further application process such as gluing and coating. The high and low cutting speed was not affected on the  $R_a$ . It is quite interesting to recognized that the interaction of MC with processing parameters could significantly affect on the  $R_a$ . The samples at 8% MC cut with using high gas pressure provided smoother surface rather that the samples cut with lower gas pressure at the same MC. This result is difficult to interpreter, due to the resulted surface is generated based on several factors and their interactions. Positioning focal point on top at samples conditioned at 12% MC was resulted as a better  $R_a$ . There is still unknown whether the rougher surface or smoother surface provides a better wood adhesive bond. If resin penetrates so much into wood structure, due to rougher surface, the bond strength reduces. However, with smoother surface, sometimes, the bondline penetration only created and wood around bondline has less interaction with the resin, may leading to a low bond strength.

The anatomical structure of the laser-cut samples: The anatomical structure of wood may damage physically when wood proceed by a contact tool. However, there were no evidence to show how would be a wood anatomical structure after laser cutting. The anatomical structure of wood can be influenced by CO<sub>2</sub> processing parameters, cutting speed and focal point position. The hydrophilic property of wood can also play an important role in an interaction with the cutting parameters, creating a new form of anatomical structure. The anatomical structure of the laser cut surface at low MC (8%) was more degraded than the surface at high MC (>FSP). Both oak and beech species with a bit different anatomical structure were shown the same behavior. This can be explained in the way that with higher moisture content, less burning on the surface occurred. A part of laser energy spends for water evaporation. The integrity of the anatomical structure of the laser cut surface weaken when a low cutting speed was used.

---

When a low cutting speed applied, the more areas of the laser cut surface becomes degraded. However, the degradation of higher molecular weight is depending on laser power. The integrity of anatomical structure was affected by focal point position. The focal point is the maximum energy of laser which can focus on surface or centre of the workpiece (beech). The maximum energy on the surface distributed better in the workpiece and resulted in a better integration. The interpretation is required more research on thermal conductivity and the specific wood species. The less anatomical integrity on the surface means less surface strength when the tensile shear strength was applied.

The chemistry of the surface cut by non-contact tool: The main chemical compounds of beech wood were degraded by thermal energy of CO<sub>2</sub> laser, based on the FTIR analysis. However, the depth of the affected layers (O/C) was mostly observed in the first and second layers (50µm each layer). Hemicellulose and lignin are two main components that mostly degraded. Therefore, the number of hydrogen bonds which can be created between resin and wood reduced. This can be one of the main reasons why the gluing properties of laser cut surface lower, compared to that the surface cut by a contact tool.

The characteristics of the bondline made of laser-cut samples are the wetting properties, the penetration behavior of the PVAc resin, bondline failure, numerical calculation of shear model.

Wetting properties of the laser-cut surface and the penetration depth of PVAc: the PVAc drop was disappeared fast on the laser-cut surface. The charred surface absorbed the PVAc drop and held it between the free spaces of a tiny charred particle. As a result, in the closed assembly time the penetration of adhesive could not possible. Even pressure from cold pressing was applied on the glued laser-cut samples, the bondline penetration was resulted. It is interesting that the penetration behavior of PVAc resin into cellular structure of the laser cut surface was the same as that of surface cut by a contact tool.

The better adhesion is achieved by a proper wetting of PVAc resin on wood. However, there is still not clear whether or not the adhesion is correlated with high penetration or low penetration depth of resin. A high glued strength of wood also achieved with a bondline penetration.

Failure analysis in the bondline made of laser cut wood: the PVAc resin was not able to properly formed the hydrogen bonds with the chemical compounds of the laser cut

---

surface. The PVAc failure was observed more in the bondline area. The reason can be explained by the present of the charred particles on the laser cut surface and mixing to the PVAc resin, acting as a boundary between wood and resin.

The kerf shape of laser-cut samples was curved. Hence, the flat surfaces of the laser cut surfaces was not achieved. Even the pressure of cold pressing was applied on the curve shapes, the bondline was not form flat. This can be one the main reason which reduce significantly the glued tensile shear strength.

Finally, the tensile shear strength of the glued laser -cut samples was reduced, compared to the surfaces cut by contact tool, the main reasons were provided as bellow:

- a) The present of charred particles on the laser-cut samples.
- b) The degradation of the wood chemical compounds.
- c) The depth of heat affected zone.
- d) The curve shape of the laser-cut samples.
- e) The disintegration of the anatomical structure of the laser-cut samples.

The glued strength of larch and spruce samples cut by a contact tool exposed to the alternating freezing and high temperatures was surprisingly the same as those without the conditioning. The changes occurred in the moisture content of the glued samples from freezing to high temperature could not impact on the glued strength. The result was rejecting the hypothesis at which the glued tensile shear strength reduced by conditioning to the varied temperatures (freezing to high temperatures). If the glued strength of the samples cut by the saw was influenced by the varied temperature conditions, the glued laser-cut samples were also subjected to the alternating freezing and high temperatures. Hence, there were no need to test the laser-cut samples under varied temperatures conditions.

---

## 4 Conclusion and future works

The quality of engineered wood products is highly dependent on the quality of the wood cutting process. The current research showed that the tensile shear strength of the glued laser cut samples reduced significantly, compared to that of samples cut by the contact tools. The quality of the glued strength depends on the quality of the surface, adhesive, and production processes.

The current research showed that glued tensile shear strength of the laser cut samples reduced significantly, compared to that of samples cut by contact tools. This supports the hypothesis at which the tensile shear strength decreased as a result of chemical and physical changes occurred on the laser cut surface.

The surface quality of the laser cut surfaces behaved differently based on the measuring method, the processing parameters of the laser, and moisture content in wood. The laser cut surface showed a lower average roughness with the processing parameters of 5000w, 3m/min, with focal point at one third from top surface, compared to those surfaces cut by the tools. This result proves the theory that in comparison to sawn surface, the average roughness of the laser cut surface decreases. When the processing parameters change to 3200 w, 3 and 3.5 m/min, 21 and 17 bar, focal point at top and centre of the workpiece, the average roughness was higher than that of cut by the tools. This disproves the theory at which in comparison to sawn surface, the average roughness of the laser cut surface decreases. The precision of the confocal microscopy used for measuring the surface profile was proven when compared with the stylus tip method. The laser cut surface of oak wood was smoother at high MC while the surface of beech wood at high MC showed rougher, as compared to the surfaces of beech and oak at low MC. Increasing gas pressure and focusing focal point at top surface was provided smoother surfaces of laser cut samples rather than those with lower gas pressure and focusing at the middle of the workpiece.

The bondline penetration was observed from both surfaces cut with laser and the contact tools. The contact angle of the resin was reducing fast on the charred layer of the laser cut surface. However, this is not indicating the higher penetration of PVAc resin. This result supports the hypothesis that wetting properties of laser cut samples reduced, due to thermal modified laser cut surface. The chemical degradation of the lignin and hemicellulose was detected on the laser cut surfaces, supporting the hypothesis, coming up with the chemical degradation of the main wood components exposed to the laser power.

---

The anatomical structure of the laser cut surfaces is influenced by the CO<sub>2</sub> laser processing parameters and the moisture contains in the wood. The anatomical structure of the surfaces conditioned to lower MC degraded as compared to higher MC. The structural integrity is better in the sample cut by laser with increasing cutting speed and focusing the focal point on top, compared with that of the samples with decreasing cutting speed and focusing at the middle of the workpiece. The hypothesis about the anatomical structure of the laser cut surface affected by laser power, is fulfilled by this result.

The findings of the current research are significantly beneficial to wood science in terms of the laser cutting process, the cut quality and finally the gluability of the laser cut samples. For example, the anatomical structure of the laser cut wood provides a new insight in wood biology. Wood scientists can employ the results of the gluability in developing a new resin, especially for laser cut surface. The results of laser cut can be modelled and optimized by scientists who are interested in laser cutting. This current research is greatly beneficial for wood industrial in practice. Cutting wood by CO<sub>2</sub> laser provides a desirable complicated shape with a short time. Wood industries can save cost by removing the sharpening process of tools.

This research has thrown up many questions in need of further investigation. Further work needs to be done to establish whether laser cutting on the softwood species behaved the same as hardwood species. Further research should usefully explore how the direction of the laser cut in the perpendicular direction vary from parallel direction. Experimental investigations are needed to estimate the mathematical model for glued shear strength with properties before and after laser cutting. Research in other adhesive systems, therefore, an essential next step in confirming the glued shear strength. Experiments, using a broader range of coatings, could shed more light on surface properties of the laser cut wood. More broadly, research is also needed to determine the diffusion and hardness behavior of the laser cut surfaces whereas the product used for exterior purposes.

---

## 5 List of used literature

- Abbott, M. D. (2006). *Advanced laser processing and photoluminescence characterisation of high efficiency silicon solar cells* (Doctoral dissertation, UNSW Sydney).
- Arnold, M., Risi, W. and Steiger, R. (2019). Qualitätskontrolle der Flächenverklebung bei Brettschichtholz aus Laubholz (QS LH-BSH). WHFF-Projekt Nr. 2017.18. Dübendorf: Empa.
- Bikerman, J. J. (2013). *The science of adhesive joints*. Elsevier.
- Bockel, S. (2020) Structural bonding of European beech wood (*Fagus sylvatica* L.) with polyurethane adhesives. thesis (PhD), Institute of Wood Technology and Renewable Materials, Austria.
- Bockel, S., Mayer, I., Konnerth, J., Harling, S., Niemz, P., Swaboda, C., ... & Pichelin, F. (2019). The role of wood extractives in structural hardwood bonding and their influence on different adhesive systems. *International Journal of Adhesion and Adhesives*, 91, 43-53.
- Barnekov, V. G., McMillin, C. W., & Huber, H. A. (1986). Factors influencing laser cutting of wood. *Forest products journal*, 36.
- Belforte, D. A. (1998). Non-metal cutting. *Ind Laser Rev*, 13(9), 11-13.
- Barnekov, V. G., McMillin, C. W., & Huber, H. A. (1986). Factors influencing laser cutting of wood. *Forest products journal*, 36.
- Bowyer, J. L., Shmulsky, R., & Haygreen, J. G. (2003). Forest products and wood science: an introduction.
- Conner, A. H. (2001). Wood: adhesives. *Encyclopedia of materials: science and technology*. Amsterdam; New York: Elsevier Science, Ltd., c2001.
- Chryssolouris, G. (2013). *Laser machining: theory and practice*. Springer Science & Business Media.
- Christiansen, A. W. (1990). How overdrying wood reduces its bonding to phenol-formaldehyde adhesives: a critical review of the literature. Part I, Physical Responses. *Wood and fiber science*. Vol. 22, no. 4 (1990): Pages 441-459.
- Dawes, C. T. (1992). *Laser welding: a practical guide*. Woodhead Publishing.
- Dinwoodie, J. M. (1983). Wood Adhesives Chemistry and Technology. *Marcel Dekker, New York*.
- Duley, W. W. (2012). *Laser processing and analysis of materials*. Springer Science & Business Media.
- Duley, W. W., & Williams, D. A. (1983). A 3.4  $\mu$  m absorption band in amorphous carbon: implications for interstellar dust. *Monthly Notices of the Royal Astronomical Society*, 205(1), 67P-70P.
- Derjaguin, B. V., & Smilga, V. P. (1967). Electronic theory of adhesion. *Journal of applied Physics*, 38(12), 4609-4616.
- Eltawahni, H. A., Olabi, A. G., & Benyounis, K. Y. (2011). Investigating the CO<sub>2</sub> laser cutting parameters of MDF wood composite material. *Optics & Laser Technology*, 43(3), 648-659.
- Eltawahni, H. A., Rossini, N. S., Dassisti, M., Alrashed, K., Aldaham, T. A., Benyounis, K. Y., & Olabi, A. G. (2013). Evaluation and optimization of laser cutting parameters for plywood materials. *Optics and lasers in engineering*, 51(9), 1029-1043.

- Frihart, C. R., & Hunt, C. G. (2010). Adhesives with wood materials: bond formation and performance. *Wood handbook: wood as an engineering material: chapter 10. Centennial ed. General technical report FPL; GTR-190. Madison, WI: US Dept. of Agriculture, Forest Service, Forest Products Laboratory, 2010: p. 10.1-10.24., 190, 10-1.*
- Hänsel, A., Sandak, J., Sandak, A., Mai, J., & Niemz, P. (2022). Selected previous findings on the factors influencing the gluing quality of solid wood products in timber construction and possible developments: A review. *Wood Material Science & Engineering, 17*(3), 230-241.
- Haller, P., Beyer, E., Wiedemann, G., Panzner, M., & Wust, H. (2001). Experimental study of the effect of a laser beam on the morphology of wood surfaces. In *Proceedings of the First International Conference of the European Society for Wood Mechanics, Lausanne, Switzerland* (pp. 19-21).
- Gardner, D. J. (2006). Adhesion mechanisms of durable wood adhesive bonds. *Characterization of the cellulosic cell wall*, 254-265.
- Green, M. A., Wenham, S. R., Zhao, J., Bowden, S., Milne, A. M., Taouk, M., & Zhang, F. (1991, October). Present status of buried contact solar cells. In *The Conference Record of the Twenty-Second IEEE Photovoltaic Specialists Conference-1991* (pp. 46-53). IEEE.
- Green, M. A., Chong, C. M., Zhang, F., Sproul, A., Zolper, J., & Wenham, S. R. (1996, September). 20% efficient laser grooved, buried contact silicon solar cells. In *Conference Record of the Twentieth IEEE Photovoltaic Specialists Conference* (pp. 411-414). IEEE.
- Gavrilović-Grmuša, I., Dunky, M., Miljković, J., & Djiporović-Momčilović, M. (2012). Influence of the degree of condensation of urea-formaldehyde adhesives on the tangential penetration into beech and fir and on the shear strength of the adhesive joints. *European Journal of Wood and Wood Products, 70*(5), 655-665.
- Hass, P. F. S. (2012). *Penetration behavior of adhesives into solid wood and micromechanics of the bondline* (Doctoral dissertation, ETH Zurich).
- Hänsel, A., Sandak, J., Sandak, A., Mai, J., & Niemz, P. (2022). Selected previous findings on the factors influencing the gluing quality of solid wood products in timber construction and possible developments: A review. *Wood Material Science & Engineering, 17*(3), 230-241.
- Hernandez-Castaneda, J. C., Sezer, H. K., & Li, L. (2010). Dual gas jet-assisted fibre laser blind cutting of dry pine wood by statistical modelling. *The International Journal of Advanced Manufacturing Technology, 50*(1), 195-206.
- Havrilla, D., & Anthony, P. (2000). Laser cutting process fundamentals and troubleshooting guidelines. *Rofin Sinar Laser publications, Germany*.
- Huber, H. E., McMillin, C. W., & Rasher, A. (1982). Economics of cutting wood parts with a laser under optical image analyzer control. *Forest Products Journal 32* (3): 16-21.
- Handbook, W. (2010). Wood as an Engineering Material. Forest Product Laboratory; United States Department of Agriculture Forest Service. *Madison, Wisconsin, USA*.
- He, X., Elmer, J. W., & DebRoy, T. (2005). Heat transfer and fluid flow in laser microwelding. *Journal of Applied Physics, 97*(8), 084909.
- Hovikorpi, J., Laakso, P., Malmberg, H., Kujanpää, V., & Miikki, N. (2004, October). Laser cutting of paper. In *International Congress on Applications of Lasers & Electro-Optics* (Vol. 2004, No. 1, p. 2103). Laser Institute of America.
- Ion, J. (2005). *Laser processing of engineering materials: principles, procedure and industrial application*. Elsevier.

- 
- International Agency for Research on Cancer. (2006). Formaldehyde, 2-Butoxyethanol and 1-tert-Butoxypropan-2-ol. In *Formaldehyde, 2-butoxyethanol and 1-tert-butoxypropan-2-ol* (pp. 478-478).
- Israelachvili, J. N., & Tabor, D. (1972). Measurement of van der Waals dispersion forces in the range 1.4 to 130 nm. *Nature Physical Science*, 236(68), 106-106.
- Jamalirad, L., Doosthoseini, K., Koch, G., Mirshokraie, S. A., & Welling, J. (2012). Investigation on bonding quality of beech wood (*Fagus orientalis* L.) veneer during high temperature drying and aging. *European Journal of Wood and Wood Products*, 70(4), 497-506.
- Johns, W. E. (1989). The chemical bonding of wood. *Wood Adhesive Chemistry and Technology*, Vol. 2.
- Jakes, J. E., Frihart, C. R., Hunt, C. G., Yelle, D. J., Plaza, N. Z., Lorenz, L., ... & Xiao, X. (2019). X-ray methods to observe and quantify adhesive penetration into wood. *Journal of materials science*, 54(1), 705-718.
- John, P. A. (1980). Textbook of wood technology: structure, identification, properties, and uses of the commercial woods of the United States and Canada. *McGraw-Hill series in forest resources (USA)*.
- Kannatey-Asibu Jr, E. (2009). *Principles of laser materials processing*. John Wiley & Sons.
- Klein, I. E., Sharon, J., Yaniv, A. E., Dodiuk, H., & Katz, D. (1983). Chemical interactions in the system anodized aluminum—primer—adhesive. *International journal of adhesion and adhesives*, 3(3), 159-162.
- Knop, A., & Pilato, L. A. (2013). *Phenolic resins: chemistry, applications and performance*. Springer Science & Business Media.
- Kreibich, R. E. (1984). Wood Adhesives: Present and Future, ed. In A. Pizzi, *Applied Polymer Symposium* (Vol. 40, pp. 1-18).
- Kúdela, J., Mrenica, L., & Javorek, L. (2018). The influence of milling and sanding on wood surface morphology. *Acta Facultatis Xylologiae Zvolen res Publica Slovaca*, 60(1), 71-83.
- Konnerth, J., Harper, D., Lee, S. H., Rials, T. G., & Gindl, W. (2008). Adhesive penetration of wood cell walls investigated by scanning thermal microscopy (SThM).
- Konnerth, J., et al. (2016) Survey of selected adhesive bonding properties of nine European softwood and hardwood species. *European Journal of Wood and Wood Products*, 74, 809–819.
- Kaboorani, A., & Riedl, B. (2011). Effects of adding nano-clay on performance of polyvinyl acetate (PVA) as a wood adhesive. *Composites Part A: Applied Science and Manufacturing*, 42(8), 1031-1039.
- Lanvermann, C. (2014). *Sorption and swelling within growth rings of norway spruce and implications on the macroscopic scale* (Doctoral dissertation, ETH Zurich).
- Lum, K. C. P., Ng, S. L., & Black, I. (2000). CO<sub>2</sub> laser cutting of MDF: 1. Determination of process parameter settings. *Optics & laser technology*, 32(1), 67-76.F
- Li, L., & Mazumder, J. (1991). A study of the mechanism of laser cutting of wood. *Forest products journal (USA)*.
- Luedtke, J., Amen, C., van Ofen, A., & Lehringer, C. (2015). 1C-PUR-bonded hardwoods for engineered wood products: influence of selected processing parameters. *European Journal of Wood and Wood Products*, 73(2), 167-178.
-

- 
- Marra, A.A. (1980). Applications of wood bonding. In: R.F. Bloomquist, A.W. Christiansen, R.H. Gillespie, and G.E.
- Malkoçoğlu, A. (2007). Machining properties and surface roughness of various wood species planed in different conditions. *Building and Environment*, 42(7), 2562-2567.
- McBain, J. W., & Hopkins, D. G. (2002). On adhesives and adhesive action. *The Journal of Physical Chemistry*, 29(2), 188-204.
- Modest, M. F., Ready, J., & Farson, D. (2001). Handbook of laser materials processing.
- McMillin, C. W., & Harry, J. E. (1971). Laser machining of southern pine. *Forest Products Journal* 21 (10): 35-37.
- Mukherjee, K., Grendzwell, T., Khan, P. A., & McMillin, C. (1990). Gas flow parameters in laser cutting of wood-nozzle design. *Forest Products Journal* 40 (10): 39-42.
- Meyer, B., & Hermanns, K. (1986). Formaldehyde release from wood products: an overview.
- Malmberg, H., Leino, K., & Kujanpää, V. (2006). *Laser cutting of paper and board*. Lappeenranta University of Technology.
- Neese, J. L., Reeb, J. E., & Funck, J. W. (2004). Relating traditional surface roughness measures to gluebond quality in plywood. *Forest products journal*, 54(1).
- Nuryawan, A., Park, B. D., & Singh, A. P. (2014). Penetration of urea-formaldehyde resins with different formaldehyde/urea mole ratios into softwood tissues. *Wood Science and Technology*, 48(5), 889-902.
- Niemz, P., & Gereke, T. (2009). Auswirkungen kurz-und langzeitiger Luftfeuchteschwankungen auf die Holzfeuchte und die Eigenschaften von Holz. *Bauphysik*, 31(6), 380-385.
- Niemz, P., Baum, S., Junghans, K., Bächle, F., & Sonderegger, W. (2006). Holzphysik:(Skript zur Vorlesung).
- Niemz, P., & Sonderegger, W. (2016). *Holzphysik*. Munich, Germany: Hanser.
- Pizzi, A. (1994). *Advanced wood adhesives technology*. CRC Press.
- Pizzi, A., & Mittal, K. L. (Eds.). (2017). *Handbook of adhesive technology*. CRC press.
- Pizzi, A., & Mittal, K. L. (2003). Urea-formaldehyde adhesives. *Handbook of adhesive technology*, 2.
- Pizzi, A., & Adhesive, W. (1983). Chemistry and technology. *New York: Marcell Deckker*.
- Pizzi, A., Horak, R. M., Ferreira, D., & Roux, D. G. (1979). Condensates of phenol, resorcinol, phloroglucinol, and pyrogallol as model compounds of flavonoid A-and B-rings with formaldehyde. *Journal of applied polymer science*, 24(6), 1571-1578.
- Pizzi, A., & Eaton, N. J. (1987). A conformational analysis approach to phenol-formaldehyde resins adhesion to wood cellulose. *Journal of Adhesion Science and Technology*, 1(1), 191-200.
- Pizzi, A. (1990). A molecular mechanics approach to the adhesion of urea-formaldehyde resins to cellulose. Part 2. Amorphous vs. crystalline Cellulose I. *Journal of adhesion science and technology*, 4(1), 589-595.
- Pizzi, A., Von Leyser, E. P., Valenzuela, J., & Clark, J. G. (1993). The chemistry and development of pine tannin adhesives for exterior particleboard.
- Pauling, L. (1940). *The nature of the chemical bond: and the structure of molecules and crystals; an introduction to modern structural chemistry* (No. 04; RMD, QD469 P3.).
- Patrick, R. L. (Ed.). (1981). Treatise on adhesion and adhesives.
-

- 
- Powell, J. (1998). Bibliography and Further Reading. In *CO<sub>2</sub> Laser Cutting* (pp. 231-239). Springer, London.
- Powell, J., & Kaplan, A. (2004, April). Laser cutting: from first principles to the state of the art. In *Pacific International Conference on Applications of Lasers and Optics* (Vol. 2004, No. 1, p. 101). Laser Institute of America.
- Peters, C. C. (1975). *Cutting wood materials by laser* (Vol. 250). Department of Agriculture, Forest Service, Forest Products Laboratory.
- Quintero, F., Riveiro, A., Lusquiños, F., Comesaña, R., & Pou, J. (2011). CO<sub>2</sub> laser cutting of phenolic resin boards. *Journal of Materials Processing Technology*, 211(11), 1710-1718.
- Qin, L., Lin, L., & Fu, F. (2016). Microstructural and micromechanical characterization of modified urea-formaldehyde resin penetration into wood. *BioResources*, 11(1), 182-194.
- Qiao, L., & Easteal, A. J. (2001). Aspects of the performance of PVAc adhesives in wood joints. *Pigment & Resin Technology*, 30(2), 79-87.
- Rabiej, R. J., Ramrattan, S. N., & Droll, W. J. (1993). Glueline shear strength of laser-cut wood. *Forest products journal*, 43(2), 45.
- Raff, R. A. V., & Silverman, B. H. (1951). Kinetics of the uncatalyzed reactions between resorcinol and formaldehyde. *Industrial & Engineering Chemistry*, 43(6), 1423-1427
- Rowell, R. M. (2005). *Handbook of wood chemistry and wood composites*. CRC press.
- Sandak, J., Orłowski, K., Sandak, A., Chuchala, D., & Taube, P. (2020). On-line measurement of wood surface smoothness. *Drvna industrija*, 71, 193-200.
- Szymani, R., & Dickinson, F. E. (1975). Recent developments in wood machining processes: novel cutting techniques. *Wood Science and Technology*, 9(2), 113-128.
- Steen, W. M., & Mazumder, J. (2010). *Laser material processing*. Springer science & business media.
- Suchsland, O. (1958). Über das Eindringen des Leimes bei der Holzverleimung und die Bedeutung der Eindringtiefe für die Fugenfestigkeit. *Holz als Roh-und Werkstoff*, 16(3), 101-108.
- Thole, V. (2017) Es ist noch nicht alles gesagt: Kleben von Holz!. In: 12. Holzwerkstoffkolloquium, December 14–15, 2017, Institut für Holztechnologie, Dresden, 99–103.
- Ülker, O. (2016). Wood adhesives and bonding theory. *Adhesives–Application and Properties*, 1st ed.; Rudawska, A., Ed, 271-288.
- Voiutskii, S. S. (1963). Autohesion and adhesion of high polymers.
- Wenham, S. R., & Green, M. A. (1988). *U.S. Patent No. 4,726,850*. Washington, DC: U.S. Patent and Trademark Office.
- White, J. T. (1995). Wood adhesives and binders. *Forest products journal*, 45(3), 21.
- Yusoff, N., Ismail, S. R., Mamat, A., & Ahmad-Yazid, A. (2008). Selected Malaysian wood CO<sub>2</sub>-laser cutting parameters and cut quality. *American Journal of Applied Sciences*, 5(8), 990-996.
- Zeppenfeld, G., & Grunwald, D. (2005). Klebstoffe in der Holz-und Möbelindustrie. 2. überarbeitete und erweiterte Auflage. *DRW-Verlag Weinbrenner GmbH & Co. KG, Leinfelden-Echterdingen*.

---

## 6 Separate articles and manuscripts

### 6.1 Interactions of monitored factors upon tensile glue shear strength on laser cut wood

**Published as:**

Milan Gaff, **Fatemeh Rezaei**, Adam Sikora, Štěpán Hýsek, Miroslav Sedlecký, Gianluca Ditommaso, Roberto Corleto et al. "Interactions of monitored factors upon tensile glue shear strength on laser cut wood." *Composite Structures* 234 (2020): 111679. DIO: 10.1016/j.compstruct.2019.111679.



## Interactions of monitored factors upon tensile glue shear strength on laser cut wood



Milan Gaff<sup>\*</sup>, Fatemeh Rezaei, Adam Sikora, Štěpán Hýsek, Miroslav Sedlecký, Gianluca Ditommaso, Roberto Corleto, Gourav Kamboj, Anil Sethy, Michal Vališ, Kamil Řípa

Department of Wood Processing, Faculty of Forestry and Wood Sciences, Czech University of Life Sciences Prague, Kamýcká 1176, Praha 6 - Suchbát, 16521, Czech Republic

### ARTICLE INFO

**Keywords:**  
Laser machine  
Tensile shear strength  
Density  
Moisture content

### ABSTRACT

Over recent decades, laser technology is at the forefront of material processing and in the near future, probably, it can be considered as a replacement for traditional techniques such as sawing. This paper reports the effect of monitor factors (cutting methods, moisture content at laser cutting, surface waviness and roughness) on tensile shear strength of glued layered wood. The process of laser cutting was applied on beech (*Fagus sylvatica* L.) and oak wood (*Quercus robur* L.). The quality of the surfaces resulted from laser cutting was measured by contact type surface profilometer. To ascertain the bonding behavior, laser cut surfaces were bonded with polyvinyl acetate adhesive and tensile glue shear strength was investigated on the bond-line. The results were compared with the results on saw cut samples. The test results revealed significant influence of monitored factors on the tensile shear strength of glued joints. The tensile glue shear strength values on laser-cut wood samples were significantly lower than those on saw cut samples.

### 1. Introduction

Wood is a renewable raw material, and widely used in construction and furniture industries. Due to the increasing demand of the increasing population, the pressure on the wood resource is tremendous. This has caused a steady increase in the prices of wood throughout the world. Hence rational utilization of available wood resource is quite important to meet the ever-increasing demand of the society. Continuous efforts are being made to minimize wastage, improve cutting precision and make the cutting process more automotive. In this endeavor, one of the modern techniques in wood processing is cutting wood with a laser beam. The use of laser technology for cutting wood goes back almost to the beginning of 1970s [1–3], particularly for cutting die in packing industries. Nowadays, the applications of laser cutting are rapidly expanded, mainly cutting wood for car interiors and wood inlays for the furniture industries [4,5]. Positive benefits of laser cutting to increase the yield can be summarized in two basic points: minimum kerf width (0.1–0.3 mm) as compared to saw cut (3–6 mm) and flexibility to start and finish cutting at any point on the board (Fig. 1). The other advantages of laser cutting over a saw cutting (conventional method) can be specified in highly precise cut, no tool wear, lack of mechanical stress in the work piece, low noise emission, and a smooth surface.

However, burning and charring are two main drawbacks of the laser cutting, leading to the reduction of the wood surface quality as well as reduction in a glued joint quality [6].

The quality of a wood surface, cut by laser, is primarily dependent on factors related to process parameters (cutting speed, laser beam power, type and pressure of the assisting gas jet and the focal point position), and also wood itself (moisture content, density, morphology, etc.) [7]. Numerous studies have been carried out to find out the mutual interaction of these factors on a cut surface quality. Branekov et al. [8] have investigated the effect of different focal point positions on the cut surface quality. A smooth surface with less charring was achieved when the focal point is at or slightly above the middle of the workpiece. Quintero et al. [9,10] demonstrated that a clean-cut quality with less roughness is a result of increasing the beam power. Lum et al. [11] reported that increase in feed speed increases the roughness of surface. Wood with relatively high moisture content cut by laser reduces feed speed [12–15]. McMillin & Harry [12] have reported that moisture in wood increases thermal conductivity resulting in considerable energy loss in the heating zone. Peters & Banas [16] have found that moisture content certainly decreases the yield of the process as compared to dry wood, however, cut quality was enhanced due to reduction in surface charring. Energy from laser beam breaks chemical bonds and therefore

<sup>\*</sup> Corresponding author.

E-mail address: [gaffmilan@gmail.com](mailto:gaffmilan@gmail.com) (M. Gaff).

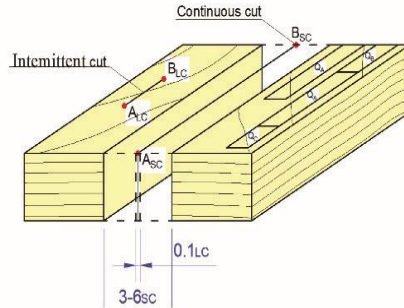


Fig. 1. Board and planks with different quality cut by laser (LC) and saw (SC).

disrupt the integrity of material. Hence, laser cutting is a type of thermo-chemical decomposition mechanism [11]. Despite several successful processes of laser cutting, laser machining of wood has not been accepted by wood industry.

It has long been investigated that the quality of a wood surface has a strong effect on wood bond quality. Influences of other factors on wood bond quality such as adhesive's types, wood species, and production process have been extensively covered by Pizzi [17] and Landrock & Ebnesajad [18]. The quality of the wood surface is affected by mechanical (cutting, sanding, and planing) and physical (drying) treatments prior to gluing. A poor bonding quality can be resulted from extremely rough surface [19]. The exact roughness value for optimal wood bonding is not yet identified [20,21]. Another issue for the formation of the poor bond is heat effects [22,23]. The heat of laser beam changes chemically the main components of wood (cellulose, hemicellulose and lignin), and also extractive substances. Lignin content reduces, and then demethoxylation takes place. Cellulose component under heat exposure degrades through its depolymerization and crystallization [24,25]. The manifestation of the monosaccharides instead of polysaccharides in the hemicellulose content implies its degradation and overall reduction [25].

There are a good number of studies concerning the surface quality of laser-cut wood but information on glue bond performance of laser-cut wood is very scanty [26]. The aim of this paper is to investigate the tensile shear strength of glued joints on laser cut surface and compared to those cut by a saw.

## 2. Experimental

### 2.1. Materials

The experiments were carried out on two wood species: Oak (*Quercus robur* L.) and European beech (*Fagus sylvatica* L.), harvested from the Vysočina region in the Czech Republic. Clear specimens of dimension of 110 mm × 25 mm × 4 mm (length × width × thickness) were used in the study. The single-component water-proof polyvinyl acetate adhesive was used for gluing wood surfaces.

### 2.2. Methods

#### 2.2.1. Laser and circular saw cutting

Wood samples with 2 moisture content regimes (8% and above fiber saturation point), were cut by CO<sub>2</sub> laser machine. Moisture content of the samples was determined according to ISO 13061-1 [27]. Wood density was determined according to ISO 13061-2 [28]. The test specimens were cut from a plank using CO<sub>2</sub> laser (BLT WoodCut) with a cutting power of 5 kW and an average cutting speed of 3 m/min. Focal point of laser beam was set at 1/3 of sample thickness from top of the plank. Thickness of plank was the width of test samples (Fig. 2). Cutting width of laser beam was 0.3 mm. In case of circular saw, standard cutting parameters for hardwoods were used.

#### 2.2.2. Milling

The milling operation was carried out with a single-spindle milling machine (FVS) with STEFF 2034 power feeder (Maggi Technology, Certaldo, Italy). The machine parameters and cutter settings are:

##### Single-spindle milling machine FVS

- Input power (kW) 3.8
- Cutting speed (m/s) 20,
- Feed speed (m/min) 4,

##### Cutter head (Ø 125 mm)

- Clearance angle ( $\alpha$ ) 25°,
- Cutting angle of wedge ( $\beta$ ) 45°
- Rake angle ( $\gamma$ ) 15°,
- Cutting angle ( $\delta$ ) 75°,

The machining was performed with three two-edge processing shaper heads (Maximus, Czech Republic) each for one angle. The milling blades were made of steel (CSN 19855) with 0.7% carbon; 4.2%

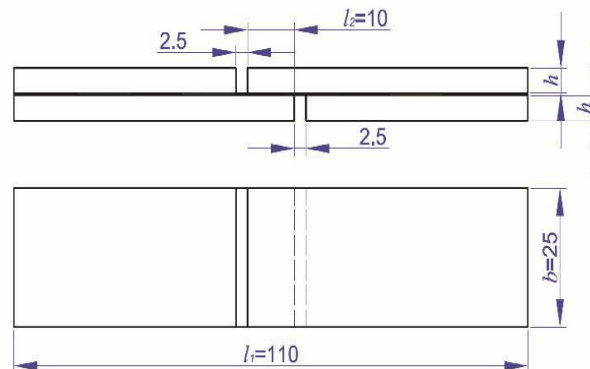


Fig. 2. Dimensions of test sample Note:  $l_1$  – sample length (mm),  $l_2$  – shear area length (mm),  $b$  – sample width/shear area width (mm),  $h$  – lamella thickness (mm).

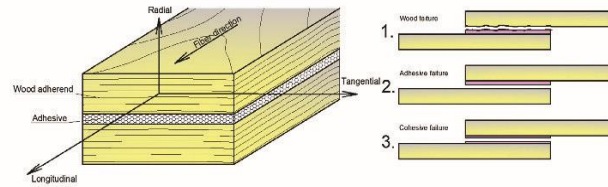


Fig. 3. Definition of Bond line Components and type of failure.

**Table 1**  
Mean values of measured parameters for samples cut by saw (SC) and laser (LC).

Cutting method	WS	W (%)	$f_v$ (Mpa)	$R_a$ ( $\mu\text{m}$ )	$W_a$ ( $\mu\text{m}$ )	Density ( $\text{kg}/\text{m}^3$ )	N
SC	O	8	5.9 (23.8)	10.2 (11.28)	18.2 (20.81)	511 (2.37)	20
SC	B	8	11.9 (17.6)	6.8 (14.49)	8.4 (13.61)	683 (2.26)	20
LC	B	8	4.2 (23.1)	5.2 (9.6)	8.5 (11.5)	667 (2.9)	20
LC	O	8	2.2 (14.2)	6.5 (11.1)	26.6 (11.0)	638 (4.8)	20
LC	B	> FSP	7.9 (11.3)	6.2 (10.9)	7.8 (12.4)	662 (3.2)	20
LC	O	> FSP	5.4 (16.2)	4.5 (19.0)	10.4 (14.9)	787 (3.0)	20

O – Oak, B – Beech, Values in parentheses are coefficients of variation (CV) in %.

**Table 2**  
One-way ANOVA evaluation for interactions of monitored factors on tensile shear strength.

Cut by laser					
Monitored factor	Sum of squares	Degree of freedom	Variance	Fisher's F – Test	Significance level P
Intercept	1718.771	1	1718.771	928.2396	***
Interaction of monitored factors	285.424	3	95.141	51.3821	***
Error	124.060	67	1.852		
The respective model explains roughly 100% of the total sum of squares.					
Cut by laser					
Monitored factor	Sum of squares	Degree of freedom	Variance	Fisher's F – Test	Significance level P
Intercept	4774.222	1	4774.222	1487.797	***
Interaction of monitored factors	531.276	1	531.276	165.562	***
Error	186.117	58	3.209		
The respective model explains roughly 55.4% of the total sum of squares.					

\*\*\* – significant. The level of significance was accepted at  $P < 0.05$ .

**Table 3**  
ANOVA evaluation for interactions of defined factors on  $R_a$ .

Cut by laser					
Monitored factor	Sum of squares	Degree of freedom	Variance	Fisher's F – Test	Significance level P
Intercept	2039.681	1	2039.681	2369.004	***
Interaction of monitored factors	46.850	3	15.617	18.138	***
Error	54.242	63	0.861		
The respective model explains roughly 87.0% of the total sum of squares.					
Cut by laser					
Monitored factor	Sum of squares	Degree of freedom	Variance	Fisher's F – Test	Significance level P
Intercept	4351.479	1	4351.479	1521.692	***
Interaction of monitored factors	179.527	1	179.527	62.780	***
Error	165.859	58	2.860		
The respective model explains roughly 60.3% of the total sum of squares.					

\*\*\* – significant. The level of significance was accepted at  $P < 0.05$ .

chromium; 18% tungsten and 1.5% vanadium.

### 2.2.3. Roughness and waviness

Surface roughness ( $R_a$ ) and surface waviness ( $W_a$ ) measurements

were performed using a stylus type surface profilometer (Form Talysurf Intra 2, Leicester, UK). The instrument records the surface profile by measuring the height, width and shape of peaks and ridges on the machine surfaces. Average surface roughness ( $R_a$ ) measured as the

**Table 4**  
ANOVA evaluation for interactions of defined factors on Wa values on samples cut by laser.

Cut by laser					
Monitored factor	Sum of squares	Degree of freedom	Variance	Fisher's F - Test	Significance level P
Intercept	11567.11	1	11567.11	1176.163	***
Interaction of monitored factors	3664.36	3	1221.45	124.199	***
Error	619.58	63	9.83		
The respective model explains roughly 58.4% of the total sum of squares.					
Cut by laser					
Monitored factor	Sum of squares	Degree of freedom	Variance	Fisher's F - Test	Significance level P
Intercept	10585.17	1	10585.17	1160.483	***
Interaction of monitored factors	1445.00	1	1445.00	158.420	***
Error	529.04	58	9.12		
The respective model explains roughly 56.4% of the total sum of squares.					

NS - not significant, \*\*\* - significant. The level of significance was accepted at  $P < 0.05$ .

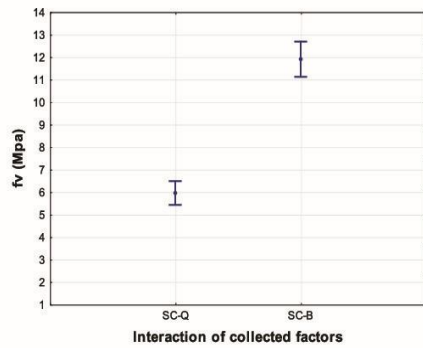


Fig. 4. Effect of the interaction of the monitored factors on tensile glue shear strength values- $f_v$  (MPa) cut by laser.

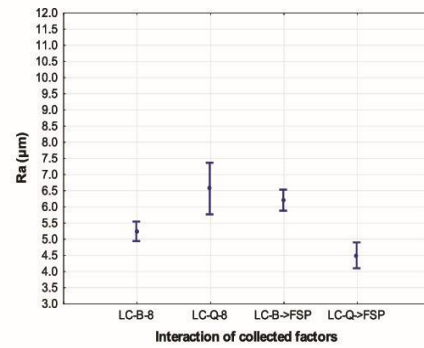


Fig. 6. Effect of the interaction of monitored factors on roughness values ( $R_a$ ) cut by laser.

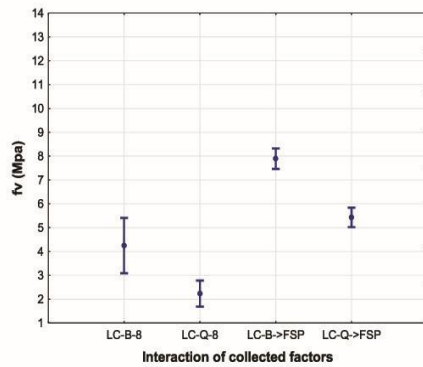


Fig. 5. Effect of the interaction of monitored factors on tensile shear strength values  $f_v$  (MPa) cut by saw.

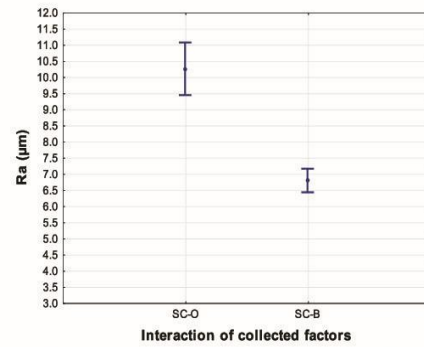


Fig. 7. Effect of the interaction of monitored factors on roughness values ( $R_a$ ) values cut by saw.

arithmetic averages of the absolute values of all the deviations of peaks and ridges from the mean. Waviness refers to the arithmetic mean deviation of the waviness profiles ( $W_a$ ) measured on the edge surface. The recorded surface profiles were processed in the connected computer and the values of  $R_a$  and  $W_a$  were displayed.

**2.2.4. Tensile shear strength (TSS)**

Adhesive was applied manually on the surface as a single-sided coating of  $150 \text{ g/m}^2$  to  $180 \text{ g/m}^2$ . Viscosity of used adhesive was 5000 to 7000 mPa s. The adhesive was applied on the wood surface and cold-pressed for 90 min. Samples were conditioned at  $65 \pm 3\% \text{ RH}$  and  $20 \pm 2 \text{ }^\circ\text{C}$  temperature to achieve an equilibrium moisture content

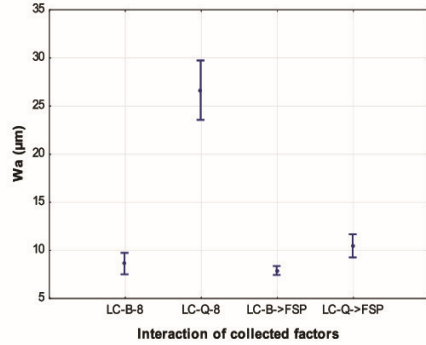


Fig. 8. Effect of the interaction of monitored factors on waviness values (Wa) cut by laser.

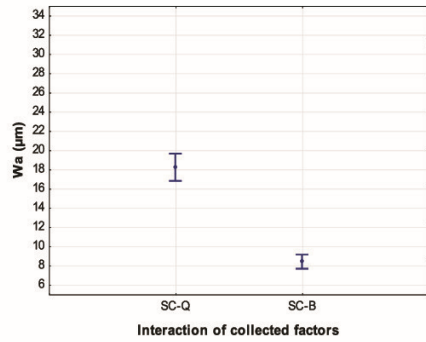


Fig. 9. Effect of the interaction of monitored factors on waviness values (Wa) cut by saw.

(EMC) of 12%. Tensile shear strength (TSS) was assessed using lap joint test according to EN 205 [28] (Fig. 2). Tensile-shear strength was determined using the universal testing machine UTS 50 (TIRA, Germany). A constant loading speed was set at  $5 \pm 0.5$  mm/min such that the time required to reach failure was between 30 s and 50 s. Maximum loading force was directly recorded into a computer.

2.3. Evaluation and calculation

The tensile-shear strength was calculated according to EN 205 [28] as per the following equation.

$$\tau = \frac{F_{max}}{l_2 \cdot b}$$

where  $\tau$  is the tensile-shear strength parallel to the fibers (MPa),  $F_{max}$  is the maximum loading force recorded at the breaking point (N),  $l_2$  is the length of the shear area (mm), and  $b$  is the width of the shear area (mm).

The shear bond strength values were evaluated using MANOVA, specifically utilizing Fisher's F-test in STATISTICA 13 software (Statsoft Inc., Tulsa, Oklahoma, USA). The results were evaluated using 95% confidence interval which reflects a significance level of 0.05 ( $P < 0.05$ ).

Table 5 Comparison of the effect of the interactions of monitored factors measured on samples cut by laser.

Tensile shear strength					
Method	Interaction of monitored factors	(1) 4.2465	(2) 2.2358	(3) 7.8898	(4) 5.4292
1	LC-B-8				
2	LC-Q-8	0.00			
3	LC-B- > FSP	0.00	0.00		
4	LC-Q- > FSP	0.01	0.00	0.00	
Ra (µm)					
Method	Interaction of monitored factors	(1) 5.21	(2) 6.54	(3) 6.18	(4) 4.47
1	LC-B-8				
2	LC-Q-8	0.000			
3	LC-B- > FSP	0.004	0.273		
4	LC-Q- > FSP	0.027	0.000	0.000	
Wa (µm)					
Method	Interaction of monitored factors	(1) 8.54	(2) 26.57	(3) 7.83	(4) 10.40
1	LC-B-8				
2	LC-Q-8	0.000			
3	LC-B- > FSP	0.521	0.000		
4	LC-Q- > FSP	0.097	0.000	0.030	

Table 6 Comparison of the effect of the interactions monitored factors measured on samples cut by saw.

Tensile shear strength values					
Method	Interaction of monitored factors	(1) 4.2465	(2) 2.2358		
1	SC-O				
2	SC-B		0.000		0.000
Ra (µm)					
Method	Interaction of monitored factors	(1) 10.246	(2) 6.7864		
1	SC-O				0.000
2	SC-B		0.000		
Wa (µm)					
Method	Interaction of monitored factors	(1) 18.190	(2) 8.3748		
1	SC-O				0.000
2	SC-B		0.000		

2.4. Categorization of type of failure

After tensile shear test, the failure occurred in the interface area of each sample was visually assessed. The failure analysis was done according to adhesive failure, wood failure and cohesive failure, as shown in Fig. 3. The failure occurred in the interface area of specimens cut by laser was compared to those cut by saw. Each failure was quantified based on the proportion of failure surface with respect to the total interface area.

2.5. Microscopy

Both the surface and the section of the glue lines were observed with a MIRA 3 electron microscope (Tescan Orsay Holding, Brno, Czech Republic) with a secondary electron detector operated at 15 kV acceleration voltage. The used working distance was 8 mm, and the spot size was 4 nm. The vacuum mode was set as follows: gun pressure,  $1 \times 10^{-8}$  Pa; column pressure,  $6 \times 10^{-4}$  Pa; chamber pressure,  $8 \times 10^{-2}$  Pa. The elemental compositions of the section of the glue line were examined by an energy dispersive spectroscopy system (Bruker XFlash X-ray detector, Karlsruhe, Germany, and ESPRIT 2 software).

**Table 7**  
Spearman's correlation for analyzed values and individual on samples cut by saw.

Variable	Interaction of monitored factors	<i>f<sub>v</sub></i> (MPa)	Ra (μm)	Wa (μm)	Density (kg/m <sup>3</sup> )
Interaction of monitored factors	1.000				
<i>f<sub>v</sub></i> (Mpa)	0.864	1.000			
Ra (μm)	-0.762	-0.724	1.000		
Wa (μm)	-0.853	-0.814	0.855	1.000	
Density (kg/m <sup>3</sup> )	0.866	0.754	-0.664	-0.801	1.000

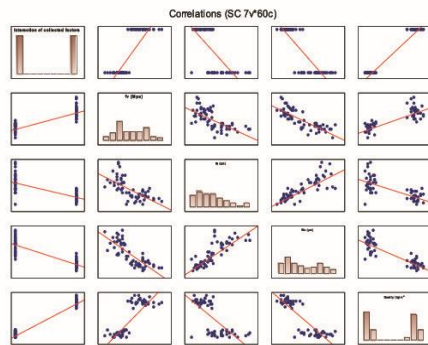


**Fig. 10.** Correlation matrix of the analyzed values and individual on samples cut by saw.

Hydrogen is not detectable by the method used.

**3. Results and discussion**

Monitored factors (MF), including moisture content, wood species (WS), and cutting methods with mean values of measured tensile shear strength (TSS) and average values of roughness (Ra) and waviness (Wa) are shown in Table 1.

Effect of all MF on TSS of samples cut by laser was analyzed and compared to those constituted of saw cut wood (Table 2). Based on one-way analysis, interaction of all MF had a statistically significant effect on TSS values of bond-line constituted of beech and oak samples cut by laser (BBL & BOL), as well as on TSS of bond-line constituted of beech and oak samples cut by saw (BBS and BOS).

One-way analysis data given in Table 3 indicates a statistically significant effect of interaction of all MF on Ra values of beech cut by laser (BL) and oak cut by laser (OL). In a similar way, Ra values of the beech cut by saw (BS) as well as oak cut by saw (OS) were also affected by interaction of all MF.

Influence of interaction of all MF on Wa values of BL and OL was proved by one-way analysis. The effect of all MF on Wa of BS and OS was also confirmed by one-way analysis. (Table 4).

Relationship between TSS of laser cut samples and the MF is shown in Fig. 4. Both wood species as well as moisture content of wood during laser cutting affected the TSS. At any particular moisture content, BL

**Table 8**  
Spearman's correlation for analyzed values and individual on samples cut by laser.

Variable	Interaction of monitored factors	<i>f<sub>v</sub></i> (Mpa)	Ra (μm)	Wa (μm)	Density (kg/m <sup>3</sup> )
Interaction of monitored factors	1.000				
<i>f<sub>v</sub></i> (Mpa)	0.371	1.000			
Ra (μm)	-0.355	-0.042	1.000		
Wa (μm)	-0.101	-0.660	0.220	1.000	
Density (kg/m <sup>3</sup> )	0.647	0.148	-0.529	-0.128	1.000

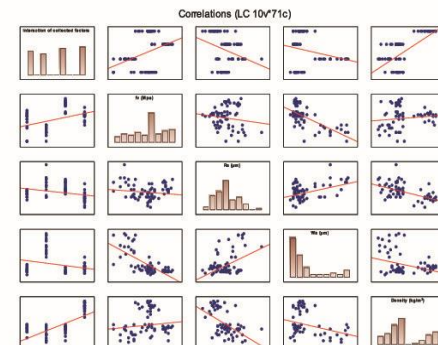


**Fig. 11.** Correlation matrix of monitored factors on measured tensile shear strength, and Ra and waviness of samples cut by laser.

samples exhibited higher TSS as compared to OL wood samples. BL samples at 8% moisture content had almost 90% higher TSS values as compared to OL samples. Similarly, the difference in TSS between both the wood species was about 46% in case of samples laser cut at moisture content above FSP. The highest TSS value (7.8 MPa) among all sets of the MF belongs to beech wood cut with a moisture content above FSP, while the lowest value belongs to oak wood (2.3 MPa) cut at a moisture content of 8%.

Moisture content of wood during laser cutting was also found to have very significant effect on the TSS of bondline irrespective of the species (Fig. 4). Samples, with moisture content above FSP, when laser cut, offered a stronger TSS than samples laser cut at 8% moisture content. The improvement in the TSS values between both the two moisture content regimes was 88% in case of beech wood samples and 145% in case of oak wood samples. Results pertaining to TSS on saw cut samples are depicted in Fig. 5. Saw cut was performed only on wood samples having 8% moisture content. Similar to laser cutting, beech wood samples exhibited significantly higher TSS as compared to oak wood and the difference was almost two times. When compared with the laser cut samples, the TSS values obtained on saw cut samples were significantly higher in both the species. Laser cutting caused 65% reduction in TSS on beech wood samples while the reduction was about 63% on Oak wood samples as compared to the saw cut samples. Similar results have been reported in the literature [29]. The authors reported 75.3% decrease in the glue bond strength on laser cut samples without

**Table 9**  
Samples (%) with different types of failures observed in the interface area.

Monitored factors	Categorization				
			(1)	(2)	(3)
Cutting method	WS	W (%)	Samples with adhesive failure (%)	Samples with wood failure (%)	Samples with cohesive failure (%)
LC	B	8	100	0	
LC	Q	8	93.4	0	6.6
LC	B	> FSP	100	0	0
LC	Q	> FSP	100	0	0
Cutting method	WS	W (%)	Samples with adhesive failure (%)	Samples with wood failure (%)	Samples with cohesive failure (%)
SC	Q	8	18.3	81.7	0
SC	B	8	26.7	73.3	0

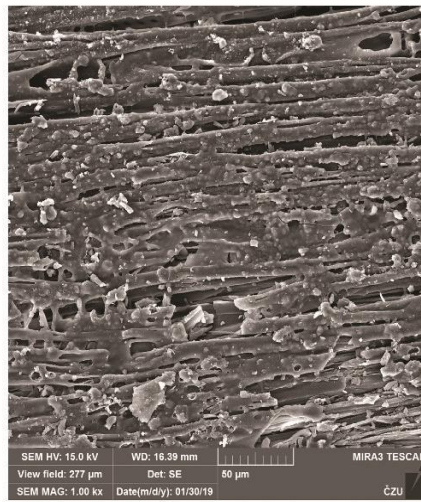


**Fig. 12a.** Surface of oak wood cut with a laser at 8% moisture content.

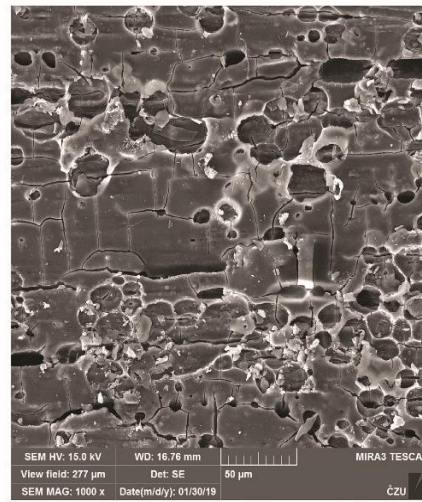


**Fig. 12b.** Surface of oak wood cut with a laser at maximum moisture content.

sanding as compared to saw cut samples. Sanding of the cut surfaces prior to gluing improved the bond strength significantly, although, it was still substantially lower (34.5%) as compared to saw cut samples. In order to find out the plausible reasons for poor TSS on laser cut samples, further analysis on surface quality, interface failure and microscopic observation of laser cut surfaces were performed.

Ra and Wa are the two important parameters of surface quality. Effect of laser cutting on the Ra was different on both the species at any particular moisture content (Fig. 6). While, it is not logical to compare the Ra of the two species (beech and oak) as the cellular composition, particularly the size and distribution of pores which also contributes to Ra, are different for both the species, the purpose of comparison was to assess the efficacy of laser cutting in providing a better surface. The Ra values of oak wood samples laser cut at 8% moisture content was 20% higher than the Ra of beech wood samples laser cut at same moisture content. However, the observations on Ra were completely opposite with oak wood having 27% lower roughness than beech wood when samples were laser cut at moisture content above FSP. The results also indicate a variable effect of moisture content on the surface quality of

laser cut wood. Ra of oak wood was reduced significantly (30%) while that of beech wood marginally increased (18%) as compared to the Ra of samples laser cut at 8% moisture content. Fig. 7, as a reference, shows the relation between the MF and the Ra of saw cut samples. The Ra of saw cut beech wood was lower than that of oak wood and the reason being the fine wood texture of beech wood over oak wood. Similar trend has been reported in the literature [29]. Comparison of two cutting methods suggest that, the surface resulted from laser cut has a lower roughness, as compared to the saw cut surface. The reduction in Ra due to laser cut was more prominent in oak (36%), a coarse texture wood than the beech (24%) which is a fine textured wood.

Ra is considered as a secondary factor (adhesive's type, wood species, processing parameters, etc.), contributing to a glue bond performance. To elucidate this contribution, the resulted data from Ra were compared to resulted data from TSS in the case of laser and saw cuts. It seemed that the rougher surface in the samples cut by saw provided higher TSS, while less roughness provided lower TSS in the samples cut by laser. This can be described by mechanical interlocking theory [30,31]. Rougher surface allows more adhesive penetration into wood,

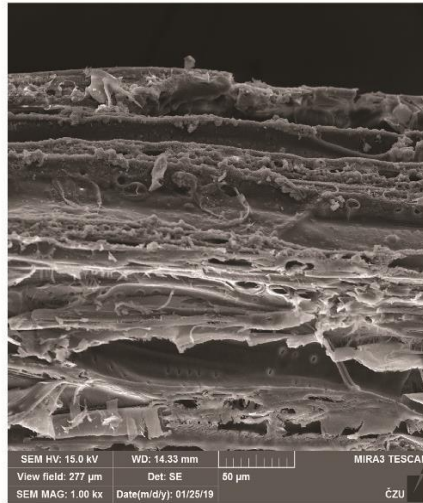


Fig. 13a. Cross section of joint after joint failure – beech specimen cut with laser

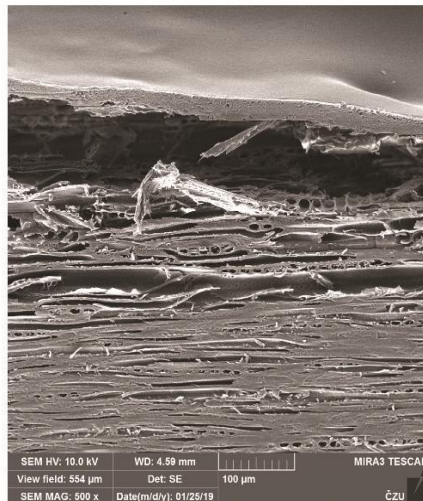


Fig. 13b. Cross section of joint after joint failure – oak specimen cut with laser.

leading to increase in surface area and glue bond strength [32,33]. Another remarkable issue probably is that micro-cracks were covered by cured adhesive on wood surface, resulting in increasing glued bond strength [33]. However, good bond strength can also be achieved on less rough surfaces with low adhesive penetration. It is noticeable to mention that the resulted data from Ra is different when comparing two species (Beech & oak) with one type of cutting method (saw or laser). The lower value of Ra, the higher tensile shear strength of samples cut

by saw was achieved. The similar trend was also found between two species when samples cut by laser. Thus, the quantity of Ra in regards to TSS was varied when comparison was made between samples with the same cutting method and different cutting method. Based on the variations, it can be argued that rougher or smoother surface did not play an important role in resulted low shear strength on samples cut by laser. Probably, other potential factors play a significant role in reduction of the shear strength.

The effect of the MF on the surface waviness of laser cut samples is shown in Fig. 8. The waviness values were lower for beech wood as compared to oak wood at both the moisture regimes. Moisture content of wood during laser cutting has a significant effect on the surface waviness. Laser cutting of greenwood (above FSP moisture content) resulted in significant decrease in surface waviness as compared to laser cutting of dry wood (8% moisture content) and the reduction was more pronounced in oak (61%), a coarse textured wood as compared to beech (8%), a fine textured wood. The results pertaining to the surface waviness of saw cut samples are shown in Fig. 9. Like laser cutting, surface waviness of oak is also higher than that of beech wood in saw cutting. While the waviness values of both the cutting methods were almost similar in beech wood samples, the waviness values were significantly lower (32%) in saw cut oak samples than laser cut samples.

Tables 5 and 6 illustrates statistical relationship between the MF and the analyzed characteristics of the samples cut by laser and saw. It is clear from Table 5 that there is a statistically significant difference between the MF and analyzed characteristics of samples cut by laser. However, there is not a statistically significant difference between the waviness values of the BL with a moisture of 8% and the OL with a moisture above the FSP. Also, the analysis of the waviness values between the BL with a moisture of 8% and the BL with a moisture above the FSP showed no statistically significant difference. It is obvious from the data in the Table 6 that there is a statistically significant different between the MF and analyzed characteristics of the samples cut by saw.

The results provided in Table 7 show numerous high degrees of dependence between the MF and the analyzed characteristics of the samples after saw-cut. Further, the degrees of dependence between the analyzed characteristics is also provided. All the characteristics affect the glue shear strength. While density affects the glue shear strength positively, Ra and surface waviness affect the TSS negatively. Fig. 10 shows the upward/downward trend occurred between the MF and the analyzed characteristics of the samples after saw cut.

The degree of dependence between the MF and the analyzed characteristics of the samples after laser-cut was considerably lower as compared to those of saw cut (Table 8). There is a relatively high degree of dependence only between waviness and TSS as well as Ra and density in the samples cut by laser. Fig. 11 shows the upward/downward trend occurred between the MF and the analyzed characteristics of the samples after laser-cut.

#### 4. Categorization of type of failure

The results pertaining to failure occurred in the interface area of specimens is shown in Table 9. It is evident from the table that the failure in the interface was due to adhesive, cohesive or wood failure. It is obvious from the table that adhesive failure is the most common failure type in laser cut samples followed by cohesive failure irrespective of the species studied. Further, adhesive failure in both the species was most prevalent than cohesive failure on samples laser cut at higher moisture content (above FSP) than samples cut at lower moisture content. None of the laser cut samples failed due to wood failure. Analysis of failure type on saw cut samples indicate quite contrasting results. Barely 10% of the saw cut samples failed due to adhesive failure while majority of the samples failed due to wood failure irrespective of the wood species. Adhesive failure on laser cut samples suggests poor bonding between wood surface and the adhesive.

Laser cutting of wood is accomplished by degradation of chemical

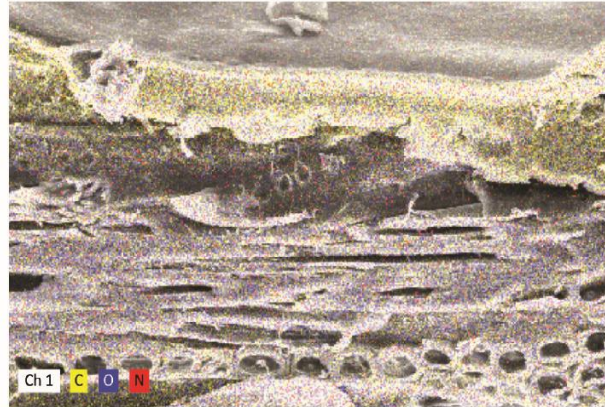


Fig. 14. Elemental analysis of the glued joint after failure – Beech wood specimen.

bonds due to the thermal effect [6]. On exposure to laser beam, wood constituents are burned in the cut zone and the resulting ash is blown out causing separation of wood elements [34,35]. Thermal degradation effect of laser can penetrate to certain depths on the cut surface and this may weaken the bonding between the wood elements resulting in loosely held surface [6]. This is quite apparent from microscopic analysis (Figs. 12a and 12b). Chemical degradation on the surface may change the hydrophilic nature of the wood which in turn might interfere adhesive bonding. Generation of ash during laser cutting might also plug the pores causing improper resin penetration into the wood and this was evident from the elemental analysis of the glued joints (see below). A cumulative effect of all these factors might be responsible for poor bonding between wood and the adhesive resulting in adhesive failure in laser cut samples. On contrary, saw cutting does not induce any chemical degradation on the wood surface and hence the bonding between the wood and adhesive was quite stable resulting in maximum wood failure and minimum adhesive failure in glue shear test.

Figs. 12a and 12b show the surface of oak specimens cut with a laser while observing the effect of the moisture content of the cut specimen. In both cases, the carbonization of the surface caused by the high temperature laser is visible. Higher surface degradation is visible in the specimen cut at lower moisture content.

Figs. 13a and 13b show the nature of the joint failure. The figures show that the failure occurred in the charred layer of the wood. Unfortunately, the charred layer is not as strong as solid wood, and the resulting strength of the glued joints was therefore lower than that of joints cut with a circular saw. The depth of degradation on the sample cross section due to laser cutting can also be observed in both the figures. About 75–100  $\mu\text{m}$  thick layer of wood from the surface appears to be degraded due to the thermal effect of laser.

The elemental analysis in Fig. 14 demonstrates the depth of penetration of the adhesive. The PVAc adhesive used has the same elemental composition as the wood, so the contrast between the wood and glue is not so prominent. However, there is a noticeable difference in the concentrations of individual elements in the wood and in the adhesive, with a higher carbon content in the PVAc adhesive. The figure shows that the glue did not penetrate the charred wood.

## 5. Conclusions

1. Gluing properties of the samples cut by laser was analyzed. It's concluded that the tensile shear strength of the samples cut by laser

was lower than those cut by saw.

2. Surface quality of the samples cut by laser was investigated. A greater roughness was resulted from samples cut by saw in comparison to those cut by laser.
3. Failure of the glued joint in specimens cut with a laser occurred in the charred layer, which is not as strong as solid wood.
4. Degradation effect of laser was more pronounced in dry wood (8% moisture content) as compared wood cut at higher moisture content (more than FSP).
5. Laser cut samples failed due to adhesive failure while saw cut samples failed due to wood failure.

## Acknowledgments

The authors are grateful for the support of “Advanced research supporting the forestry and wood-processing sectors adaptation to global change and the 4th industrial revolution”, No. CZ.02.1.01/0.0/0.0/16\_019/0000803 financed by OP RDE“ and for the support of the University-wide Internal Grant Agency (CIGA) of the Faculty of Forestry and Wood Sciences at Czech University of Life Sciences Prague, project 2016 – 4308.

## Appendix A. Supplementary data

Supplementary data to this article can be found online at <https://doi.org/10.1016/j.compstruct.2019.111679>.

## References

- [1] Powell J. CO<sub>2</sub> laser cutting. New York: Springer; 1993.
- [2] Belforte DA. Non-metal cutting. *Ind Laser Rev* 1998;13(9):11–3.
- [3] Pires MC, et al. Plywood inlays through CO<sub>2</sub> laser cutting. CO<sub>2</sub> laser and applications. *SPIE Proceedings* 1989;1042:97–102.
- [4] Barcikowski S, Koch G, Odermatt J. “Characterization and modification of the heat affected zone during laser material processing of wood and wood composites”. *Holz als Roh – und Werkstoff* 2006;64(2):94–103.
- [5] Pires MC, Araújo JL, Teixeira MR, Rodrigues FC. “Plywood inlays through CO<sub>2</sub> laser cutting. CO<sub>2</sub> laser and applications. *SPIE Proceedings* 1989;1042:97–102.
- [6] Martínez-Condé A, Krenke T, Frybort S, Müller U. Review: Comparative analysis of CO<sub>2</sub> laser and conventional sawing for cutting of lumber and wood-based materials. *Wood Sci Technol* 2017;51:943–66.
- [7] Pili H, Hirvimäki M, Salminen A. (2009). “Repeatability of laser cutting of uncoated and coated boards.” In: *Nolamp*, 24-26.8 2009, Copenhagen Denmark.
- [8] Barnekov VG, McMillin CV, Huber HA. Factors influencing laser cutting of wood. *For Prod J* 1986;36(1):55–8.
- [9] Quintero F, Riveiro A, Lusquiños F, Comesaña R, Pou J. CO<sub>2</sub> laser cutting of

- phenolic resin boards. *J Mater Process Technol* 2011;21(11):1710-8.
- [10] Quintero F, Riveiro A, Lusiños F, Gomesaño R, Pou J, et al. Feasibility study on the laser cutting of phenolic resin boards. *Phys Procedia* 2011;12:578-83.
- [11] Lum KCP, Ng SL, Black I. Determination of process parameter setting. *Opt Laser Technol* 2000;32(1):67-76.
- [12] McMillin CW, Harry JE. Laser machining of southern pine. *For Prod J* 1971;21(10):34-7.
- [13] Peters CC, Marshall HL. Cutting wood materials by laser. *US For Prod Lab Res Pap* 1975.
- [14] Li L, Mazumder J. A study of the mechanism of laser cutting of wood. *For Prod J* 1991;41(10):53-9.
- [15] Powell J. *CO<sub>2</sub> Laser cutting*. 2nd edn. London: Springer; 1998.
- [16] Peters CC, Barnes CM. Cutting wood and wood-base products with a multikilowatt CO<sub>2</sub> laser. *Forest Prod J* 1977;27(11):41-5.
- [17] Pizzi A, Mittal KL. *Handbook of adhesive technology*. 2nd edition New York, Basel: Marcel Dekker Inc; 2003. p. 61-100.
- [18] Landrock AH, Ebneshajad S. *Adhesive technology handbook*. 2nd edition, Nourwich, New York: William Andrew Inc; 2008. p. 11-24p.
- [19] Marra AA. *Technology of Wood Bonding: Principles in Practice*. New York: Van Nostrand Reinhold; 1992. p. 153-233p.
- [20] Neese J, Reeb J, Funck J. Relating traditional Ra measures to gluebond quality in plywood. *Forest Prod J* 2004;54:67-73.
- [21] Aydın I. Activation of wood surfaces for glue bonds by mechanical pre-treatment and its effects on some properties of veneer surfaces and plywood panels. *Appl Surface Sci* 2004;233:268-74.
- [22] Christiansen AW. How overdrying wood reduces its bonding to phenol-formaldehyde adhesives - A critical review of the literature I Physical responses. *Wood Fiber Sci* 1990;22:441-59.
- [23] Christiansen AW. How overdrying wood reduces its bonding to phenol-formaldehyde adhesives: a critical review of the literature. Part II. Chemical reactions. *Wood Fiber Sci* 1991;23:69-84.
- [24] Polettoab M, Zatterab AJ, Forte MMC, Santanaa RMC. Thermal decomposition of wood: Influence of wood components' and cellulose crystallite size. *Bioresour Technol* 2012;109:148-53.
- [25] Özgeçen Ö, Durmaz S, Boyacı IH, Eksi-Kocak H. Determination of chemical changes in heat-treated wood using ATR-FTIR and FT Raman spectrometry. *Spectrochim Acta Part A Mol Biomol Spectrosc* 2017;171:395-400.
- [26] Kačík F, Šmíra P, Kačíková D, Velková V, Nasswetrová A, Vacek V. Chemical alterations of pine wood saccharides during heat sterilisation. *Carbohydr Polym* 2015;117:681-6.
- [27] Rabiej RJ, Ramrattan SN, Droll WJ. Gluing shear strength of laser-cut wood. *Forest Prod J* 1993;43(2):45-54.
- [28] **ISO 13061-1 (2014): Physical and mechanical properties of wood - Test methods for small clear wood specimens - Part 1: Determination of moisture content for physical and mechanical tests.**
- [29] **EN 205 (2003): Adhesive for load-bearing timber structures - Test methods - Part I: determination of longitudinal tensile shear strength.**
- [30] Thoma H, Peri L, Lato E. Evaluation of wood surface roughness depending on species characteristics. *Maderas. Ciencia y tecnología* 2015;17(2):285-92.
- [31] Pizzi A, Mittal KL. *Handbook of adhesive technology*. New York: Marcel Dekker; 2003.
- [32] Rahayu I, Darmawan W, Nugroho N, Marchal R. The effect of jaban veneer quality on laminated veneer lumber glue bond and bending strength. *J Ilmu Teknol Kayu Tropis* 2015;13(2).
- [33] **Gent, A., and Lai, S. Adhesion and autohesion of rubber compounds: Effect of Ra. Rubber Chem. Technol. 68, 13-25.**
- [34] Kamke FA, Lee JN. Adhesive penetration in wood- a review. *Wood Fiber Sci* 2005;39(2):205-20.
- [35] Poccorní J, Powell J, Ilar T, Schwarz A, Kaplan AFH. (2013). **Measuring the state-of-the-art in laser cut quality. In-14th Nordic Laser Materials Processing (NOLAMP) Conference held at Gothenburg, Sweden.**

---

## 6.2 Surface quality measurement by contact and laser methods on thermally modified spruce wood after plain milling

**Published as:**

**Fatemeh Rezaei**, Milan Gaff, Anil Kumar Sethy, Peter Niemz, Gourav Kamboj, Gianluca Ditommaso, Roberto Corleto, Sumanta Das, and Miroslav Gašparík. "Surface quality measurement by contact and laser methods on thermally modified spruce wood after plain milling." *The International Journal of Advanced Manufacturing Technology* 110, no. 5 (2020): 1653-1663. DOI:10.1007/s00170-020-05983-7.



## Surface quality measurement by contact and laser methods on thermally modified spruce wood after plain milling

Fatemeh Rzaei<sup>1</sup> · Milan Gaff<sup>1</sup> · Anil Kumar Sethy<sup>1</sup> · Peter Niemz<sup>1</sup> · Gourav Kamboj<sup>1</sup> · Gianluca Ditommaso<sup>1</sup> · Roberto Corleto<sup>1</sup> · Sumanta Das<sup>1</sup> · Miroslav Gašparík<sup>1</sup>

Received: 12 May 2020 / Accepted: 20 August 2020 / Published online: 27 August 2020  
© Springer-Verlag London Ltd., part of Springer Nature 2020

### Abstract

The accuracy and reliability of a measuring device is crucial to determine the quality of wood surface. This paper compares the surface quality of thermally modified spruce wood measured by two different methods. Spruce wood specimens were thermally modified at different temperatures (160, 180, and 210 °C) and then milled with a single-spindle milling machine operated at different combinations of processing parameters (cutting speed, rake angle, and feed rate). Surface quality (surface roughness and surface waviness) of the specimens were measured by laser as well as contact method. Higher values of surface roughness and waviness were obtained by the laser method compared with the contact method. Average surface roughness was 31% higher, while average waviness was 35% higher in laser method as compared with the contact method. Based on the surface quality obtained by laser method and energy consumption during milling, the optimum combination of parameters for milling of thermally modified spruce wood was ascertained. The best surface quality with lower energy consumption during machining was obtained in spruce wood thermally modified at 210 °C and processed at a cutting speed of 20 m/s, rake angle of 20°, and a feed rate of 4 m/min.

**Keywords** Spruce · Laser method · Contact method · Surface quality · Thermal modification · Energy consumption

### 1 Introduction

The surface quality of wood is one of the important parameters in wood processing as it affects the aesthetics from a macroscopic perspective to the coating and gluing process from microscopic and functional aspects [1]. While outer appearance is necessary to attract customers, a quality surface on machined wood is a prerequisite to ensure optimal use of coatings and improved coating performance. Performance of a wood-adhesive bond is also correlated with the characteristics of wood surfaces [2]. Mechanical surface preparation techniques such as planing and sanding can have significant influence on the performance of wood-adhesive bond [3]. Extreme rough wood surfaces cause poor bonding

performance by the overpenetration of resin into the rough areas [4]. In spite of the known effect of surface quality on glue bond strength, information on the exact roughness value for optimal wood bonding is still uncertain [5, 6].

Surface quality is quantitatively represented in terms of surface roughness and waviness. While roughness refers to microscopic irregularities, waviness indicates macroscopic irregularities on the wood surface [7, 8]. Procedures for surface quality assessment and energy consumption during milling are well-established in metal processing industry using Taguchi design [9, 10]. However, in wood processing industry, the knowledge is still developing. Different methods of measurement have been reported in the literature for surface roughness, and every method has its own advantages and disadvantages in terms of accuracy, complexity, and cost. The most common and easiest method is the ocular inspection; however, the method is very subjective and depends on the experience of the person [11]. Visio-tactile assessment is a basic method [12, 13], while a stylus profilometer is the most commonly used method in laboratories [14, 15]. Although the accuracy of the stylus profilometer method has been proven by several researchers [1, 16], about 10% error on surface

✉ Anil Kumar Sethy  
sethyanil@gmail.com

<sup>1</sup> Department of Wood Processing and Biomaterials, Faculty of Forestry and Wood Sciences, Czech University of Life Sciences Prague, Kamýcká 1176, Prague 6, 16521 Suchbát, Czech Republic

roughness of softwood species has been reported for this method [17]. Moreover, variation in the wood surface due to the anatomical structures makes the use of stylus profiler complicated [11].

The ideal method for assessing surface quality can be a noncontact method with no physical interaction between the sensor and the wood surface [18]. In this context, the use of optical profilometer has been stressed by various researchers [19, 20]. Lundberg and Porankiewicz [9] performed surface roughness measurement on limited number of samples using two optical noncontact methods and correlated the result with that obtained by contact stylus profiler. Laser method was found to measure the surface roughness with sufficient accuracy. Sandak and Tanaka [18] compared the roughness profile obtained by a contact stylus with a laser displacement sensor and reported that the accuracy of laser displacement sensor depends on color and density of wood, position of the sensor, and profile shape. Costes and Larricq [21] used optical roughness device for assessment of surface quality following high-speed cutting and reported superior surface quality with increasing cutting speed. Although, there have been a quite good number of studies on the surface quality assessment of wood and wood-based products by various methods, comparative study on the relative accuracy of contact and noncontact method is very limited.

Inherent material character, tools used, and the processes followed during machining greatly influence the surface quality of wood and energy consumption during milling. Energy consumption during wood milling is important as it adds to the price of the processed wood [22]. Studies show that power consumption and surface quality are hugely affected by wood density and wood anatomy [23, 24]. Davim [25] explained that, although increasing cutting speed is greatly useful for surface quality, an increase in the cutting speed induces tool wear, resulting in higher power consumption. Hence, the tools and machining parameters to be used for milling wood need optimization.

Thermal modification of wood is gaining commercial importance, and thermally modified wood is becoming more popular over traditional preservative treated wood. However, from a material point of view, the properties of thermally modified wood are different to that of unmodified wood [26]. Thermal modification is energy intensive, while machining of thermally modified wood has been reported as less energy demanding compared with unmodified wood [27, 28]. Machining of thermally modified wood has been reported to produce more dust as compared with unmodified wood. Optimizing milling parameters for thermally modified wood is necessary to obtain superior surface quality with minimum energy consumption [29, 30]. This paper establishes the effect of machining parameters such as cutting speed, feed rate, and rake angle on the surface quality of milled spruce wood measured by both contact and laser methods. Power consumption

during milling was also measured. Based on the surface quality values, obtained by the most accurate method, and energy consumption during milling, the optimum combination of machine parameters for milling of spruce wood has also been suggested.

## 2 Material and method

### 2.1 Material

Norway spruce (*Picea abies* L.) was selected due to its wide applicability for construction purposes. This species was collected from the Vysocina forest in the Czech Republic. Samples of 100 mm (width) × 20 mm (thickness) and 200 mm length along the grain were used in this study. A total of 108 samples were prepared for this study.

### 2.2 Experimental methods

#### 2.2.1 Thermal modification

Spruce wood samples were thermally modified in an open-system thermal chamber (S400/03, LAC Ltd., Czech Republic). The process consisted of three stages based on the ThermoWood® method prescribed by the ITA, Finland. The first stage involves a gradual increase in temperature to the desired level (160 °C, 180 °C, or 210 °C). In the second stage, the desired temperature was maintained for a period of 3 h. The third and final stage involves gradual cooling and conditioning of the samples to a moisture content of 5–7%.

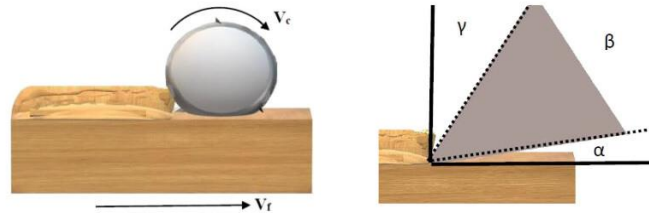
#### 2.2.2 Milling

Milling was performed by a single-spindle milling machine (FVS) containing feeder STEFF 2034 (Maggi Technology, Italy). The processing parameters used for the milling operation were cutting speed (m/s), 20, 30, and 40; feed rate (m/min), 4, 8, and 11; clearance angle ( $\alpha$ ), 30°, 25°, and 20°; wedge angle ( $\beta$ ), 45°; rake angle ( $\gamma$ ), 15°, 20°, and 25° (Fig. 1); and input power (kW), 3.8. Three two-edge processing shaper heads (Maximus, Czech Republic) were used. The milling blades were of steel and composed of 0.7% carbon, 4.2% chromium, 18% tungsten, and 1.5% vanadium. The thickness of material removed during the entire milling process was 1 mm.

#### 2.2.3 Roughness and waviness measurement

Surface roughness ( $R_a$ ) is the measurement of fine irregularities, i.e., small peaks and ridges found on the surface of the processed sample and measured as the mean deviation from

**Fig. 1** Configuration of cutting angles during the milling operation,  $\alpha$ , clearance angle;  $\beta$ , wedge angle;  $\gamma$ , rake angle.  $V_c$  stands for cutting speed and  $V_f$  stands for feed rate



the nominal surface. Waviness ( $W_a$ ) are widely spaced surface irregularities having greater sampling length than roughness and measured on the surface of the sample. For surface quality measurement, each sample was divided into 5 segments, leaving 1 cm from both ends. Then, each segment was further divided into 2 identical parts with 6-mm gap in between.

Surface profile measurements were carried out by two different methods, i.e., a contact and contactless (laser) method (Fig. 2). In the contact method, the surface profiles were measured using a contact tool (Form Talysurf 50 Intra) with a 50-mm horizontal measurement range with a tip radius of 2  $\mu\text{m}$ . Its straightness deviation per 50 mm is 0.4  $\mu\text{m}$ , and the measurement error is  $\pm 2\%$ . The contactless (laser) measurement of the surface profile was carried out using an Olympus laser microscope. Its semiconductor laser has a light source of 405 nm, and the measurement accuracy was  $\pm 2\%$ . It is necessary to mention that the settings of both devices (contact and contactless) were identical based on the standards [31, 32].

#### 2.2.4 Measurement of cutting power

The power consumption during milling was measured by a computerized digital power meter MI 2392 Power Q Plus (Metrel d.d., Slovenia) in both working and idle state. The measurements were recorded automatically by the computer

connected to it at a 1-s interval. The average cutting power was the difference between the total cutting power and the idling power.

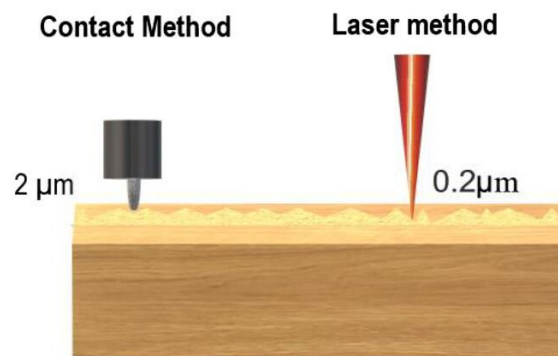
#### 2.2.5 Statistical analysis

The results were analyzed with a four-factor analysis of variance using Statistica (Tibco Software Inc.). The analysis evaluates the effect of each factor on the used characteristics. Based on the  $P$  value, it determined whether a factor affected the evaluated characteristics or not. Diagrams were made for 95% confidence levels, and the results were verified with Duncan's test.

#### 2.2.6 Value analysis for optimization of machining parameters

The combination of milling parameters (cutting speed, rake angle, and feeding rate) on thermally modified spruce is considered optimum when the milling process results in superior surface quality (lower  $R_a$  and  $W_a$ ) with lower energy consumption. In order to achieve this level, the resulting values of  $R_a$ ,  $W_a$ , and energy consumption were sorted according to their weights. Their ranks were then combined and further sorted to display the best combination of milling parameters for processing thermally modified spruce wood.

**Fig. 2** Diameter of laser tip (0.2  $\mu\text{m}$ ) and contact tip (2  $\mu\text{m}$ )



### 3 Results and discussion

#### 3.1 Effect of milling parameters on surface quality and cutting power

The effects of milling parameters and thermal modification on the surface roughness and waviness (Ra, Wa), obtained by the contact method as well as the laser method, are shown in Table 1 and Table 2, respectively. Ra values obtained by the contact method were significantly affected by all factors ( $p < 0.05$ ) except the rake angle (Table 1), whereas Ra values obtained by the contactless method (laser) were affected by all processing factors except modification temperature (Table 2). Waviness values obtained by the contact method were found to be significantly affected by all processing factors except cutting speed (Table 1). On the contrary, when the waviness profile was measured using the laser method, only the feed rate was found to have a significant effect on it (Table 2).

#### 3.2 Cutting speed

The statistical relationship between cutting speed and surface quality of spruce (Ra and Wa) resulting from the contact and laser methods is depicted in Fig. 3 and Fig. 4. Ra values decreased as cutting speed increased, and the trends are consistent for both contact and laser methods. However, it is to be noted that the Ra values obtained by the laser method were

higher than the Ra values obtained by the contact method at each level of cutting speed. The reason for this is the effective penetration of the laser into minute crevices smaller than the diameter of the stylus, which is inaccessible by the tip of the stylus. This indicates a greater resolution of roughness measurement by the laser method. Gašparik and Gaff [33] reported a reduction in average surface roughness with increasing cutting speed. At higher cutting speed, the number of teeth passing frequency increased, resulting in shorter thickness of the chip [34]. Sütçü and Karagöz [35] demonstrated a rougher surface in an MDF panel as a consequence of decreasing spindle speed of the CNC machine.

The surface waviness value was found to decrease with an increase in cutting speed; however, unlike the Ra, the variation in the Wa due to an increase in cutting speed is minimal. Wa values ranged between 6.0 and 6.25  $\mu\text{m}$  with the contact measurement, while they were between 7.75 and 8.4  $\mu\text{m}$  with the laser method. Like the Ra, the values of Wa obtained by the laser method were significantly higher than those measured with the contact method at each level of cutting speed. Similar findings have been reported in earlier studies [36, 37].

#### 3.3 Rake angle

The influence of the rake angle on surface quality (Wa and Ra) of spruce wood as measured by the contact and laser methods is shown in Fig. 5 and Fig. 6, respectively. Ra values of

**Table 1** Statistical analysis of the effect of processing parameters on surface quality of spruce wood measured by contact method

Surface waviness ( $\mu\text{m}$ )					
Factors	Sum of squares	Degree of freedom	Variance	F value	Level of significance
Intercept	39,808.58	1	39,808.58	1174.825	***
Cutting speed (m/s) (1)	18.56	2	9.28	0.274	NS
Rake angle ( $^\circ$ ) (2)	647.57	2	323.79	9.556	***
Feed rate (m/min) (3)	304.14	2	152.07	4.488	***
Treatment temperature ( $^\circ\text{C}$ ) (4)	517.54	3	172.51	5.091	***
1 * 2 * 3 * 4	2489.16	24	103.71	3.061	***
Error	32,935.91	972	33.88		
The respective model explains 57.3% of the total sum of squares					
Surface roughness ( $\mu\text{m}$ )					
Intercept	24,195.13	1	24,195.13	7149.685	***
Cutting speed (m/s) (1)	64.96	2	32.48	9.597	***
Rake angle ( $^\circ$ ) (2)	13.28	2	6.64	1.963	NS
Feed rate (m/min) (3)	205.18	2	102.59	30.315	***
Treatment temperature ( $^\circ\text{C}$ ) (4)	44.98	3	14.99	4.430	***
1 * 2 * 3 * 4	393.19	24	16.38	4.841	***
Error	3289.33	972	3.38		
The respective model explains 88.3% of the total sum of squares					

NS not significant, \*\*\*Significant,  $P < 0.05$

**Table 2** Statistical analysis of the effect of processing parameters on surface quality of spruce wood measured by laser method

Surface waviness ( $\mu\text{m}$ )					
Factors	Sum of squares	Degree of freedom	Variance	F value	Level of significance
Intercept	72,974.61	1	72,974.61	2426.545	***
Cutting speed (m/s) (1)	86.17	2	43.09	1.433	NS
Rake angle ( $^{\circ}$ ) (2)	39.21	2	19.60	0.652	NS
Feed rate (m/min) (3)	190.87	2	95.44	3.173	***
Treatment temperature ( $^{\circ}\text{C}$ ) (4)	74.65	3	24.88	0.827	NS
1 * 2 * 3 * 4	3003.33	24	125.14	4.161	***
Error	29,231.41	972	30.07		
The respective model explains 72.3% of the total sum of squares					
Surface roughness ( $\mu\text{m}$ )					
Intercept	41,082.48	1	41,082.48	6117.799	***
Cutting speed (m/s) (1)	196.95	2	98.47	14.664	***
Rake angle ( $^{\circ}$ ) (2)	109.26	2	54.63	8.135	***
Feed rate (m/min) (3)	168.98	2	84.49	12.582	***
Treatment temperature ( $^{\circ}\text{C}$ ) (4)	36.73	3	12.24	1.823	NS
1 * 2 * 3 * 4	792.23	24	33.01	4.916	***
Error	6527.21	972	6.72		
The respective model explains 86.7% of the total sum of squares					

NS not significant, \*\*\*Significant,  $P < 0.05$

spruce, when measured by the contact method, did not show any significant change with an increase in rake angle. The Ra values ranged between 4.6 and 4.75  $\mu\text{m}$  when the rake angle increased from 15 to 25 $^{\circ}$  (Fig. 5). This is in accordance with the results of previous studies [38, 39]. However, when the measurement was carried out by the laser method, the Ra values decreased from 6.6 to 5.8  $\mu\text{m}$  with an increase in the rake angle from 15 to 25 $^{\circ}$ . On the contrary, Wa values, when measured by the contact method, were found to increase with an increase in rake angle, and maximum Wa values of 7.2  $\mu\text{m}$

were obtained with the highest rake angle studied (25 $^{\circ}$ ). Measurement of Wa by the laser method showed a marginal increase when the rake angle was increased to 20 $^{\circ}$  and then declined to level off with the initial values (with 15 $^{\circ}$ ) when the rake angle was further increased to 25 $^{\circ}$ . Again, the Ra and Wa values obtained by the laser method were significantly higher than the values obtained by the contact method, suggesting better capture of surface irregularities by laser beam.

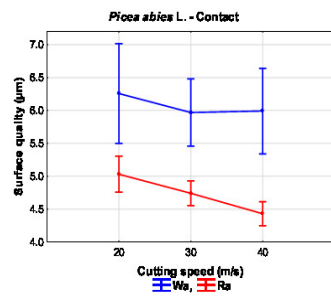


**Fig. 3** The effect of cutting speed on waviness and roughness of spruce wood—contact method

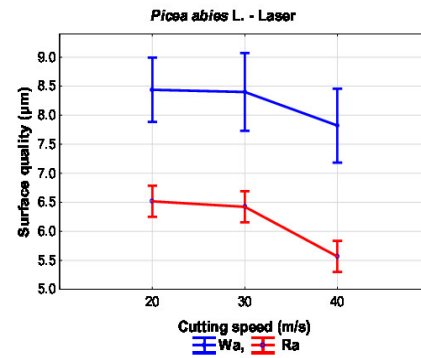


**Fig. 4** The effect of cutting speed on waviness and roughness of spruce wood—laser method

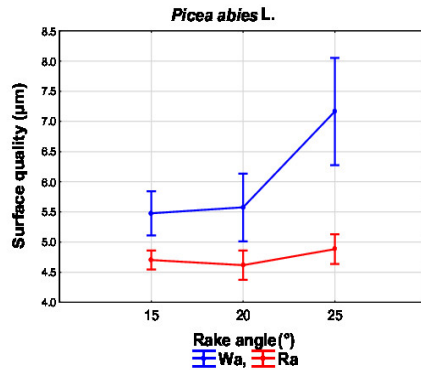


Fig. 5 The effect of rake angle on waviness and roughness of spruce wood—contact method

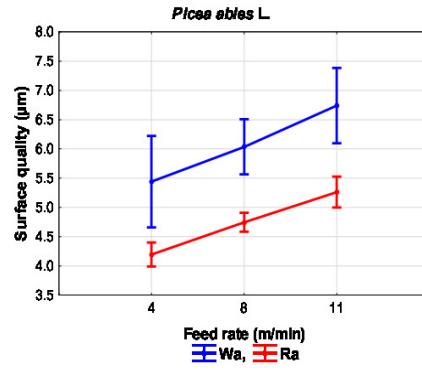


Fig. 7 The effect of feed rate on waviness and roughness of spruce wood—contact method

3.4 Feed rate

The relationship between feed rate and the surface quality of spruce as measured by the contact and laser methods is shown in Figs. 7 and 8, respectively. It is quite apparent from both figures that the Ra values increased irrespective of measurement method as the feed speed increased. As mentioned earlier, the values obtained by the laser method were significantly higher than the values obtained by the contact method at every feed rate. Increased feed rate causes vibration, both in the work piece as well as in the cutting tool, which in turn contributes to increased Ra values. A temperature increase between the interaction areas as a consequence of the vibration has also been reported [40]. Davim et al. [41] investigated the influence of drilling parameters (spindle speed, feed rate, and

drilling diameter) on the Ra of MDF panel. The result of the study showed that feed rate is the most important factor affecting the Ra in MDF. In another study, Deus et al. [42] proved that Ra values could be minimized with higher spindle speeds and a lower feed rate.

With respect to surface waviness, it can be seen that minimum Wa values were obtained at a lower feed rate (4 m/min) as obtained by both measurement methods, and the values increased as the feed rate increased. However, in the laser method, Wa values increased as the feed rate increased from 4 to 8 m/min, and a further increase in feed rate to 11 m/min did not cause any significant change in the Wa values. Again, the reason for this can be related to shear vibrations as the cutting tool has to remove more material per unit time when the feed speed increases [39, 43].

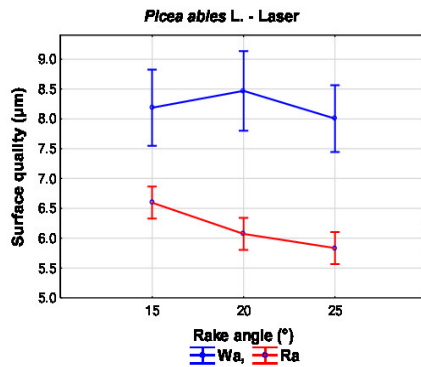


Fig. 6 The effect of rake angle on waviness and roughness of spruce wood—laser method

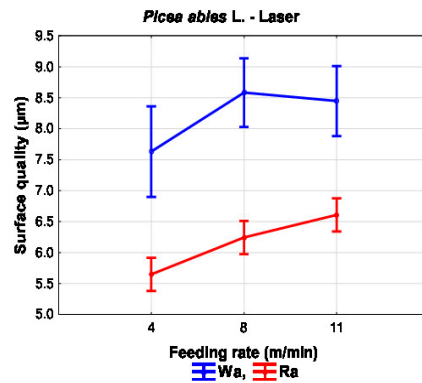


Fig. 8 The effect of feed rate on waviness and roughness of spruce wood—laser method

### 3.5 Thermal modification temperature

The relationship between surface quality parameters measured by the contact method and the thermal modification temperature is depicted in Fig. 9. Thermal modification at temperatures above 180 °C caused a significant increase in Ra values. Ra values of unmodified wood and wood modified at 160° were similar. The trend in Ra values remained unchanged when the measurement was performed with the laser method, except that the values were significantly higher in the laser method at each thermal modification temperature (Fig. 10). These findings are in contrast to earlier findings, where thermal treatment of wood has been reported to decrease the surface roughness of wood and wood-based materials [44, 45]. The Wa measured by the contact method (Fig. 9) remained almost constant up to a modification temperature of 180 °C, and the value increased steadily on samples modified at 210 °C. When measurement was performed using the laser method, there was no significant change in Ra values once the thermal temperature increased from 180 °C to 210 °C.

All foregoing results indicate that the laser method showed higher values of surface waviness and roughness than the contact method. When, the data were pooled together and averaged, roughness and waviness values obtained by laser method were 5.90 μm and 7.95 μm, respectively, while those obtained by contact method were 4.66 μm and 6.11 μm, respectively. The roughness value measured by laser method was found 31% higher than that obtained by contact method. Similarly, the waviness value obtained by laser method was 35% higher than that obtained by contact method. Variable results obtained from laser and contact devices indicate that every machine has its own defined parameters. The precision of laser device is related to the diameter of the laser beam (0.2 μm), which is considerably less (10 times) than that of a

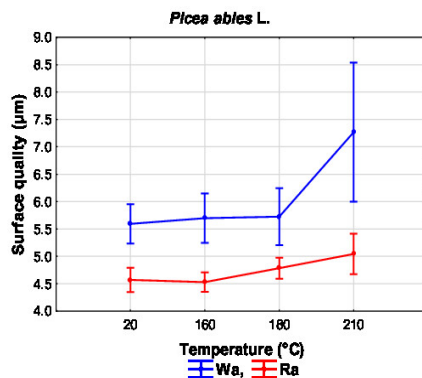


Fig. 9 Effect of modification temperature on waviness and roughness—contact method

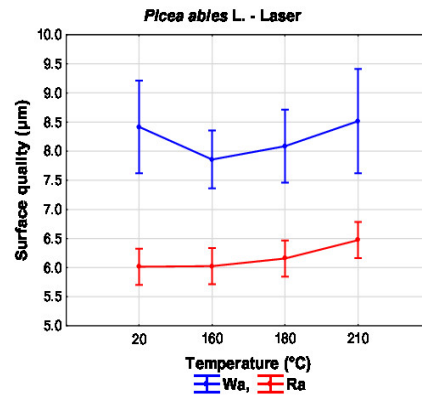


Fig. 10 Effect of modification temperature on waviness and roughness—laser method

diamond tip used in a contact device (2 μm). As a result, the contact tip can measure only irregularities above 2 μm in size, while the laser beam can measure irregularities from 0.2 μm. This confirms that the laser method is capable of measuring smaller irregularities than the contact machine, thereby providing more precise information. However, smaller irregularities were overlooked when using the contact method, leading to lower values of surface waviness and roughness. Hence, the values obtained by the contact method were found to underestimate the true surface quality. At the same time, it should be noted that the contact machine is faster and more frequently used in wood industries because of the lower cost. The results are in concurrence with the results reported in literature [11]. The authors compared the roughness values of two optical noncontact methods with reference to the values of contact stylus profiler and reported that laser scan method can measure surface roughness with sufficient accuracy.

### 3.6 The relationship between measurement methods in terms of surface quality data

Both measurement methods have their own merits and demerits. While the laser method is more accurate and captures the surface quality to minute details, the measurement is time-consuming and requires expensive setup. On the other hand, the contact method is very quick and less expensive, though it underestimates the real surface quality. In order to ascertain the degree of association of the values obtained by both methods, the surface roughness data were correlated. The relation is shown in Fig. 11. A moderate correlation ( $r=0.63$ ) was obtained between both measuring methods when surface roughness values were correlated.

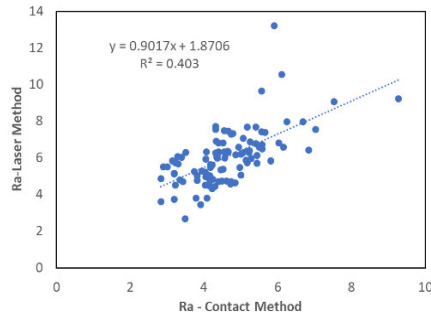


Fig. 11 Correlation between contact and laser methods with respect to surface roughness (Ra) values

**3.7 Surface roughness and chemical changes of spruce wood under thermal modification**

The chemical changes in spruce wood exposed to different thermal modification temperatures have already been reported [46]. Ra values resulting from the milling operation were also found to increase with an increase in the modification temperature (Fig. 9). To determine if changes in the chemical composition of spruce can have an influence on variations in the surface roughness, the percentage of chemical constituents and surface roughness corresponding to each modification temperature were correlated (Fig. 12). A strong correlation was observed between chemical changes, particularly the hemicelluloses, and variations in the quantity of surface roughness. This indicates that chemical changes occurring during thermal modification create irregularities on the wood surface at a microscale. In addition, the anatomical structure of wood also slightly distorts due to thermal treatment. This distortion can be due to the rupture in the ray parenchyma cell,

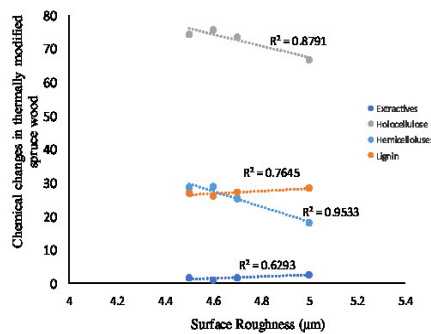


Fig. 12 Correlation between chemical changes and surface roughness of spruce thermally modified at 160 °C, 180 °C, and 210 °C.

**Table 3** Optimum combination of processing parameters with regard to Wa

Cutting speed (m/s)	Rake angle (°)	Feed rate (m/min)	Temperature (°C)	Wa (µm)	Ra (µm)	Energy consumption (W)
30	25°	4	180 °C	3.95	4.32	505
40	20°	4	180 °C	4.44	4.72	1208
...	...	...	...	...	...	...
20	20°	11	210 °C	17.66	10.56	425
30	15°	4	20 °C	24.75	13.21	651

development of checks in the secondary wall and middle lamella, and hydrolyzation of bordered pits [47, 48].

**3.8 Optimum cutting parameters**

For ascertaining the optimum combination of processing parameters, surface quality data obtained by laser method was used. Data in Table 3 show the combination of milling parameters and thermal modification temperature on the increasing order of surface waviness. The corresponding values of surface roughness as well as energy consumption have also been included. Due to a large number of data, only the best two and worst two combinations have been presented. The lowest surface waviness of 3.95 µm was obtained on samples thermally modified at 180 °C and machined with milling parameters of 30 m/s cutting speed, 25° rake angle, and 4 m/min feed rate. The highest surface waviness, 24.75 µm, was obtained on unmodified samples with a milling machine operated at a cutting speed of 30 m/s, rake angle of 15°, and feed rate of 4 m/min.

Data in Table 4 represent the combination of milling parameters and thermal modification temperature on the increasing order of surface roughness. The corresponding values of surface waviness as well as energy consumption have also been included. Due to a large number of data, only the best two and worst two combinations have been presented. The

**Table 4** Optimum combination of processing parameters with regard to Ra

Cutting speed (m/s)	Rake angle (°)	Feed rate (m/min)	Temperature (°C)	Wa (µm)	Ra (µm)	Energy consumption (W)
40	25°	4	210 °C	4.59	3.62	1138
40	25°	8	20 °C	7.25	3.46	1100
...	...	...	...	...	...	...
20	20°	11	210 °C	17.66	10.56	425
30	15°	4	20 °C	24.75	13.21	651

**Table 5** Optimum combination of processing parameters with regard to energy consumption

Cutting speed (m/s)	Rake angle (°)	Feed rate (m/min)	Temperature (°C)	Wa (μm)	Ra (μm)	Energy consumption (W)
20	25°	8	210 °C	9.94	6.35	345
20	25°	11	180 °C	8.68	6.27	353
...	...	...	...	...	...	...
40	15°	4	160 °C	5.07	5.04	1496
40	15°	4	20 °C	6.73	4.77	1517

lowest surface waviness of 3.62 μm was obtained on samples thermally modified at 210 °C and machined with milling parameters of 40 m/s cutting speed, 25° rake angle, and 4 m/min feed rate. The highest surface waviness, 13.21 μm, was obtained on unmodified samples with a milling machine operated at a cutting speed of 30 m/s, rake angle of 15°, and feed rate of 4 m/min

Table 5 shows the combination of milling parameters and thermal modification temperature on the increasing order of energy consumption. The corresponding values of surface waviness as well as surface roughness have also been included. The lowest energy consumption was obtained while milling spruce wood samples thermally modified at 210 °C with the machine parameters set at 20 m/s cutting speed, 25° rake angle, and 8 m/min feed rate. The highest energy consumption was obtained with unmodified samples.

While milling parameters can be regulated based on the importance of any one of the individual characteristics (Ra, Wa, or energy consumption), it will be more appropriate if all the three monitored characteristics are combined to obtain the best combinations of processing parameters. Table 6 shows the two best and two worst combination of processing parameters in terms of surface roughness, surface waviness, and energy consumption. Lower energy consumption and optimum surface quality were obtained with spruce wood samples thermally modified at 210 °C and milled at 20 m/min cutting speed, 20° rake angle, and 4 m/min feed rate.

**Table 6** Optimum combination of processing parameters for all three characteristics

Cutting speed (m/s)	Rake angle (°)	Feed rate (m/min)	Temperature (°C)	Wa (μm)	Ra (μm)	Energy consumption (W)
20	20°	4	210 °C	5.36	3.86	405
30	25°	4	180 °C	3.95	4.32	505
...	...	...	...	...	...	...
40	25°	11	210 °C	15.78	9.23	1026
40	20°	8	180 °C	14.24	8.88	1303

## 4 Conclusions

Spruce wood samples were subjected to thermal modification and subsequently milled with different combinations of processing parameters. The surface quality of the specimens was assessed using both laser and contact methods. Energy consumption during milling was also measured. The salient findings of this study are as follows:

1. Average roughness and waviness values obtained by laser method were 5.90 μm and 7.95 μm, respectively, while those obtained by contact method were 4.66 μm and 6.11 μm, respectively.
2. Higher surface roughness (31%) and surface waviness (35%) values were obtained by the laser method compared with the contact method, suggesting that the laser method is more accurate than the contact method in capturing surface irregularity.
3. A moderate correlation ( $r=0.63$ ) was found between the surface roughness data measured by both methods.
4. Milling parameters influenced the surface quality of wood. Increase in cutting speed and rake angle improved the surface quality while increase in feed speed caused a deterioration in the surface quality.
5. Lower energy consumption during milling with optimum surface quality (Ra 3.86 μm and Wa 5.36 μm) was achieved on spruce wood samples thermally modified at 210 °C and machined at a cutting speed of 20 m/s, rake angle of 20°, and a feed rate of 4 m/min.

**Funding Information** This study was financially supported by the “Advanced research supporting the forestry and wood-processing sector’s adaptation to global change and the 4th industrial revolution.” no. CZ.02.1.01/0.0/0.0/16\_019/0000803 financed by OP RDE as well as the Internal Grant Agency (IGA) of the Faculty of Forestry and Wood Sciences, project no. B-20\_04.

## References

1. Kılıç M, Hiziroğlu S, Burdurlu E (2006) Effect of machining on surface roughness of wood. *Build Environ* 41:1074–1078. <https://doi.org/10.1016/j.buildenv.2005.05.008>
2. Jakerst RW, Steward HA (1976) Knife-versus abrasive planed wood: quality of adhesive bonds. *Wood Fiber Sci* 8(2):107–113
3. Kamke FA, Lee JN (2007) Adhesive penetration in wood—a review. *Wood Fiber Sci* 39(2):205–220
4. Singh AP, Anderson CR, Warnes JM, Matsumura J (2002) The effect of planing on the microscopic structure of *Pinus radiata* wood cells in relation to penetration of PVA glue. *Holz Roh Werkst* 60(5):333–341. <https://doi.org/10.1007/s00107-002-0321-1>
5. Neese JL, Reeb JE (2004) Funck JW (2004) Relating traditional Ra measures to glue bond quality in plywood. *For Prod J* 54:67–73
6. Aydın I (2004) Activation of wood surfaces for glue bonds by mechanical pre-treatment and its effects on some properties of veneer surfaces and plywood panels. *Appl Surf Sci* 233:268–274. <https://doi.org/10.1016/j.apsusc.2004.03.230>

- wood. *Bioresour Technol* 99(6):1861–1868. <https://doi.org/10.1016/j.biortech.2007.03.038>
46. Gaff M, Kačik F, Dick S, Turčani M, Niemz P, Hanzlík P (2019) The effect of chemical changes during thermal modification of European oak and Norway spruce on elasticity properties. *Compos Struct* 220:529–538. <https://doi.org/10.1016/j.compstruct.2019.04.034>
47. Fengel D, Wegener G (1989) *Wood: chemistry, ultrastructure, reactions*. Walter de Gruyter, Berlin
48. Dashi H, Tarmian A, Faezipour M, Hejazi S, Shahverdi M (2012) Effect of pre-steaming on mass transfer properties of fire wood (*Picea abies* L.); A gymnosperm species with torus margo pit membrane. *BioResources* 7(2):1907–1918. <https://doi.org/10.15376/biores.7.2.1907-1918>

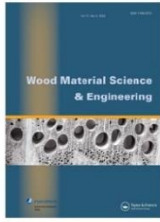
**Publisher's note** Springer Nature remains neutral with regard to jurisdictional claims in published maps and institutional affiliations.

---

### **6.3 Anatomical and morphological characteristics of beech wood after CO<sub>2</sub> laser cutting**

**Published as:**

**Fatemeh Rezaei**, Rupert Wimmer, Milan Gaff, Claudia Gusenbauer, Stephan Frömel-Frybort, Anil Kumar Sethy, Roberto Corleto, Gianluca Ditommaso, and Peter Niemz. "Anatomical and morphological characteristics of beech wood after CO<sub>2</sub>-laser cutting." *Wood Material Science & Engineering* (2022): 1-10.



## Anatomical and morphological characteristics of beech wood after CO<sub>2</sub>-laser cutting

Fatemeh Rezaei, Rupert Wimmer, Milan Gaff, Claudia Gusenbauer, Stephan Frömel-Frybort, Anil Kumar Sethy, Roberto Corleto, Gianluca Ditommaso & Peter Niemz

To cite this article: Fatemeh Rezaei, Rupert Wimmer, Milan Gaff, Claudia Gusenbauer, Stephan Frömel-Frybort, Anil Kumar Sethy, Roberto Corleto, Gianluca Ditommaso & Peter Niemz (2022): Anatomical and morphological characteristics of beech wood after CO<sub>2</sub>-laser cutting, Wood Material Science & Engineering, DOI: [10.1080/17480272.2022.2134820](https://doi.org/10.1080/17480272.2022.2134820)

To link to this article: <https://doi.org/10.1080/17480272.2022.2134820>



© 2022 The Author(s). Published by Informa UK Limited, trading as Taylor & Francis Group



Published online: 19 Oct 2022.



Submit your article to this journal [↗](#)



Article views: 113



View related articles [↗](#)



View Crossmark data [↗](#)

Full Terms & Conditions of access and use can be found at  
<https://www.tandfonline.com/action/journalInformation?journalCode=swoo20>

## Anatomical and morphological characteristics of beech wood after CO<sub>2</sub>-laser cutting

Fatemeh Rezaei<sup>a</sup>, Rupert Wimmer<sup>b</sup>, Milan Gaff<sup>a,c</sup>, Claudia Gusenbauer<sup>b</sup>, Stephan Frömel-Frybort<sup>b</sup>, Anil Kumar Sethy<sup>a,d</sup>, Roberto Corleto<sup>a</sup>, Gianluca Ditommaso<sup>a</sup> and Peter Niemz<sup>a,e,f</sup>

<sup>a</sup>Department of Wood Processing, Faculty of Forestry and Wood Sciences, Czech University of Life Sciences Prague, Suchbát, Czech Republic; <sup>b</sup>Institute of Wood Technology and Renewable Materials, University of Natural Resources and Life Sciences, Tulln, Austria; <sup>c</sup>Department of Furniture, Design and Habitat Brno, Mendel University in Brno, Brno, Czech Republic; <sup>d</sup>Institute of Wood Science and Technology, Bangalore, India; <sup>e</sup>Wood Science and Engineering, Luleå University of Technology, Skellefteå, Sweden; <sup>f</sup>Institute for Building Materials, ETH Zürich, Zürich, Switzerland

### ABSTRACT

This study aimed to characterize the surface quality of beech wood (*Fagus sylvatica* L.) cut by a CO<sub>2</sub>-laser. Boards were conditioned to a low (about 8% moisture content), 12% and a high, (about 18% moisture content). Laser cutting was performed at varying processing parameters, i.e. cutting speed, gas pressure and focal-point position. A confocal microscope was used to determine the average surface roughness perpendicular to the grain. The anatomical structures of the laser-cut surfaces were examined with scanning electron microscope. The result showed that smoother surfaces were obtained at the low moisture content when processed at a gas pressure of 21 bar. Focal-point positioning did only have an effect on the surface roughness at 12% moisture content whereas the value was substantially lower for focal-point positioned on the surface. The surfaces cut at 18% moisture content, and at a cutting speed of 3.5 m/min generated a rougher surface than cut at low moisture content and at a lower speed. Laser cutting produced a rougher surface as compared to sawn surface (circular saw). The structural integrity of the laser-cut surface was more intact when the wood was having high moisture content and processed at a high cutting speed.

### ARTICLE HISTORY

Received 10 April 2022  
Revised 6 October 2022  
Accepted 7 October 2022

### KEYWORDS

CO<sub>2</sub>-laser; surface roughness; moisture content; anatomical structure

### 1. Introduction

Traditional wood-machining processes involve the interaction between a wooden piece and a cutting tool. However, laser-beam machining utilizes a focused laser beam to melt and/or vapourise material to produce a cut edge. Due to their higher efficiency and accuracy, this technology has become attractive in various fields of wood-industrial applications (Kubovský *et al.* 2020). For example, laser-beam cutting is applied in the furniture industry with the aim to reduce the cutting costs (Badoniya 2018) and this technology has already been widely implemented in the metal-, ceramic- and plastic-processing industries. In general, traditional wood machining potentially causes changes only in the physical properties of the processed surface (Kilic *et al.* 2006), while laser-beam machining is accompanied by structural, chemical and physical changes (Haller *et al.* 2001, Kačík and Kubovský 2011, Kubovský and Kačík 2013).

A laser beam cuts material by extremely fast heating of the structure, ejected from a nozzle by applying a reflecting beam from a mirror through focusing lenses. A high-energetic beam spot is focused by a lens on the wood surface (Powell 1993). The coherent laser beam of infrared light (wavelength 10.6 µm) usually has a power above 20 kW. However, in modern industrial laser-cutting machines, power ranging from 3.5 kW to 5.5 kW is sufficient to achieve very high

production rates (Peters and Banas 1977, Powell and Kaplan 2004). The energy absorbed by the wood largely depends on the laser power and the related exposure time (Barnekov *et al.* 1986). When more energy is absorbed, the number of polysaccharides in wood declines due to the degradation processes in hemicelluloses and also in part of the amorphous regions of cellulose (Kačík and Kubovský 2011). Laser power forms an unavoidable charred cut on the wood surface due to pyrolysis. Across the width of a wooden piece, the internal wood structure is directly subjected to laser heat, which is referred to as the heat affected zone (HAZ). The formation of a HAZ is affected by the growth rings (i.e. density variation) (Barnekov *et al.* 1986), the fiber orientation, the laser-power input, and the workpiece thickness (Powell and Kaplan 2004). The surface quality of the HAZ is different from conventional processes such as sawing. The effect of HAZ can be determined by quantifying surface characteristics such as surface roughness or surface waviness.

Solid-wood surfaces are naturally uneven due to the existing variations in the anatomical structure of wood, caused by the growth rings, the ratio of earlywood and latewood, and the varying wood density (Forest Products Laboratory 1987, Barcikowski *et al.* 2006, Korkut and Donertas 2007, Bekhta *et al.* 2009, Brémaud *et al.* 2011). This is one reason why existing standards for measuring and evaluating surface quality

**CONTACT** Fatemeh Rezaei  rezaei@fd.czu.cz 

© 2022 The Author(s). Published by Informa UK Limited, trading as Taylor & Francis Group  
This is an Open Access article distributed under the terms of the Creative Commons Attribution-NonCommercial-NoDerivatives License (<http://creativecommons.org/licenses/by-nc-nd/4.0/>), which permits non-commercial re-use, distribution, and reproduction in any medium, provided the original work is properly cited, and is not altered, transformed, or built upon in any way.

are not applicable to wood since they only measure roughness due to a machining process (Funck *et al.* 1992, Thoma *et al.* 2015, Thibaut *et al.* 2016). Numerical values assessed with different methods (light sectioning, confocal microscopy, tactile measurement, gloss meters, pneumatic, laser) are used to determine surface irregularity. There are advantages and disadvantages while using each of these methods (Hiziroglu 1996, Hiziroglu and Graham 1998, Hirata *et al.* 2001, Merrild and Christensen 2009). For example, the disadvantage of image analysis (confocal or laser microscopy) is that it is tricky to differentiate between features with similar optical characteristics (Leban and Triboulot 1994).

The inherent properties of wood, the characteristics of applied processing tools, and the employed processing parameters all influence the surface quality of processed wood (Hazır and Koç 2016). Optimization of the processing parameters of CO<sub>2</sub> laser is therefore critical to achieve better quality of laser-cut surfaces than sawn surfaces. Microscopic analyses showed that laser-cut wood surfaces are smoother than sawn surfaces (Haller *et al.* 2001, Dolan 2014). It is also well documented that surface roughness declines when the laser power increases (Barnekov *et al.* 1989, Quintero *et al.* 2011a, 2011b, Eltawahni *et al.* 2011). Gurau and Petru (2018) engraved maple wood with a laser and reported that surface roughness increased as a negative response to laser power. Increased feed rate has been reported as a cause of increased roughness on MDF surfaces cut by laser (Lum *et al.* 2000, Eltawahni *et al.* 2011). An increased wood moisture content (MC) also plays an important role in the quality of laser-cut wood surfaces. A high MC requires a low feed rate (Pili *et al.* 2009) which can be explained by high thermal conductivity that leads to a reduction in the amount of energy concentrated on HAZ (McMillin and Harry 1971). At high MC, a substantial part of the laser energy vaporizes water and hence the amount of energy required to burn the material is reduced (Hernandez-Castaneda *et al.* 2011).

During laser cutting of wood, the quality of the cut surface is influenced by the laser parameters (focal-point position, laser power, gas pressure), processing parameters (cutting speed) and material parameters (moisture content, density, grain direction). Ascertaining the effect of these parameters may lead to increased cutting efficiency and improved surface quality. Characterization of laser-cut surfaces in terms of physical, chemical and anatomical properties is of paramount importance to ascertain its suitability for different applications. A much-debated question is whether or not a low cutting speed, a high gas pressure, and a focal point focused on the middle of a workpiece result in a smooth surface. Another question is to what extent the adjacent anatomical wood structures change due to laser-cutting, with a varying cutting speed, gas pressure and focal-point position. Because wood disintegrates through in several laser-induced ablation processes, there is a strong possibility that smoother surfaces can be achieved by laser-cutting, compared with sawing. It is also assumed that a lower cutting speed provides sufficient time for melting, and higher gas pressure partly prevents undesirable vaporization, leading to a smoother surface of the laser-cut surfaces. It has

commonly been assumed that replacing the focal-point position from the top surface to the workpiece center will result in better energy distribution and thus a smoother surface after laser-cutting. Due to different levels of thermal degradation of chemical compounds during laser cutting, it is probable that the structural integrity of the laser-cut surface becomes weak.

## 2. Materials and methods

### 2.1. Materials

Kiln dried European beech (*Fagus sylvatica* L.) wood was purchased from the Wood Store<sup>®</sup> company, Czech Republic. The measured average wood density was 770 kg/m<sup>3</sup> ( $\pm 12$  kg/m<sup>3</sup>), while the moisture content was 16% ( $\pm 0.8\%$ ). Six pieces of sawn timber with a dimension of 50 × 25 × 3 cm (length × width × thickness) were prepared and stored in a semi-opened outdoor space for two weeks.

### 2.2. Methods

#### 2.2.1. CO<sub>2</sub>-laser cutting process

To study the effect of moisture content, the two pieces of sawn timber from the six pieces were conditioned in a climatic chamber at 20 ± 2 °C and 65 ± 5% relative humidity (RH) until the weight became constant, while the other two pieces were submersed in water. The average moisture content of the pieces conditioned in a climatic chamber was 12%, while that of the water-soaked pieces was about 18% (high MC). The remaining two pieces were conditioned to achieve a moisture content of about 8% (low MC). The moisture content was calculated using representative samples according to ISO 13061-1 (2014).

A CO<sub>2</sub>-laser machine (TRUMPF<sup>®</sup>, Czech Republic) was used to cut the boards. The radial sections of the pieces were placed perpendicular to the laser beam in a such a way that the cutting was achieved in the tangential section along the grain (Figure 1). The applied processing parameters are outlined in Table 1.

Nozzle diameter and cutting power were kept constant at 2.7 mm and 3200 W, respectively. Six sample strips were cut (parallel to grain direction) with every processing parameter combination from each of the boards representing different MC. The dimensions of the cut sample strips were 50 cm × 3 cm × 5 mm (length × width × thickness) as shown in Figure 1.

To compare the laser-cut surface with a sawn surface, sawing was performed in parallel direction to the grain on the tangential section using a circular saw of blade diameter of 300 mm, blade thickness of 2.2 mm, tooth thickness of 3.2 mm, rotating speed of 4000 RPM and blade height of 60 mm.

#### 2.2.2. Electron microscopy

Samples sized 5 × 5 × 5 mm (length × width × thickness) were cut from the specimen (laser-cut strips) to observe the cross-sections with electron microscope FEI Quanta 250 FEG (Thermo Fisher Scientific, Hillsboro, USA) under high-

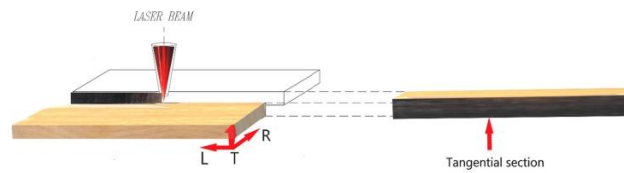


Figure 1. CO<sub>2</sub>-laser cutting process on beech wood (L- longitudinal, R- Radial and T- Tangential direction).

Table 1. CO<sub>2</sub>-laser machine processing parameters.

CO <sub>2</sub> -laser	Focal-point position	Gas pressure (bar)	Cutting speed (m/min)
Variations in the processing parameters	On the top surface of the workpiece	17	3
	At the center of the workpiece	21	3.5

vacuum conditions. Micrographs were recorded with the Everhart-Thornley-Detector to collect the secondary electrons and back-scattered electrons at an accelerating voltage of 20 kV. The laser-cut samples were mounted with conductive double-sided carbon tape on an aluminum stub,

which was sputter coated with a 10 nm thin gold layer under Argon atmosphere in a Scaancoat Six sputter coater (Edwards, Burgess Hill, UK) for sufficient electrical conductivity. The surfaces were assessed immediately after laser cutting and after airbrushing of carbon dusts.

### 2.2.3. Confocal microscopy

Samples with dimensions of 3 cm × 3 cm × 5 mm (length × width × thickness) were cut from the specimen. The surface profile of the laser-cut samples (on tangential section) was measured with confocal microscope (Olympus OLS5100, Japan) with a Gaussian filter (Figure 2(a)). The incident light

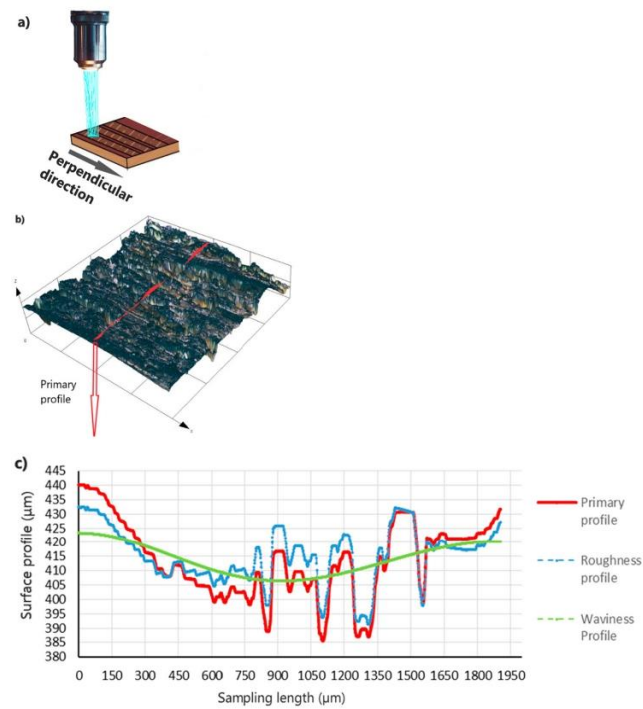


Figure 2. (a) Configuration of a laser-cut sample for measuring a surface profile with a confocal microscope, (b) a 3D image of the laser-cut sample (c) a primary profile of the 3D image filtering the shortest wavelength components from a roughness measurement.

in the microscope shines from a collimated light source on the tangential surface of the sample providing 3D images of the surface by image stacking (Figure 2(b)). Primary profiles of the 3D images were obtained (Figure 2(c)). The three laser-cut samples from each group (cutting speed, focal point and gas pressure) were prepared and three readings were taken from each laser-cut sample. Measurements were carried out across the grain directions.

The waviness was removed from the measured profile to numerically evaluate the roughness (Figure 2(c)). A cutoff value of 2.5 mm, as reported by Gurau *et al.* (2006) was used to segregate waviness. In the present study, the roughness average was obtained pursuant to ISO 4287 (2009),  $R_a$  is the arithmetic mean of the absolute coordinate values Z (profile peak height) within sampling length.  $R_a$  can be expressed by Equation (1).

$$R_a = \frac{1}{L} \int_0^L |z(x)| dx \quad (1)$$

Statistical analysis of the experimental data was performed by applying an analysis of variance (ANOVA) as well as Fischer's F-Test with STATISTICA™ 14 (StatSoft Inc; Oklahoma, USA) software.

### 3. Results and discussion

#### 3.1. Effect of CO<sub>2</sub> laser processing parameters on surface roughness

##### 3.1.1. Cutting speed

The first set of analyses was aimed to reveal the effects of laser processing on the surface quality. Table 2 shows a two-way ANOVA of the effect of the interaction of cutting speed (3 and 3.5 m/min) and moisture content (8%, 12%, and 18%) on the average surface roughness ( $R_a$ ). Constant parameters were 3200 W laser power, 21 bar gas pressure and the focal-point position on the top surface of the work-piece. No significant difference between  $R_a$  values cut at speed of 3 and 3.5 m/min with 8% / 12%, or 18% MC was obtained (Table 2). Data in Figure 3 showed that as the MC increased, particularly from low to the samples conditioned at 12% MC, the  $R_a$  values increased significantly when cut at 3.5 m/min (Table 2). This result may be explained by the

**Table 2.** Two-way analysis of variance (ANOVA) of average roughness ( $R_a$ ) perpendicular to the grain for the effects of cutting speed (3 m/min or 3.5 m/min), and the specimens conditioned at 8%, 12% or 18% MC.

Monitored factors	Sum of squares	Degree of freedom	Mean squares	F-value	Probability
Cutting speed (m/min)	6.36	1	6.36	2.33	NS
Moisture content (%)	20.63	2	10.32	3.78	***
Interaction between cutting speed (m/min) and Moisture content (%)	14.61	2	7.30	2.67	NS
Error	131.11	48	2.73		

Multiple  $R^2 = 0.24$

Note: \*\*\* significant. The level of significance was accepted at  $P < 0.05$ . NS: not significant.  $P > 0.05$ .

fact that with a higher MC, a greater part of the energy was consumed for the evaporation of water, thereby reducing the energy available for thermochemical degradation of the wood elements leading to higher surface roughness.

A study by Lum *et al.* (2000) has shown that in MDF, by increasing cutting speed, the average roughness of laser-cut samples increased. The authors highlighted that a lower cutting speed enabled thorough penetration of the laser beam into the wood, creating thermochemical degradation and thereby delivering a smooth transition across the cut kerf. The authors have also stated that the beam was bypassing the exposed region without full thermochemical degradation at a higher cutting speed, resulting in incomplete char formation. Eltawahni *et al.* (2011) reported an increase in the roughness values for MDF, with an increasing cutting speed and air pressure, but, they did not provide an explanation for these increases. Barnekov *et al.* (1989) provided an explanation for the smoother surface of a five-layered panel as a result of a lower cutting speed of a CO<sub>2</sub>-laser. The authors mentioned that with lower speed, excess heat builds up and a char layer generates. In the present study, solid beech wood was less homogenous than MDF but the latter includes adhesives and other additives. The components, other than wood, may require a greater exposure time to be fully degraded.

Wood as a heterogenous material has a low thermal conductivity (Ashby 2012), and with its varying chemical composition, it requires different temperature ranges and exposure time to achieve the most efficient degradation of the wood constituents. As demonstrated, a rougher or smoother surface of the laser-cut surface was not achieved when the cutting speed increased by 0.5 m/min. At a constant cutting power of 3200 W, the faster cutting speed was sufficient for cutting the 30 mm beech wood, particularly with respect to energy savings and cost reduction.

##### 3.1.2. Focal-point positions

To study the effect of focal-point position, laser cutting was performed at a power of 3200 W, a cutting speed of 3.5 m/min and a gas pressure of 17 bar. The result has been presented in Figure 4. Two-way ANOVA of the effect of the

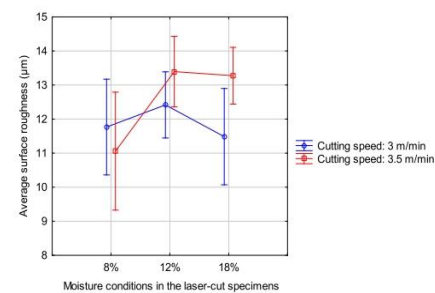


**Figure 3.** The effect of cutting speed and the moisture content of laser-cut specimens on average surface roughness ( $R_a$ ) measured perpendicular to the grain (bars denote 95% confidence intervals).

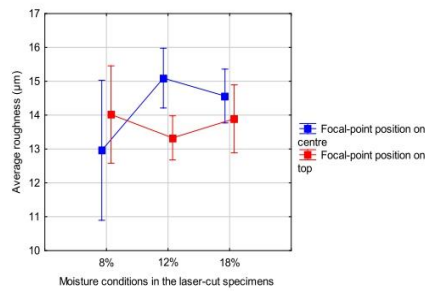


**Figure 4.** The effect of focal-point positions and moisture content on average surface roughness ( $R_a$ ) measured perpendicular to the grain. (bars denote 95% confidence intervals).

interaction of focal-point positions and moisture levels on the average surface roughness was carried out and the results are shown in Table 3. The focal-point position on the surface produced a better surface quality compared to the center position, particularly in samples conditioned to 12% MC (Figure 4). When only the focal-point position is considered, the  $R_a$  differences between both the focal-point positions studied were not significant (Table 3), however, their interaction with MC had a significant effect on the surface roughness. This outcome is contrary to that of Barnekov *et al.* (1986) who studied the effect of different focal-point positions on the surface quality and reported a smooth surface with less charring when the focal point was at or slightly above the workpiece center. The heat distribution rate is highly depending on the anatomical structure and wood properties (its discussed in part 3.2.2).

### 3.1.3. Gas pressure

To study the effect of gas pressure, 17 and 21 bar, laser cutting was performed at a laser power of 3200 W, a cutting speed of 3.5 m/min and a focal-point positioned on the surface of the sample. Figure 5 shows the results pertaining to the effect of gas pressure and MC (8%, 12%, or 18%), on the average surface roughness of the samples. The data were analyzed using two-way ANOVA and the results are shown in Table 4.

**Table 3.** Two-way analysis of variance (ANOVA) of average roughness ( $R_a$ ) perpendicular to the grain for the effects of focal point on the top surface and at the workpiece center, and the specimens conditioned at 8%, 12% or 18% MC.

Monitored factors	Sum of squares	Degree of freedom	Mean squares	F-value	Probability
Focal-point position	2.87	1	2.87	1.11	NS
Moisture content (%)	6.38	2	3.19	1.23	NS
<b>Interaction between focal-point position and Moisture content (%)</b>	<b>18.25</b>	<b>2</b>	<b>9.13</b>	<b>3.52</b>	<b>***</b>
Error	124.32	48	2.59		

Multiple  $R^2 = 0.18$

Note: \*\*\* significant. The level of significance was accepted at  $P < 0.05$ . NS: not significant.  $P > 0.05$ .

In Figure 5, it is quite apparent that the  $R_a$  value of the cut at 21 bar gas pressure increased significantly as the MC of the sample increased from 8% to 18%. However, at a gas pressure of 17 bar, the  $R_a$  values for each of the MC, 8–18%, studied were more or less comparable without any significant difference. The pooled data indicates a significant effect of gas pressure on the surface roughness (Table 4), however this difference is mainly contributed by the extreme roughness values of samples at low MC (Figure 5). A low MC (8%) ensures maximum absorption of energy by the wood resulting in faster degradation and instantaneous production of smoke and carbon dust. A high gas pressure helps in faster removal of smoke and carbon dust thereby promoting efficient cut with smoother surface. Such benefits of higher gas pressure could not be seen with a MC of 18% due to the fact that higher MC limits the degradation process and the generated carbon particles get trapped with the evaporated moisture from the wood and sticks to the wood surface thereby contributing to a rough surface.

Lum *et al.* (2000) used two different shield gas pressures (0.5 and 2.5 bar) to cut medium density fiberboards (MDF) and reported comparable surface roughness values at both gas pressures without any significant difference. In contrast, Eltahwani *et al.* (2011) studied the effect of gas pressure, which ranged between 4.5 and 6.0 bar, on the surface quality of laser-cut MDF and reported a decrease in surface roughness ( $R_a$ ) values with an increase in the gas pressure. When wood is cut with a laser beam, a jet of gas is needed to exhaust the smoke, control the excessive burning, and protect the lens and a gas pressure up to 4 bar is usually employed in cutting solid wood (Barnekov *et al.* 1986). Hernandez-Castaneda *et al.* (2011) stated that when the gas pressure increased, the interaction between the laser beam and the material also improved. The lens is protected against fumes and carbon dust. In addition, charring on the laser-cut surface is also reduced (Powell 1993, Quintero *et al.* 2011a). It is important to note that the gas pressure experimented with in this study was between 17 and 21 bar, such a high gas pressure was applied due to the high wood density ( $677 \text{ kg/m}^3$  to  $863 \text{ kg/m}^3$ ), and a fast cutting speed.

The average roughness parameter ( $R_a$ ) obtained with a circular saw was  $5.25 \mu\text{m}$  which was significantly lower than the

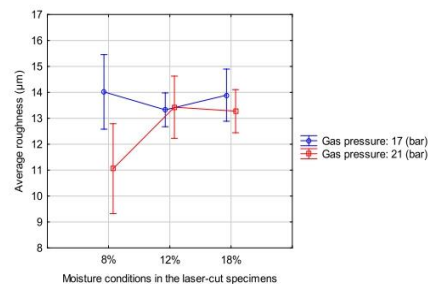


**Figure 5.** The effect of the interaction between gas pressure and moisture content on average surface roughness ( $R_a$ ) measured perpendicular to the grain (vertical bars denote 95% confidence intervals).

**Table 4.** Two-way analysis of variance (ANOVA) of average roughness ( $R_a$ ) perpendicular to the grain for the effects of gas pressures of 17, or 21 bar and the specimens conditioned at 8%, 12% and 18% MC.

Factors	Sum of squares	Degree of freedom	Mean squares	F-value	Probability
Gas pressure (bar)	17.81	1	17.81	7.49	***
Moisture content (%)	10.97	2	5.48	2.30	NS
The interaction between gas pressure (bar) and Moisture content (%)	22.62	2	11.31	4.75	***
Error	111.84	47	2.38		

Multiple  $R^2 = 0.32$

Note: \*\*\* significant. The level of significance was accepted at  $P < 0.05$ . NS: not significant.  $P > 0.05$ .

average  $R_a$  of laser-cut surfaces. The higher  $R_a$  value for the laser-cut can be attributed to the formation of charred layers and different charring rates for earlywood (lower rate) and latewood (higher rate). In addition, the laser cutting marks observed may be due to the small vibration of the wood pieces during laser cutting.

### 3.2. The effect of $CO_2$ processing parameters on the anatomical structure of laser-cut beech samples

#### 3.2.1. Cutting speed and the anatomical structure

To discover the changes that likely occurred in the anatomical structure of the specimen during the laser cutting, a scanning

electron microscope (SEM) was used. SEM micrographs of the specimen conditioned to 8% MC and laser-cut at different cutting speeds (3.5 m/min and 3 m/min), with the focal point focused on the top surface, are shown in Figure 6. Figures 6(a) (magnification: 2625x) and 6b (magnification: 10662x) show different magnified micrographs taken from the specimen cut at a speed of 3.5 m/min, while Figures 6(c) (magnification: 3075x) and 6d (magnification: 11748x) show micrographs of a specimen cut at speed of 3 m/min. It is evident from the micrographs that the anatomical integrity of the specimen cut at 3 m/min in most of the areas (Figure 6(a,b)) is lower than that obtained at 3.5 m/min (Figure 6(c,d)). The middle lamella between the fiber walls was completely degraded when the specimen was cut at a low speed (Figure 6(c)), while at a high speed the degradation of middle lamella was only partial. The middle lamella is in general mostly composed of lignin, pectic polysaccharides and a small amount of proteins (Lazić *et al.* 2018), and the lignin proportion can be up to 84%. The lignin proportion decreases and the cellulose proportion increases from the middle lamella towards the  $S_3$  layer (adjacent to the lumen) (Rowell 2005). The thermal degradation of lignin is slower at 200–500°C than cellulose and hemicellulose components of biomass (Brebū and Vasile 2010). However, the accessibility of lignin is quite higher than that of cellulose. Electron transitions are caused by visible and ultraviolet (UV-VIS) radiation, mostly creating

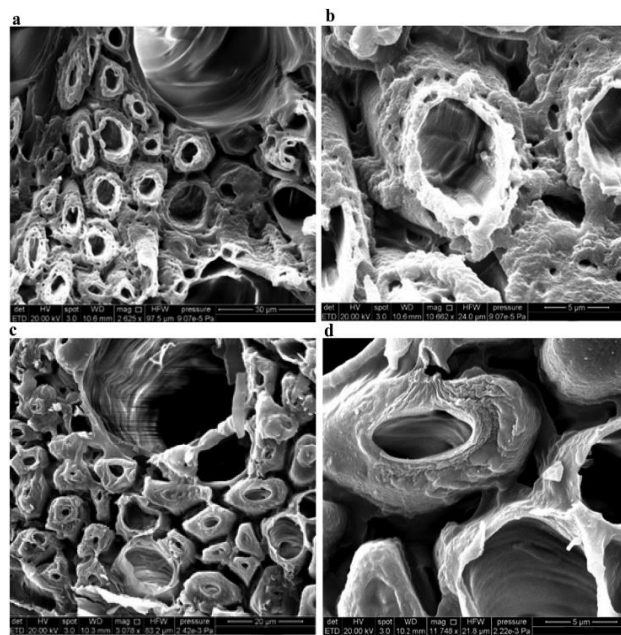


**Figure 6.** SEM micrographs taken from the cross-section of laser-cut samples: (a) and (b) are from specimen laser-cut at speed of 3.5 m/min; (c) and (d) are from specimen laser-cut at speed of 3 m/min.

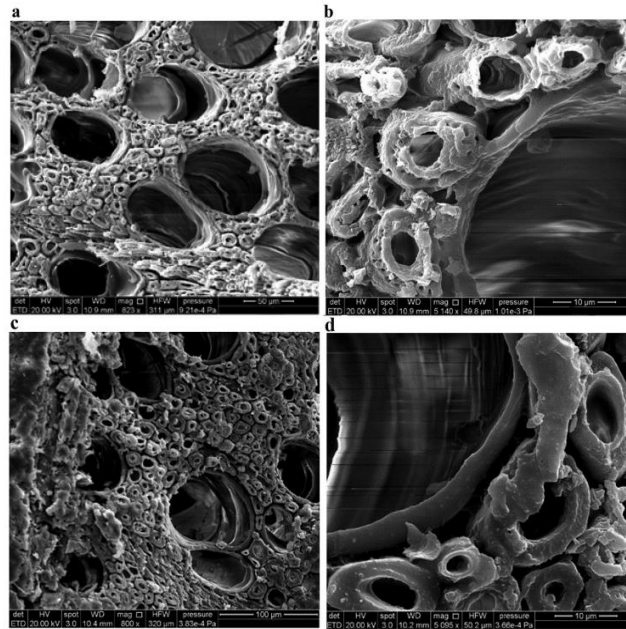


**Figure 7.** SEM photos taken from the cross-section of laser-cut samples with: (a) and (b) are from specimen laser-cut with the focal-point position on top surface, (c) and (d) are from specimen laser-cut with the focal-point position at the workpiece center.

changes in lignin. A CO<sub>2</sub> laser in the range of far infrared does not the same. Particular vibrational changes in the molecules caused by the CO<sub>2</sub>-laser result in thermal action (Haller *et al.* 2001, Kačik and Kubovský 2011). What can be clearly seen in Figure 6(b) is apparently a portion of polymer chains, maybe the crystalline portion of cellulose, in the deeper walls of fiber, S<sub>2</sub> and S<sub>3</sub>, remained unchanged by thermal degradation and looks like a white portion protruding out from the end of fibers in the samples cut at higher speed. In contrast, at a lower speed, as shown in Figure 6(d), the polymer chains were completely degraded without any polymer chains remaining. This may be explained by the fact that at lower speed the exposure time of the wood to the laser is higher and the heat energy generation surpasses the energy dissipation through conduction. The residual energy (difference between heat energy generated and heat energy dissipated due to conduction) at the exposure point is high enough to thermally degrade the polymer chains completely. When the speed is increased, the exposure time is reduced and the residual energy at the exposure point is comparatively lower due to energy dissipation through conduction. The residual energy is still sufficient enough to degrade the lignin and cellulose polymers at the point of exposure; however, the energy conducted through the probably cellulose gets dissipated to the underlying lignin and seems sufficient enough to degrade the underlying lignin up to a certain distance (~ 1 μm) from the exposure point, leaving

the crystalline portion of cellulose unaffected. As a result, the unaffected cellulose protrudes from the cut end of the fibers, as can be seen in Figure 6(b). These projections are more towards the cell lumen, as the cellulose content is higher towards that side. Further, selective degradation (more lignin and less cellulose) at higher speed did not affect the micro voids present in the fiber walls; however, these voids have been covered by the degradation by-products in samples cut at a lower speed.

The remaining polymer chains as projections, and the absence of middle lamella as cavities on the cross-section of the laser-cut samples, can be a signal for changes in the surface roughness profile. Observing the anatomical changes of the samples in the cross-section, the anatomical changes are expected to be roughly the same on the tangential surface, leading to changes in the surface roughness profile. As explained earlier in Figure 3, the average roughness of the samples cut by laser in the tangential plane was not affected by increasing the cutting speed from 3 to 3.5 m/min. This indicates that potential anatomical changes in the tangential plane do not affect the  $R_a$ .

### 3.2.2. Focal-point positions and the anatomical structure

The result of SEM analyses of the laser-cut samples cut by different focal-point positions is shown in Figure 7. Samples conditioned to 8% MC were cut at a constant cutting speed

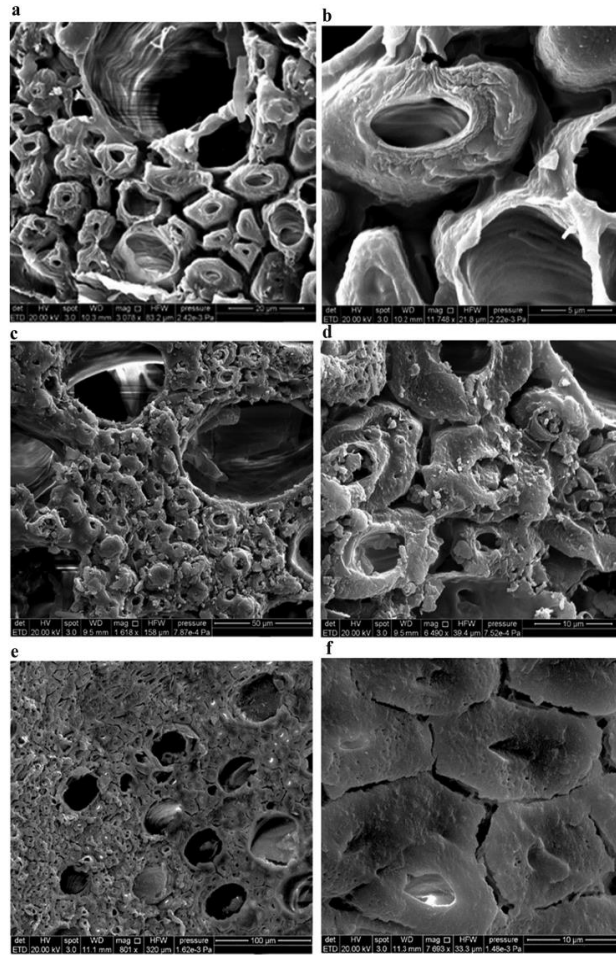


**Figure 8.** SEM photos taken from the cross-section of laser-cut samples conditioned at: (a) and (b) 8% MC, (c) and (d) 12% MC, and (e) and (f) 18% MC (with constant cutting parameters of 3 m/min, 21bar, focal-point at workpiece center)

of 3.5 m/min, gas pressure of 17 bar and conditioned to 8% MC. Figure 7(a) (magnification: 823x) and 7b (Magnification: 5140x) depict the SEM micrographs (with different magnification) of the cross-section of a sample cut with the focal-point positioned on the sample's surface, while 7c (magnification: 800x) and 7d (magnification: 5095x) depict the cross-section of a sample cut with the focal-point positioned in the middle of the sample's thickness. The lower part of laser-cut samples (cross-section) was selected for SEM analysis. When the focal point is on the surface, the concentration of energy is initially higher on the surface, and then it

distributes from the upper parts of the samples to the lower parts. The lower part of the laser-cut samples absorbed less energy than the upper parts. This resulted in better anatomical integrity of the lower part and less burning. This may be one of the reasons why the middle lamella in most parts disappeared less between cells in the laser-cut samples with the focal point on the surface (Figure 7(a,b)). The absence of a middle lamella provides empty spaces in the cross-section of the laser-cut samples, which probably leads to changes in the surface roughness profile. The empty spaces on the cross-section of the laser-cut samples can

presumably also occur in the tangential phase. As explained earlier in Figure 4, laser-cut samples at 12% MC were rougher in the tangential plane when the focal point was relocated from the top to the workpiece center. The empty spaces may therefore be one of the possible reasons for the rougher surfaces. It can also be stated that when the focal point is placed on the surface, energy distributes equally on the surface and less burning occurs, finally enhancing the material integrity. More detailed observations of the SEM photo (Figure 7(d)) indicated the presence of small bubbles mostly on the cell wall. This is probably due to the pressure of liquid or vapor under laser power (Ghany and Newishy 2005), as well as gas pressure, which formed during the pyrolysis process (carbon monoxide, hydrogen, carbon dioxide, methane and other light hydrocarbons) (Commandré *et al.* 2011).

### 3.2.3. The effect of moisture content on the anatomical structure of wood

SEM micrographs of the cross-section of the samples cut at different MC are presented in Figure 8. All the samples were cut at a constant speed of 3 m/min, laser power of 3200 W, and gas pressure of 21 bar, with the focal-point positioned at the workpiece center. Figure 8(a,b) shows the cross-section of samples conditioned to 8% MC (with different magnification levels), Figure 8(c,d) shows the cross-section of samples conditioned to 12% MC, and Figure 8(e,f) shows the cross-section of a sample conditioned to 18% MC. The SEM micrographs show that high MC in the samples improves the quality of the laser-cut surface. At low MC, the middle lamella between the fiber walls is seen completely disintegrated and the fiber lumens are seen devoid of any deposits. At a low MC, the thermal degradation and evaporation seems quite efficient, as most of the laser energy is absorbed by the wood elements. As MC increases, the thermal disintegration of the middle lamella is restricted. This may be due to increased thermal conductivity of wood with increased MC (MacLean 1941, Vay *et al.* 2015) leading to faster energy dissipation through conduction. In addition, a part of the thermal energy is also consumed for evaporation of moisture (Barnekov *et al.* 1986, Piili *et al.* 2009, Hernandez-Castaneda *et al.* 2011). The byproducts of thermal degradation combined with the water vapor may form a slurry and get deposited on the cut surface, thereby sealing the fiber lumens as well as the crevices of the middle lamella and creating an even surface, as seen in Figure 8(d,f).

## 4. Conclusion

Sawn timber of European beech was cut by CO<sub>2</sub> laser using different cutting speeds, gas pressure, focal-point positions and wood moisture content (MC). The effect of these parameters on surface quality and anatomical changes on the cut surface was assessed. The results show that cutting speed has no effect on the average surface roughness. Positioning the focal point at the center in the thickness of the workpiece rather than on the surface also did not cause any significant effect on the surface roughness, except in the laser-cut samples at 12% MC. However, an increase in gas

pressure resulted in a lower average surface roughness, particularly in laser-cut samples with lowest moisture content. Overall, the laser-cut surfaces were rougher than those cut by a circular saw. Anatomical study revealed reduced structural integrity of the laser-cut samples at low cutting speed. The middle lamella between the fiber walls was completely degraded when the samples were cut at a low speed, while at a high cutting speed the middle lamella was only partially disintegrated.

## Disclosure statement

No potential conflict of interest was reported by the author(s).

## ORCID

Rupert Wimmer  <http://orcid.org/0000-0002-7023-6209>

## References

- Ashby, M. F. (2012) *Materials Selection in Mechanical Design*. Butterworth-Heinemann, In 4, Elsevier Ltd, 640. doi:10.1016/C2009-0-25539-5.
- Badoniya, P. (2018) CO<sub>2</sub> laser cutting of different materials—a review. *International Research Journal of Engineering and Technology (IRJET)*, 5, 1–12.
- Barcikowski, S., Koch, G. and Odematt, J. (2006) Characterisation and modification of the heat affected zone during laser material processing of wood and wood composites. *Holz als Roh- und Werkstoff*, 64 (2), 94–103. doi:10.1007/s00107-005-0028-1
- Barnekov, V. G., McMillin, C. W. and Huber, H. A. (1986) Factors influencing laser cutting of wood. *Forest Products Journal*, 36(1), 55–58.
- Barnekov, V., Huber, H. A. and McMillin, C. W. (1989) Laser machining wood composites. *Forest Products Journal*, 39(10), 76–78.
- Bekhta, P., Hiziroglu, S. and Shepelyuk, O. (2009) Properties of plywood manufactured from compressed veneer as building material. *Materials & Design*, 30(4), 947–953. doi:10.1016/j.matdes.2008.07.001
- Brebu, M. and Vasile, C. (2010) Thermal degradation of lignin—a review. *Cellulose Chemistry & Technology*, 44(9), 353.
- Brémaud, I., Gril, J. and Thibaut, B. (2011) Anisotropy of wood vibrational properties: Dependence on grain angle and review of literature data. *Wood Science and Technology*, 45(4), 735–754. doi:10.1007/s00226-010-0393-8
- Commandré, J. M., Lahmidi, H., Salvador, S. and Dupassieux, N. (2011) Pyrolysis of wood at high temperature: The influence of experimental parameters on gaseous products. *Fuel Processing Technology*, 92(5), 837–844. doi:10.1016/j.fuproc.2010.07.009
- Dolan, J. A. (2014) *Characterization of laser modified surfaces for wood adhesion* (Doctoral dissertation, Virginia Tech).
- Eltawahni, H. A., Olabi, A. G. and Benyounis, K. Y. (2011) Investigating the CO<sub>2</sub> laser cutting parameters of MDF wood composite material. *Optics & Laser Technology*, 43(3), 648–659. doi:10.1016/j.optlastec.2010.09.006
- Forest Products Laboratory (US) (1987) *Wood Handbook: Wood as an Engineering Material* (No. 72). The Laboratory.
- Funck, J. W., Forrer, J. B., Buttler, D. A., Brunner, C. C. and Maristany, A. G. (1992) Measuring surface roughness on wood: A comparison of laser-scatter and stylus-tracing approaches. The International Society for Optical Engineering (SPIE), 1821, 173–184.
- Ghany, K. A. and Newishy, M. (2005) Cutting of 1.2 mm thick austenitic stainless-steel sheet using pulsed and CW Nd:YAG laser. *Journal of Materials Processing Technology*, 168(3), 438–447. doi:10.1016/j.jmatprotec.2005.02.251
- Gurau, L. and Petru, A. (2018) The influence of CO<sub>2</sub> laser beam power output and scanning speed on surface quality of Norway maple (*Acer platanoides*). *BioResources*, 13(4), 8168–8183. doi:10.15376/biores.13.4.8168-8183

- Gurau, L., Mansfield-Williams, H. and Irlle, M. (2006) Filtering the roughness of a sanded wood surface. *Holz als Roh- und Werkstoff*, 64(5), 363–371. doi:10.1007/s00107-005-0089-1
- Haller, P., Beyer, E., Wiedemann, G., Panzner, M. and Wust, H. (2001, April) Experimental study of the effect of a laser beam on the morphology of wood surfaces. In *First International Conference of the European Society for Wood Mechanics*, 19A21 April, Lausanne, Switzerland. Accessed 9 January 2002, available at: <https://www.researchgate.net/publication/237543545>
- Hazir, E. and Koç, K. H. (2016) Optimization of wood surface machining parameters in CNC routers: Response surface methodology (RSM) approach. *International Journal of Scientific Research Engineering & Technology*, 5(10), 494–501.
- Hernandez-Castaneda, J. C., Sezer, H. K. and Li, L. (2011) The effect of moisture content in fibre laser cutting of pine wood. *Optics and Lasers in Engineering*, 49(9-10), 1139–1152. doi:10.1016/j.optlaseng.2011.05.008
- Hirata, S., Ohta, M. and Honma, Y. (2001) Hardness distribution on wood surface. *Journal of Wood Science*, 47(1), 1–7. doi:10.1007/BF00776637
- Hiziroglu, S. (1996) Surface roughness analysis of wood composites: A stylus method. *Forest Products Journal*, 46(7, 8), 67.
- Hiziroglu, S. and Graham, M. (1998) Effect of press closing time and target thickness on surface roughness of particleboard. *Forest Products Journal*, 48(3), 50.
- ISO 13061-1. (2014) Physical and mechanical properties of wood - test methods for small clear wood specimens - Part 1: Determination of moisture content for physical and mechanical tests.
- ISO, E. 4287. (2009) Geometrical product specifications (GPS). Surface texture. Profile method. Terms. Definitions and surface texture parameters. International Organization for Standardization. 1997+ Amd1: 2009.
- Kačík, F. and Kubovský, I. (2011) Chemical changes of beech wood due to CO<sub>2</sub> laser irradiation. *Journal of Photochemistry and Photobiology A: Chemistry*, 222(1), 105–110. doi:10.1016/j.jphotochem.2011.05.008
- Kilic, M., Hiziroglu, S. and Burdurlu, E. (2006) Effect of machining on surface roughness of wood. *Building and Environment*, 41(8), 1074–1078. doi:10.1016/j.buildenv.2005.05.008
- Korkut, I. and Donertas, M. A. (2007) The influence of feed rate and cutting speed on the cutting forces, surface roughness and tool-chip contact length during face milling. *Materials & Design*, 28(1), 308–312. doi:10.1016/j.matdes.2005.06.002
- Kubovský, I. and Kačík, F. (2013) Changes of the wood surface colour induced by CO<sub>2</sub> laser and its durability after the xenon lamp exposure. *Wood Research*, 58(4), 581–590. Available online: <http://www.woodresearch.sk/wr/201304/07.pdf> (accessed on 21 January 2014).
- Kubovský, I., Krišťák, L., Suja, J., Gajtanska, M., Igaz, R., Ružiak, I. and Réh, R. (2020) Optimization of parameters for the cutting of wood-based materials by a CO<sub>2</sub> laser. *Applied Sciences*, 10(22), 8113. doi:10.3390/app10228113
- Lazić, B. D., Pejić, B. M., Kramar, A. D., Vukčević, M. M., Mihajlovski, K. R., Rusmirović, J. D. and Kostić, M. M. (2018) Influence of hemicelluloses and lignin content on structure and sorption properties of flax fibers (*Linum usitatissimum* L.). *Cellulose*, 25(1), 697–709. doi:10.1007/s10570-017-1575-4
- Leban, J. M. and Triboulot, P. (1994) Défauts de forme et états de surface. Lum, K. C. P., Ng, S. L. and Black, I. (2000) CO<sub>2</sub> laser cutting of MDF: 1. Determination of process parameter settings. *Optics & Laser Technology*, 32(1), 67–76. doi:10.1016/S0030-3992(00)00020-7
- MacLean, J. D. (1941) Thermal conductivity of wood. In *Heating, Piping & Air Conditioning*, 13, 380–391.
- McMillin, C. W. and Harry, J. E. (1971) Laser machining of southern pine. *Forest Products Journal*, 21(10), 35–37.
- Merrild, H. and Christensen, T. H. (2009) Recycling of wood for particle board production: accounting of greenhouse gases and global warming contributions. *Waste Management & Research: The Journal for a Sustainable Circular Economy*, 27(8), 781–788.
- Peters, C. C. and Banas, C. M. (1977) Cutting wood and wood-based products with a multikilowatt CO<sub>2</sub> laser. *Forest Production*, 27(11), 41–45.
- Piili, H., Hirvimäki, M., Salminen, A. and Lindell, H. (2009) Repeatability of laser cutting of uncoated and coated boards. In *Proceedings of the NOLAMP* (conference paper, Copenhagen), pp. 24–26.
- Powell, J. (1993) *CO<sub>2</sub> Laser Cutting* (Vol. 214) (London: Springer-Verlag).
- Powell, J. and Kaplan, A. (2004, April) Laser cutting: from first principles to the state of the art. In *Pacific International Conference on Applications of Lasers and Optics* (Vol. 2004, No. 1) (Laser Institute of America), p. 101. doi:10.1007/s00226-010-0393-8
- Quintero, F., Riveiro, A., Lusquiños, F., Comesaña, R. and Pou, J. (2011a) Feasibility study on laser cutting of phenolic resin boards. *Physics Procedia*, 12, 578–583. doi:10.1016/j.phpro.2011.03.073
- Quintero, F., Riveiro, A., Lusquiños, F., Comesaña, R. and Pou, J. (2011b) CO<sub>2</sub> laser cutting of phenolic resin boards. *Journal of Materials Processing Technology*, 211(11), 1710–1718. doi:10.1016/j.jmatprotec.2011.05.014
- Rowell, R. M. (2005) *Handbook of Wood Chemistry and Wood Composites* (Baco raton: CRC Press).
- Thibaut, B., Denaud, L., Collet, R., Marchal, R., Beauchêne, J., Mothe, F., Méausoone, P. J., Martin, P., Larricq, P. and Eyma, F. (2016) Wood machining with a focus on French research in the last 50 years. *Annals of Forest Science*, 73(1), 163–184.
- Thoma, H., Peri, L. and Lato, E. (2015) Evaluation of wood surface roughness depending on species characteristics. *Maderas. Ciencia y tecnología*, 17(2), 285–292.
- Vay, O., De Borst, K., Hansmann, C., Teischinger, A. and Müller, U. (2015) Thermal conductivity of wood at angles to the principal anatomical directions. *Wood Science and Technology*, 49(3), 577–589. doi:10.1007/s00226-015-0716-x

---

## **6.4 CO<sub>2</sub> laser cutting on the bondline characteristics of beech wood**

### **Submitted manuscript:**

**Fatemeh Rezaei**, Milan Gaff, Robert Nemeth, Jerzy Smardzewski, Anil Kumar sethy, Peter Niemz, Luigi Todaro, Gourav Kamboj, Sumanta Dass, Roberto Corleto, Gianluca Ditommaso, Mikos Bak. “Effect of CO<sub>2</sub> laser parameters on tensile-shear strength of laser-cut wood” (under review).

## CO<sub>2</sub> laser cutting on the bondline characteristics of beech wood

Fatemeh Rezaei <sup>a</sup>, Milan Gaff <sup>a, b, c</sup>, Róbert Nemeth <sup>d</sup>, Jerzy Smardzewski <sup>e</sup>, Peter Niemz <sup>f</sup>, Anil Kumar Sethy <sup>a, g</sup>, Luigi Todaro <sup>h</sup>, Gourav Kamboj <sup>a</sup>, Sumanta Das <sup>a</sup>, Roberto Corleto <sup>a</sup>, Gianluca Ditommaso <sup>a</sup>, Miklós Bak <sup>d</sup>

<sup>a</sup> *Department of Wood Processing, Faculty of Forestry and Wood Sciences, Czech University of Life Sciences Prague, Kamýcká 1176, Praha 6 - Suchbát, 16521, Czech Republic*

<sup>b</sup> *Department of Furniture, Design and Habitat Brno, Mendel University in Brno, Brno 61300, Czech Republic*

<sup>c</sup> *Czech Technical University in Prague, Faculty of Civil Engineering, Experimental Centre, Thakurova 7, 166 29 Prague 6, Czech Republic*

<sup>d</sup> *Institute of Wood Technology and Technical Sciences, University of Sopron, Sopron, 9400, Hungary*

<sup>e</sup> *Poznan University of Life Sciences, Faculty of Forestry and Wood Technology, Department of Furniture Design, Wojska Polskiego 28, 60-637 Poznan, Poland*

<sup>f</sup> *ETH Zürich, Institute for Building Materials, Stefano-Franscini-Platz 3  
CH 8093 Zürich  
Luleå University of Technology*

<sup>g</sup> *Institute of Wood Science and Technology, 18<sup>th</sup> Cross, mallewaram, Bangalore-560003, India*

<sup>h</sup> *School of Agricultural Forestry, Food, and Environmental Science, University of Basilicata, Viale dell'AteneoLucano 10, 85100 Potenza, Italy*

### ABSTRACT

The performance of engineered wood products is highly associated with an efficient cutting method and the proper assembly. This paper investigates the influence of CO<sub>2</sub> laser parameters on the bondline characteristics in terms of surface chemistry, wetting property, adhesive penetration, and numerical analysis of stress-strain model. The laser disintegrated beech wood with varying amount of cutting speed, gas pressure, and focal point position. A tensile shear test was applied on the laser-cut samples bonded with polyvinyl acetate adhesive (PVAc). A scanning electron microscopy was used to assess the adhesive penetration of the bondline. The surface modified chemically was assessed by using a Fourier transform infrared spectroscopy. The wetting properties of the laser surface was investigated by using a contact angle goniometer. The results showed that the numerical model of the strain-stress curve confirmed the experimental model of the strain-stress curve. A PVAc drop disappeared on the laser-cut surface immediately (30s) rather than a PVAc drop on the sawn surface. The bondline penetration of PVAc adhesive was observed in both laser-cut and sawn surfaces. Among the analyzed chemical components of the laser-cut samples, hemicellulose and lignin, became partially degraded subjected to the laser power.

**Keyword:** CO<sub>2</sub> laser, cutting speed, focal point position, gas pressure

## 1. INTRODUCTION

Laser technology dates back to the early nineteenth century for cutting die in packing industries. Today, laser-cut wood is used in car interiors and inlays for the furniture industries (Powell 1993, Belforte 1998, Barcikowski et al. 2006). One of the main advantages of using a laser over mechanical tools (conventional method for cutting wood) is a lower kerf width, between 0.1–0.3 mm, compared to a saw cut kerf width ranging from 3 mm to 6 mm (Gaff et al. 2020). Developing more complex models of cutting for decorative applications in the furniture and flooring industries is another advantage of using a laser (Martínez-Conde 2017). A CO<sub>2</sub> laser, a gas laser, is more powerful with a very long wavelength of around 10.6 micrometers, compared to others (solid-state, liquid, and semiconductor). The powerful laser beam originates from a mixture of gases (carbon dioxide, nitrogen, hydrogen and helium) that are excited by an electric current. The excited state of atoms releases energy in the form of photons (Badoniya 2018). Wood is chemically disintegrated by the thermal energy of the laser. Physical changes follow the chemical changes in thermally affected regions. (Esteves & Pereira 2009, Kačík & Kubovský 2011). The surface quality of laser-cut wood in terms of chemical and physical properties is important for further applications of coating and glueing. The quality of laser-cut samples depends on the processing parameters of the laser such as cutting speed, focal point position, assist gas pressure, etc. Wood properties such as density, moisture content, anatomical structure, etc., are other factors that affect the cut quality (Piili et al. 2009, Riveiro et al. 2019).

In terms of the processing parameters of CO<sub>2</sub> lasers, Barnekov et al. (1989) reported that when the focal point is focused slightly above the surface of a wooden workpiece, the energy density declined, leading to a wider kerf width and the formation of a charred layer. In contrast, focusing the focal point on the surface caused the surface energy density to reach its highest level. The authors also mentioned that when the focal point was placed at or slightly above the centre of the workpiece, more homogenous and narrower kerf widths were achieved. A smoother surface with less charring was also observed. Other studies (Powell 1993, Quintero et al. 2011) reported a reduction in charred layer with the increase in the gas pressure, however, the kerf width and cutting speed were not influenced by the higher gas pressure. Brankove et al. (1989) and Lum et al. (2000) reported that increased cutting speed reduced the laser exposure time on wood and decreased wood char formation. From the perspective of wood characteristics, the higher the moisture content of wood, the higher the thermal conductivity, resulting in a reduction in energy being concentrated in the affected region (McMillin and Harry 1971). In addition, the water content in wood requires some energy to be boiled and vaporized, therefore the overall energy of the CO<sub>2</sub> laser touching the wood decreases (Hernandez-Castaneda et al. 2011). An increase in the density of ligno-cellulose materials requires a longer exposure time for the melting process (cutting) (Piili, et al. 2009).

There is a continuous challenge in making bonded wood products due to the variability of wood sources, the desire for more remarkable performance, and the tendency for lower costs (Koning 2010). The wood bond formation is a molecular interaction between wood and an adhesive (adhesion), and between the adhesive molecules (cohesive). Interaction between the adhesive and wood increases by the penetrating resin into the porous structure of wood (cell lumen) and even at a lower scale, into cell walls (Pocius 2012). To obtain a strong and durable bond, the resin must wet the wood surface properly and cure efficiently to provide strength and sufficient deformability. (Baier et al. 1968). The efficiency of the wood adhesive bond is strongly related to the anatomical, physical, and mechanical properties of wood, as well as the properties of the adhesive (viscosity,

pH, etc.) and bonding processes (pressure, temperature, etc.). The density, porosity, anisotropy and grain angle of wood can modify the adhesive flow. Adhesive wetting is influenced by wood moisture content, pH, buffering capacity and extractives (Hunt 2018). Haller et al. (2002) reported that the pine wood surface irradiated with a CO<sub>2</sub> laser (without carbonization) showed higher contact angle (86 °angle - 102 °angle) and longer spreading time (40s) with distilled water drop to full spread, compared to the surface obtained by a saw tool (contact angle: 11 °angle - 47 °angle, spreading time: 18s). Inversely, Dolan (2014) claimed that the wetting properties improved by the irradiated surfaces. Changes in the chemical wood structure can affect the wetting and gluing properties. Kačík and Kubovský (2011) proved that CO<sub>2</sub> laser caused thermal action by giving rise to particular vibrational changes in the molecules. Saccharides, especially hemicelluloses and amorphous part of cellulose, showed fast degradation and less stability.

The ratio of damage and distortion of wood under the bonding process is associated with the mechanical properties of wood (Hunt 2018). With higher wood density, higher adhesion strength was achieved in all cases. However, for almost all cases, with higher shear strength, higher adhesion strength was achieved (Aicher et al. (2018).

Research to date has not yet determined the bondline characteristics made of laser-cut wood. A recent study (Gaff et al. 2020) focused on the tensile shear strength of wood cut by CO<sub>2</sub> laser. The tensile shear strength of laser-cut wood bonded with Polyvinyl acetate decreased significantly compared to that of sawn samples. However, understanding of the weakness in the strength of the glued laser-cut samples requires scientific investigations and monitoring on the bondline. The numerical and experimental model of the stress-strain curve, the wettability properties of PVAc resin, the possible chemical degradation on the laser-cut surface are considered to be investigated.

## 2 MATERIALS AND METHODS

### 2.1 Materials

Kiln-dried European beech (*Fagus sylvatica* L.) wood was purchased from the Wood Store®, Czech Republic, with an average density of 770 kg/m<sup>3</sup>. The average moisture content of the lumber was 16%. The dimensions of the two beech lumbers were 25 cm × 3 cm × 50 cm (in radial, tangential, and longitudinal direction). Single-component, water-proof polyvinyl acetate (PVAc) Ag-Coll 8761/L D3 adhesive was used, with a viscosity ranging from 7000 to 13,000 mPa.s at 23 °C and a density ranging between 0.9 and 1.1 g/cm<sup>3</sup>.

### 2.2 Methods

The wood samples were conditioned in a climatic chamber at 20±2 °C and 65±5% RH until the weight became constant. The average moisture content of conditioned samples was 12%. The moisture content was calculated using representative samples according to ISO 13061-1.

#### 2.2.1.Saw cutting

Wood samples were cut in a parallel direction to the grain. The characteristics of the circular saw used for cutting the reference samples are shown below:

- Blade diameter (mm): 300
- Blade thickness (mm): 2.2
- Tooth thickness (mm): 3.2
- RPM during cutting: 4000

- Feed rate: 4 m/min
- Blade height during cutting: 60 mm.

After cutting, the samples were sanded using an abrasive paper with a P280 grit size. Twelve number of the samples were prepared (15cm x 2 cm x 0.5 cm) according to EN 302-1(2013).

### 2.2.2. Laser cutting

A CO<sub>2</sub> laser machine (TRUMPF®, Czech Republic) was used to cut the beech wood samples. The samples were placed perpendicular to the laser beam to cut parallel to the grain. The cut sample strips had a dimension of 3 cm × 1 cm × 50 cm (in tangential × radial × longitudinal direction). The number of the samples was 54.

The applied processing parameters were:

- Cutting speed: 3 m/min and 3.5 m/min
- Focal point position: on surface and ½ from surface
- Gas pressure (oxygen, nitrogen, mixed gas, and high-pressure air systems): 17 bar and 21 bar
- Nozzle diameter was 2.7 mm.

### 2.2.3. Tensile shear strength test

The strips obtained by laser cutting had an uneven shape (V shape cross section) from the top surface to the bottom. To minimize the effect of unevenness, 5 mm was cut from each edge along the longitudinal direction (Figure 1a). The final width of the samples for the glued shear test was 2 cm. The length and thickness of the samples was 15 cm and 5 mm, respectively. The total samples (108 pieces) were subsequently divided into two groups of sanded (36 pieces) and non-sanded (72 pieces) samples (Figure 2b). Sand paper of grit size P280 was used to remove the charred layer in case of samples meant for sanding. Average roughness values of sanded samples along the grain direction were obtained using a stylus type surface profilometer (Form Talysurf Intra 2, Leicester, UK). Then glue shear samples were prepared using polyvinyl acetate adhesive (150 ±10 g/m<sup>2</sup>) using both sanded and non-sanded samples separately (Figure 1). The assembled samples were subsequently cold pressed using a pressure of 0.7 ±0.1 N/mm<sup>2</sup> (Figure 1c). In total 54 shear test samples, 18 with sanded samples and 36 with non-sanded samples were prepared. For each variable of processing (cutting speed, gas pressure, focal point position, sanding) six replicate samples were tested. Tensile shear test was performed using a universal testing machine equipped with a video extensometer (INSTRON® 5882, NORWOOD, USA). Load was applied through the movable head of the machine moved at a constant speed of 5 ± 0.5 mm/min. The data for the maximum force were acquired based on EN 302-1 (2013) as per the following equation.

$\tau = F_{\max} / l_2 \cdot b$	(1)
---------------------------------	-----

where  $\tau$  is the tensile-shear strength parallel to the fibres (MPa),  $F_{\max}$  is the maximum loading force recorded at the breaking point (N),  $l_2$  is the length of the shear area (mm), and  $b$  is the width of the shear area (mm).

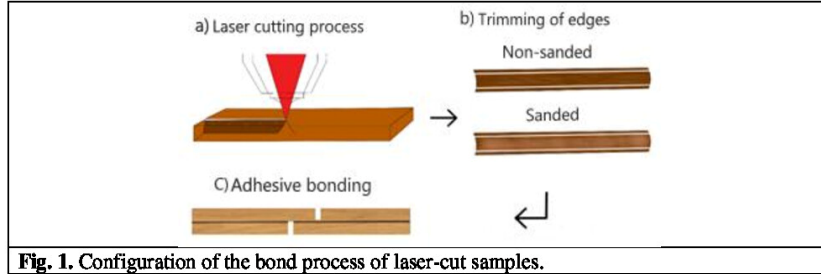


**Fig. 1.** Configuration of the bond process of laser-cut samples.

#### 2.2.4. Glue line shear modulus

After the tensile shear test, analysis was carried out based on the load and displacement data obtained from the extensometer's software (Figure 2).

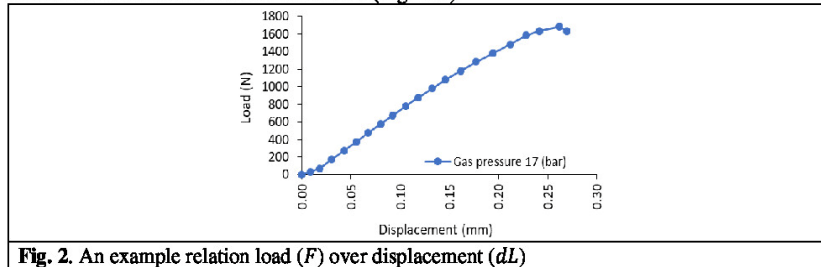


**Fig. 2.** An example relation load ( $F$ ) over displacement ( $dL$ )

Figure 3 presents a deformation model of joints. The external tensile load  $F$  (N) is divided between wooden claddings and glue line.

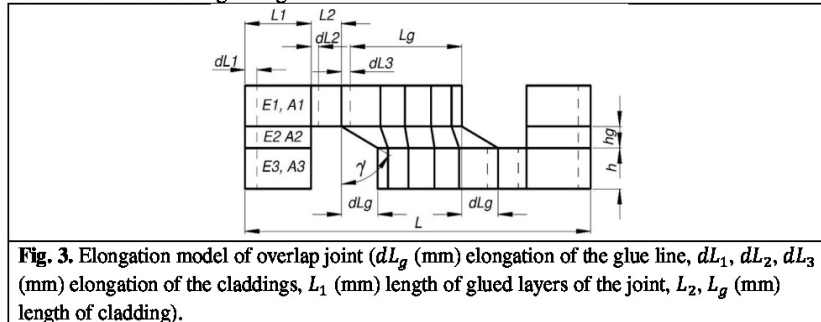


**Fig. 3.** Elongation model of overlap joint ( $dL_g$  (mm) elongation of the glue line,  $dL_1$ ,  $dL_2$ ,  $dL_3$  (mm) elongation of the claddings,  $L_1$  (mm) length of glued layers of the joint,  $L_2$ ,  $L_g$  (mm) length of cladding).

Suppose the module of linear elasticity of claddings  $E_1 = E_3$  (MPa), the module of the linear elasticity of the glue line  $E_2 = 0.1E_1$  (MPa) (Kamboj et al. 2020), and the surface of the cross-section of the cladding and glue line, respectively  $A_1 = A_3$ ,  $A_2 = 0.002A_1$  (mm<sup>2</sup>). In that case, internal loads  $F_1 = F_3$ , and  $F_2$  (N) in separate layers of the lap joint are equal:

$F_i = \frac{FE_i A_i}{\sum_{i=1}^n E_i A_i}$	(2)
$F_1 = F_3 = \frac{FE_1 A_1}{\sum_{i=1}^3 E_i A_i} = \frac{FE_1 A_1}{E_1 A_1 + E_1 A_1 + 0.1E_1 0.002A_1} = 0.499F$	(3)
$F_2 = \frac{FE_2 A_2}{\sum_{i=1}^3 E_i A_i} = \frac{F0.1E_1 0.002A_1}{E_1 A_1 + E_1 A_1 + 0.1E_1 0.002A_1} = 0.001F$	(4)

For this reason, the loads in the glue line were omitted for further calculations, and only loads in cladding were considered. To calculate the shear module of the glue line, it was first to be computed elongation  $dL_g$  (mm):

$dL_g = dL - 2dL_1 - 2dL_2 - 2dL_3$	(5)
-------------------------------------	-----

where:  $dL_g$  (mm) elongation of the glue line,  $dL$  (mm) elongation of the whole sample (experimental result),  $dL_1$  (mm) elongation of the glued layers of joint,  $dL_2$ ,  $dL_3$  (mm) elongation of the claddings:

$dL_1 = \frac{FL_1}{E_1 b(2h + h_g)}$	(6)
---------------------------------------	-----

$dL_2 = \frac{FL_2}{E_2 bh}$	(7)
------------------------------	-----

$dL_3 = \frac{FL_g}{E_1 bh}$	(8)
------------------------------	-----

where:  $F$  (N) external load,  $L_1$  (mm) length of glued layers of the joint,  $L_2$  (mm) length of cladding,  $L_g$  (mm) length of the cladding with glue line,  $b$  (mm) joint width,  $h$  (mm) thickness of the cladding,  $h_g$  (mm) glue line thickness. Assuming that:

$E_w = E_1 = E_3$	(9)
-------------------	-----

where:  $E_w$  (MPa) modulus of linear elasticity of wood,  $E_1$ ,  $E_3$  (MPa) the module of elasticity of claddings:

$dL_g = dL - \frac{2F}{E_w b} \left( \frac{L_1}{(2h + h_g)} + \frac{L_2}{h} + \frac{L_g}{h} \right)$	(10)
--	------

The shear modulus  $G_g$  (MPa) of the glue line was calculated from the equation:

$G_g = \frac{\tau}{\gamma} = \frac{Fh_g}{bL_g(dL_g)}$	(11)
---	------

where:  $\tau$  (MPa) shear stress in the glue line,  $\gamma$  (rad) shear strain,

$\gamma = \text{actan} \left( \frac{dL_g}{h_g} \right) = \frac{dL_g}{h_g}$	(12)
--	------

The module of linear elasticity of glue line  $E_g$  (MPa) was calculated by assuming that the Poissons ratio is equal  $\vartheta = 0.3$  (Kamboj et al. 2020),

$E_g = 2(1 + \vartheta)G_g$	(13)
-----------------------------	------

The results of analytical calculations were verified by the method of finite elements. For this purpose, a numerical model was prepared, as shown in Figure 4.

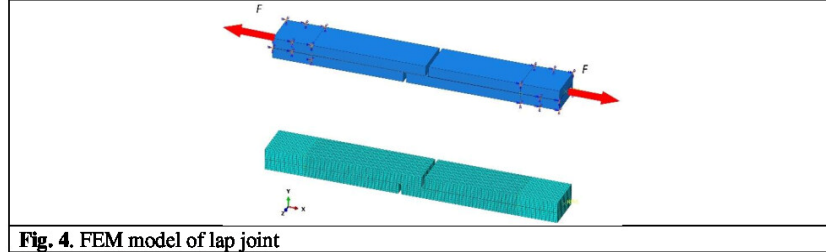


**Fig. 4.** FEM model of lap joint

The constitutive model of wood is shown in Figure 5. Wood material data was calibrated using standard Abaqus tools.  $E_g$  (MPa) adhesive weld modules for individual types of connections were calculated on the basis of equation (13). A method of non-linear calculations was used. The given extension  $dL$  forced the load values (mm) obtained based on experimental tests. The sample was immobilized by assigning freedom levels adequate to the experimental tensile test. The weld and cladding were modeled with the use of C3D8R elements (an 8-node linear brick, reduced integration, hourglass control, the total number of nodes: 71778, total number of elements: 54120). Quicking was made on the commercial version of the Abaqus v. 6.13 (Dassault System Simulia Corp. Providence, RI, USA). The correctness of the model calibration is presented in the form of numerical calculations and their comparisons with the results of experimental research.

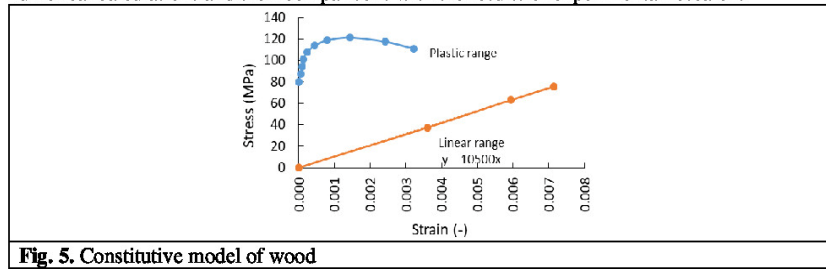


**Fig. 5.** Constitutive model of wood

Figure 6 presents the method of measuring the elongation of the connection appropriate for elongations in the mathematical model. The results of all measurements were collected and compiled in the form of stress and deformation accounts, as well as calculated modulus of glue lines.

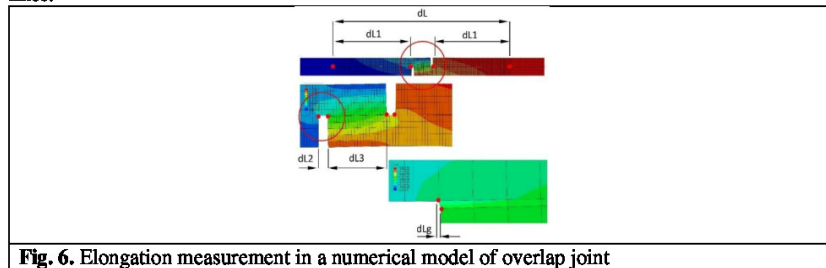


**Fig. 6.** Elongation measurement in a numerical model of overlap joint

### **2.2.5. Microscopy analyses**

Samples of  $5 \times 5 \times 5 \text{ mm}^3$  were used and a smooth surface was prepared using a sledge microtome (Leica SM 2000R, Leica Biosystems Nussloch GmbH, Germany) after softening with water, to reduce the back crack, cutting resistance, tool wear and increase wood plasticity (Xu et al. 2017). The bond line in the cross section was observed with a scanning electron microscope (SEM Tescan Vega 4, TESCAN ORSAY HOLDING, a.s., Czech Republic). The scans were prepared in a RESOLUTION scanning mode in a high vacuum with a detector of secondary electrons (SE detector). A low energy imaging method was applied in order to prevent charging of non-conductive samples without sputter coating. The optimised parameters were as follows: beam current 6 pA, landing energy 800 eV, scan speed 3 ( $1 \mu\text{s}/\text{pixel}$ ), image averaging with an accumulation of 50 images with image dimensions  $1536 \times 1152$  pixels. The magnification of the microscope was set to 250x and 1000x.

In this study, energy dispersive X-ray (EDX) spectrometry was used to identify the chemical changes in the samples through the changes in elemental composition (O/C ratio). An EDX analysis of the laser-cut surface (1L) and 6 other layers below (2L-7L) was performed to investigate how deep the laser cutting affects the chemical composition (O/C ratio) of wood. Every layer was  $50 \mu\text{m}$  thick and prepared by sliding microtome (Thermo Scientific Microm HM 430). Slices were made after softening with only droplets of distilled water at room temperature ( $21^\circ\text{C}$ ) to avoid changes in the chemical composition of the wood samples. As a first step, the surface layer was positioned and cut to a  $50 \mu\text{m}$  thick slice. Subsequently, 6 more slices of  $50 \mu\text{m}$  thick were cut, making  $300 \mu\text{m}$  the deepest layer that was investigated this way. After cutting, the slices were placed in desiccators with silica gel to dry. The EDX analysis was performed at 3 points on each layer. The device used for the test was a Hitachi S-3400N scanning electron microscope, equipped with a Bruker XFlash 5010 EDX detector.

### **2.2.6. Fourier transform infrared spectroscopy (FTIR-ATR)**

Fourier transform infrared spectroscopy studies were performed using a FTIR spectrometer, (Nicolet, Křelovická, Czech Republic). The obtained samples were analyzed in a transmittance range of  $4000 - 500 \text{ cm}^{-1}$ .

### **2.2.7. Contact angle measurement**

The degree of wettability on the laser-cut samples, with and without sanding, was determined by measuring the contact angle between the PVAc adhesive and the sample surface. The contact angle of the laser-cut samples was measured with the sessile drop method using a goniometer Krüss DSA 30E device (Krüss, Hamburg, Germany) and compared with the reference samples. A volume of  $10 \mu\text{l}$  was applied to the sample surface. Five measurements per sample were taken. Changes in the contact angles were recorded immediately after PVAc drop was applied on the surface (Figure 7). The time taken by the PVAc drop to wet the laser-cut surface is also crucial. The contact angle measurement continued until the PVAc drop completely disappeared on the surface or attained a constant contact angle. This is quite important for closed or open assembly time prior to gluing (cold press).

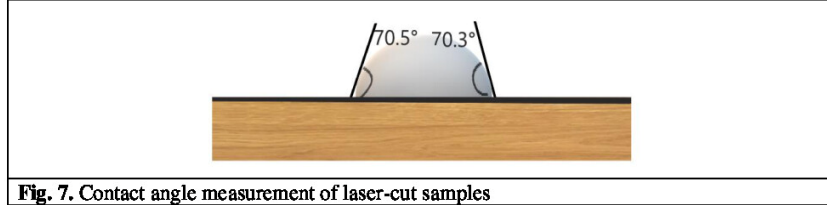


**Fig. 7.** Contact angle measurement of laser-cut samples

A statistical analysis of the experimental data was performed through analysis of variance (ANOVA) and Fischer's F-Test using STATISTICA™ 14 (StatSoft Inc; Oklahoma, USA).

### 3 RESULTS AND DISCUSSION

#### 3.1.1 Linear and shear modulus of glue line

Figure 7 shows the relationship between normal stresses and strains for all joints. The results include experimental research (Figure 7a) and numerical calculations (Figure 7b). The modules of the linear elasticity of the glue line used for numerical computations are presented in Figure 9 and discussed in the next part of the work. Figure 7 shows that the results of numerical calculations correspond to the results of experimental research. The differences in stress values sets for the same strains are insignificant and range from 5% to 15%, with a predominance on the numerical calculations side. In addition, the slope of the curves determines the rigidity of the joints. In Figure 7a, values of joint modules of linear elasticity based on the experimental tests were presented. From both figures, it can be concluded that the most significant rigidity that characterizes joint Sanding (on top surface) was the module of linear elasticity  $E_L = 7582$  (MPa). The modulus of elasticity of the other joints are lower, respectively: Cutting speed 3 (m/min) 6%, Gas pressure 21 (bar) 21%, Cutting speed 3.5 (m/min) 29%, On top surface 33%, Solid beech wood 45 %, 1/2 from top surface 47%, and Gas pressure 17 (bar) 48%.

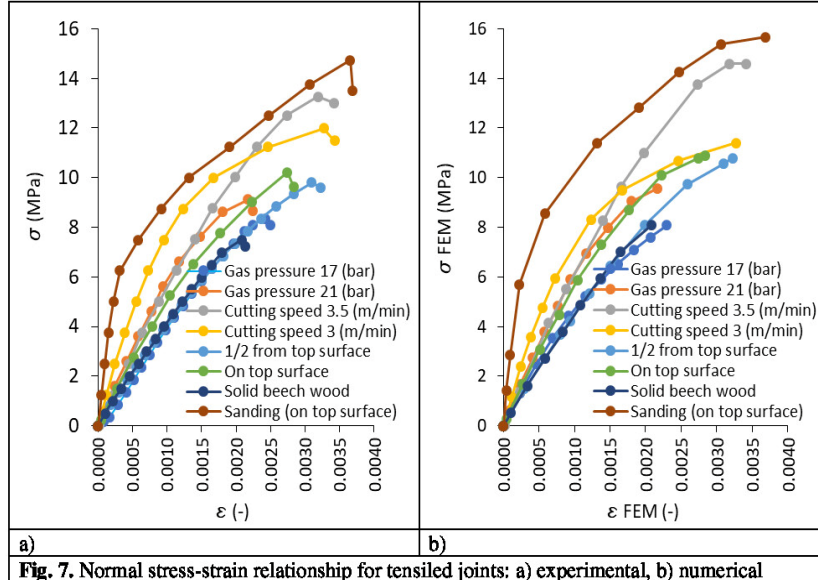


**Fig. 7.** Normal stress-strain relationship for tensiled joints: a) experimental, b) numerical

Considering the high compliance of the results of numerical calculations with the results of experimental research, the quality of the mathematical model was also verified. Therefore, on the basis of equation (13) the module of linear elasticity of glue line was calculated. In the case of the selected joint, Gas pressure 17 (bar), appropriate elongations were illustrated in Table 1. This table shows that the maximum differences between the results obtained in both methods do not exceed 8.2%. Therefore, it can be considered that the elaborated mathematical model is adequate and can be used for further calculations of the module of linear elasticity in other joints. Using the developed mathematical model in Figure 8, the relationship between the shear stress and the shear strain of the glue line was presented. On this basis, the values of the Kirchhoff module of the glue line  $G_g$  (MPa) were determined for the range of linear elasticity. Figure 8 shows that the joint Gas pressure 21 (bar) is characterized by the largest module of elasticity equal  $G_g = 660$  MPa. The elastic modulus of the other joints is lower, respectively: Cutting speed 3.5 (m/min) 7%, On top surface, 22%, Cutting speed 3 (m/min) 27%, Gas pressure 17 (bar) 34%. 1/2 from Top surface 35%, Solid beech wood 39%, and Sanding (on top surface) 39%.

**Table 1.** Elongations in joint according to mathematical and FEM analysis (Gas pressure 17 (bar) joint)

Elongation	Unit	Load (N)	Model		Difference (%)
			Mathematical	FEM	
$dL_1$	mm	1084	0.02428	0.02434	-0.28
$dL_2$			0.00155	0.00142	8.20
$dL_3$			0.01032	0.00983	4.83

$dL_2$			0.00155	0.00142	8.20
$dL_1$			0.02428	0.02434	-0.28
$dL_g$			0.03723	0.03784	-1.66
$dL$			0.09920	0.09920	

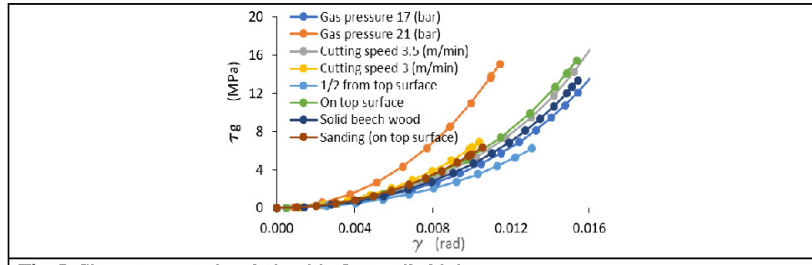


**Fig. 8.** Shear stress-strain relationship for tensiled joints

Ultimately, Figure 9 presents the calculated modulus of linear elasticity of the glue line  $E_g$  (MPa) used for numerical models. It is worth noting that the  $E_g$  depends on the type of mechanical processing of gluing surfaces. The Gas pressure 21 (bar) joint is characterized by the highest value of  $E_g=1716$  MPa. It means that the shear strain  $\gamma$  (rad) of the glue line was the lowest among the tested joints. Therefore, the used glue showed the best adhesion to the surface. For other joints, the differences are shaped in the same way as in the case of the Kirchhoff  $G_g$  module.

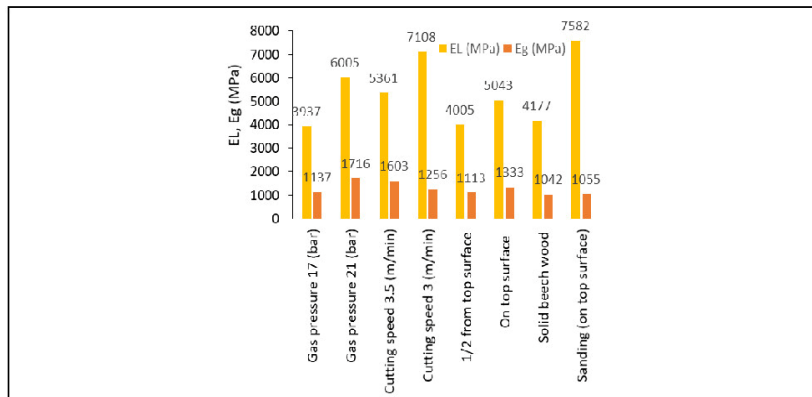
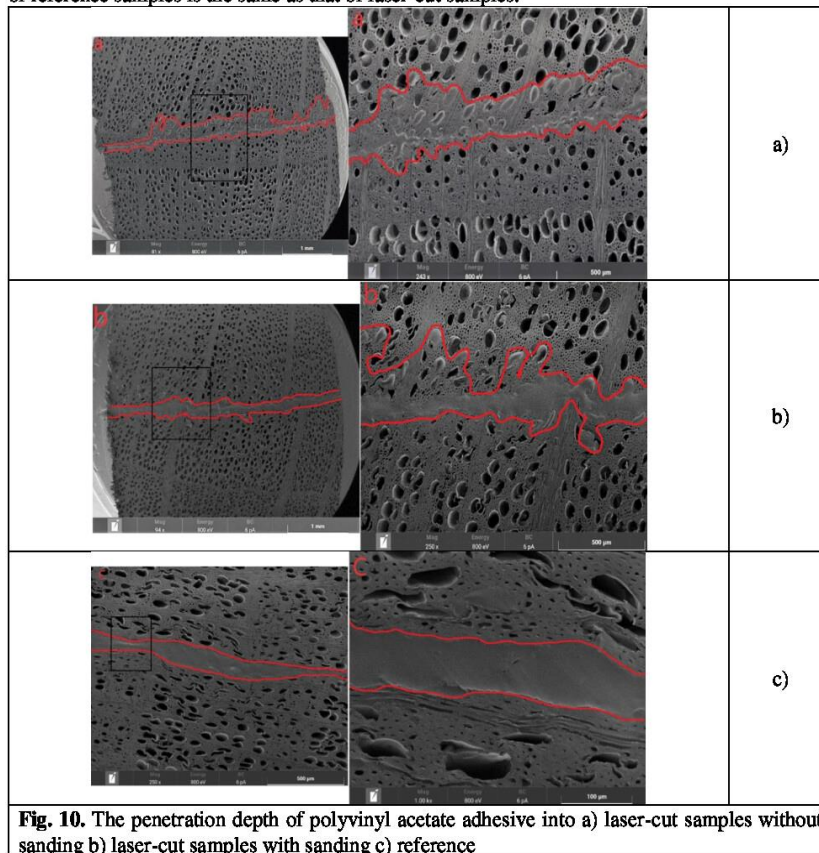


**Fig. 9.** Modulus of linear elasticity of joints and glue line

### 3.2 Microscopy analyses

#### 3.2.1 Adhesive penetration

The penetration depth of PVAc adhesive into the porosity structure of the glued laser-cut samples with and without sanding is shown in Figure 10. The penetration depth of PVAc adhesive into the bonded area of the laser-cut samples is the same as that of the laser-cut samples with sanding. It seems possible that these results are due to a great amount of char on the laser-cut samples without sanding, which greatly reduces the amount of penetration. However, the effect of adhesive penetration on the bond performance depends on other factors, including adhesive characteristics and the production process. The penetration behavior of PVAc adhesive into the porosity structure of reference samples is the same as that of laser-cut samples.



### 3.2.2 EDX analyses

The elemental composition of the laser-cut surfaces showed a different pattern in the depth of the beech material depending on cutting parameters. Cutting speed had a significant effect on changes in the main chemical components of the cut surface, but the hypothesis that slower cutting speed will result in higher degradation of the surface (indicated by a lower O/C ratio) was not supported by the results (Figure 11), as higher cutting speed resulted in a lower O/C ratio. The effect of laser cutting on the chemical composition of the beech wood was not significant with a 3 m/min cutting speed in any of the investigated layers, including the surface layer. On the other hand, increasing the cutting speed to 3,5 m/min resulted in a severe decrease in the O/C ratio. Specifically, the ratio of carbon increased on the cut surface as a result of the high temperature of the laser beam. With a higher cutting speed, this effect was significant to a depth of 150  $\mu$  (4L) compared to the reference sample, and no effect was observed deeper into the beech material. This may be explained by the fact that the wood was in contact with the laser beam for a longer time, allowing more temperature driven oxidative reactions of the cell wall components. This result indicates that laser cutting with smaller heat degradation of the surface is possible with a slower cutting speed.

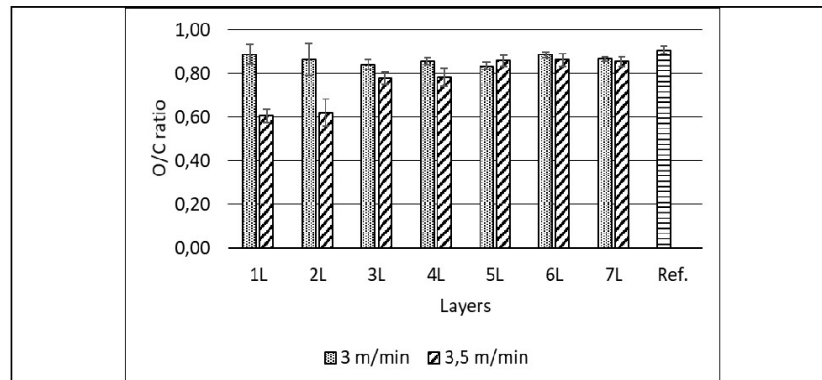


**Fig. 11.** The effect of different cutting speeds in different depths on the O/C ratio of laser-cut surfaces. 1L: cut surface; 2L: 50  $\mu$ m; 3L: 100  $\mu$ m; 4L: 150  $\mu$ m; 5L: 200  $\mu$ m; 6L: 250  $\mu$ m; 7L: 300  $\mu$ m

Gas pressure had a significant effect on the chemical components of the cut surface. Higher gas pressure resulted in higher degradation of the surface, indicated by a lower O/C ratio in every investigated layer (Figure 12). The effect of laser cutting on the chemical composition of the beech wood was significant with both 17 bar and 21 bar gas pressure, mostly on the surface layer. However, with 17 bar gas pressure, the effect diminished to an insignificant level at a depth of 50  $\mu$ m (2L). On the other hand, increasing the gas pressure to 21 bar resulted in a severe decrease in the O/C ratio in deeper layers as well. With higher gas pressure, this effect was significant to a depth of 150  $\mu$ m (4L) compared to the reference sample, while no effect was observed deeper into the beech material. All of this may indicate that the lower gas flow rate associated with lower gas pressure resulted in a higher smoke concentration, which could reduce the effect of the laser beam on heating the wood. This result indicates that laser cutting with smaller heat degradation of the surface is possible with lower gas pressure.

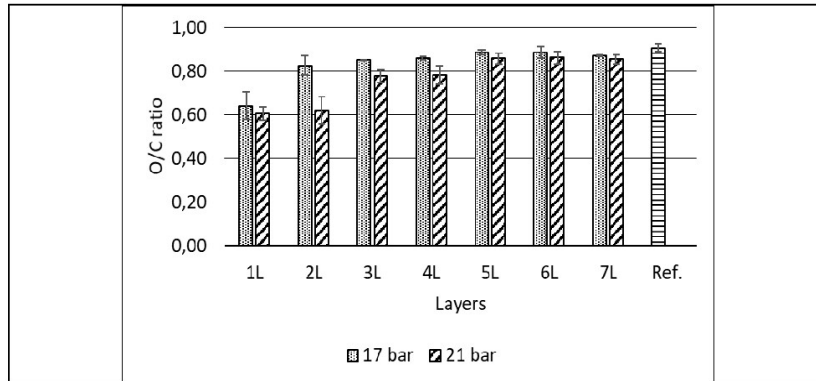


**Fig. 12.** The effect of different gas pressure at different depths on the O/C ratio of laser-cut surfaces. 1L: cut surface; 2L: 50  $\mu\text{m}$ ; 3L: 100  $\mu\text{m}$ ; 4L: 150  $\mu\text{m}$ ; 5L: 200  $\mu\text{m}$ ; 6L: 250  $\mu\text{m}$ ; 7L: 300  $\mu\text{m}$

The focal point had a significant effect on the chemical components of the cut surface. The focal point on the top surface resulted in significantly higher degradation of the cut surface, indicated by a lower O/C ratio, compared to cutting with a focal point on the centre of the sample (Figure 13). However, the effect diminished to an insignificant level at a depth of 50  $\mu\text{m}$  (2L) in both investigated focal point positions compared to the reference sample, while no effect was observed deeper into the beech material. This result indicates that laser cutting with smaller heat degradation of the surface is possible with a focal point in the centre of the material instead of on its surface.

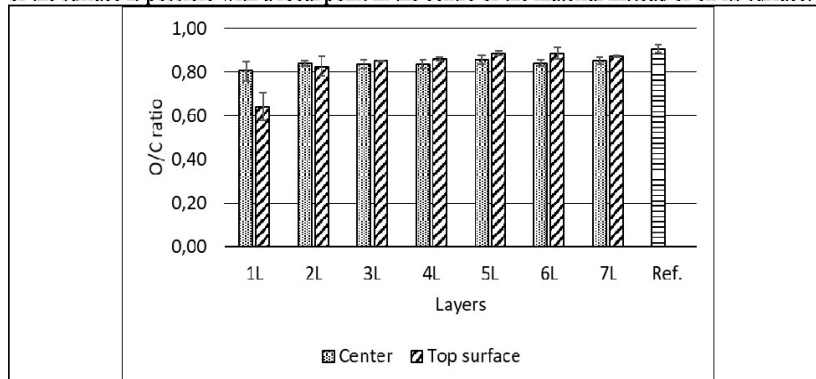


**Fig. 13.** The effect of different focal points at different depths on the O/C ratio of laser-cut surfaces. 1L: cut surface; 2L: 50  $\mu\text{m}$ ; 3L: 100  $\mu\text{m}$ ; 4L: 150  $\mu\text{m}$ ; 5L: 200  $\mu\text{m}$ ; 6L: 250  $\mu\text{m}$ ; 7L: 300  $\mu\text{m}$

The elemental analysis of the glue layer demonstrates the penetration of the adhesive (Figure 14.). The PVAc adhesive used has the same elemental composition as the wood (C, O, H), thus the

contrast between the wood and adhesive is not highly visible. However, there is a slight difference in the ratio of individual elements in the wood and in the adhesive. As a result, higher carbon content in the PVAc adhesive is visible in Figure 14. The figure shows that the adhesive did not penetrate the charred wood efficiently.



**Fig. 14.** Elemental analysis of the glued joint after failure

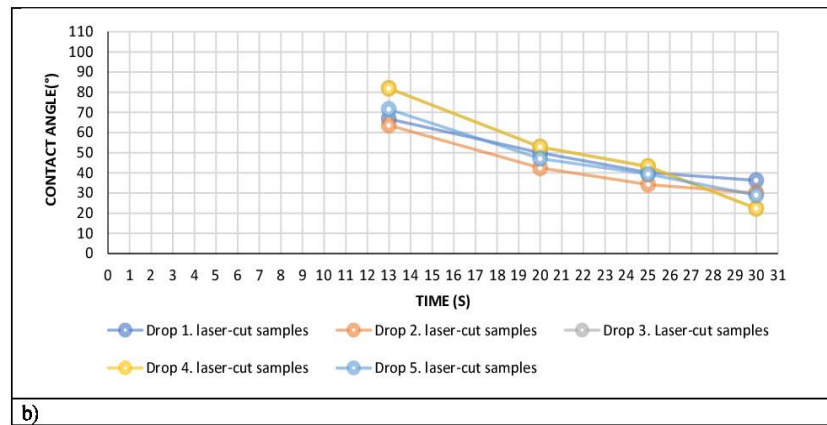
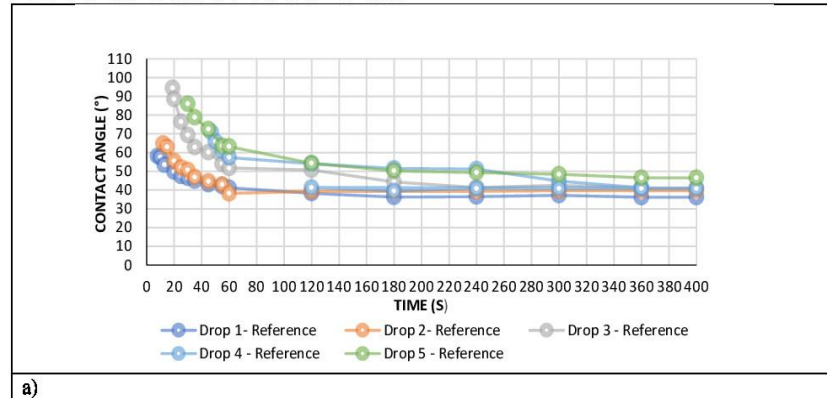
More red color on the upper part of the specimen indicates a higher carbon content of the PVAc adhesive.

### 3.3 Wetting properties

The level of wettability of laser-cut samples with PVAc adhesive before gluing is shown in Figure 15. It is apparent from Figure 15b that the contact angle between the PVAc adhesive and the laser-cut samples started in the range of  $85^{\circ}$  to  $60^{\circ}$  at 13s and continuing to decline very fast between  $38^{\circ}$  to  $20^{\circ}$  at 30s. Surprisingly, at 30s the PVAc drop was completely absorbed by the laser-cut surface. As shown in Figure 15c, the contact angle of the laser-cut samples with sanding was initially in the range of  $80^{\circ}$  -  $69^{\circ}$  between 8 to 20s. After this, the angle was sharply reduced by  $30^{\circ}$  -  $40^{\circ}$  at 60s, followed by a slow reduction to  $20^{\circ}$  at 180s. From 180s to more or less 360s, the PVAc drop was completely absorbed by the sanded surface.

The data in Figure 15a show the changes in the contact angle between solid beech wood (as a reference sample) and PVAc adhesive over time. From the very first moments, 8-30s, the contact angle was in the range of  $97^{\circ}$  -  $58^{\circ}$ . The angle declined fast around  $65^{\circ}$  -  $40^{\circ}$  up to 60s. As time passed, there was a small fluctuation in the angles that continued to remain on the reference surface in the range of  $47^{\circ}$  -  $35^{\circ}$  after 300s. Surprisingly, the adhesive drop was not completely absorbed by the reference surface. It, therefore, seems that the laser-cut samples generally absorbed the PVAc drop faster and completely than the reference samples. This may be explained by the fact that char particles on the surface had free spaces between them and the PVAc drop penetrated into the free spaces faster. Another possible reason is that the char compound is physically or chemically attracted by the PVAc compound. However, this requires further investigation. When the charred layer was removed (sanding), the sample surface absorbed the PVAc slowly compared to a surface with a charred layer (without sanding), but still faster than the reference sample. This result strengthens the possibility of a physical attraction between PVAc and the sample surface. The layers under the charred layers were thermally affected, and they may be able to physically absorb the PVAc adhesive to some degree. The penetration behavior of PVAc into the cellular structure of the laser-cut surface remained in the bondline area (Figure 10, 14), so even the drop was

absorbed very fast by the laser-cut surface, it mixed with charred layer and did not penetrate deeply into the cellular structure of the beech surface.



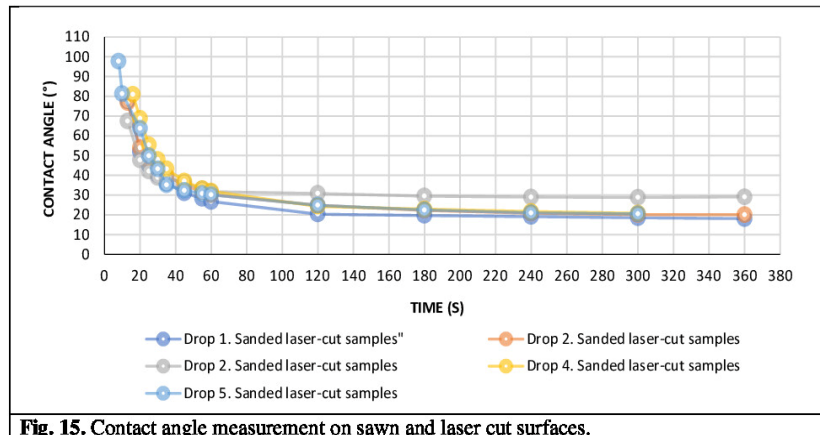


**Fig. 15.** Contact angle measurement on sawn and laser cut surfaces.

### 3.4 FTIR analysis

The FTIR method can provide broad and rapid information on the structural compositions of wood (Esteves et al. 2013). However, the method cannot directly allocate bands to every single component of wood (Owen & Thomas 1989). Hemicellulose  $[(C_5(H_2O)_4)_n]$ , cellulose  $[(C_6(H_2O)_5)_n]$ , and lignin  $[(C_{10}H_{12}O_3)]$  are the main chemical components of wood. Nader et al. (1999) reported that wood surfaces cut with a  $CO_2$  laser are subjected to heating, oxidation and formation of a charcoal layer on the wood surface. The pyrolysis process of wood that occurred during laser-cutting was proven by Barcikowski et al. (2006) and Wang et al. 2013. The spectrum of the investigated laser-cut samples and reference samples is shown in Figure 16. The spectra showed O-H stretching at around  $3336\text{ cm}^{-1}$ . The intensity of the O-H bands was slightly higher in the laser-cut samples compared to that of the reference sample. This is due to the decomposition of various oxygen-containing groups (Yang et al. 2006) and the cleavage of aliphatic hydroxyl groups in the lateral chains (Liu et al. 2008). C-H stretching band methyl and methylene groups were observed in the range of  $2918\text{-}2928\text{ cm}^{-1}$  in the laser-cut samples and nearly in the same range of the reference sample,  $2922\text{ cm}^{-1}$ . The spectrum of the reference sample showed the presence of C=O carboxyl groups and acetyl groups in hemicellulose at around  $1735\text{ cm}^{-1}$ . However, the spectrum was removed or showed a slight curve in the laser-cut samples, indicating the absence of the C=O band. This result indicates that the laser power induces the deacetylation of hemicellulose by the cleavage of acetyl groups (Altgen et al. 2018a, b). The pick at around  $1237\text{ cm}^{-1}$  demonstrated an abundance of C-O, C-C, C-O, and C-O stretching in lignin and xylan in the reference sample, while the intensity of the bands is lower in the laser-cut samples at the same wavenumber. A significant change occurred during pyrolysis in the range of  $1900\text{-}1600\text{ cm}^{-1}$ , indicating the presence of organic compounds with the carbonyl group (C=O) belonging to numerous organic species, such as aldehydes, esters and ketones (Yang et al. 2006).

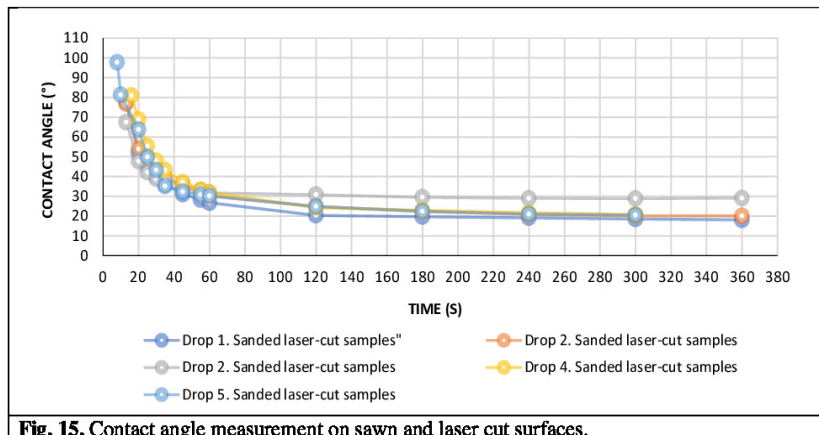


**Fig. 15.** Contact angle measurement on sawn and laser cut surfaces.

### 3.4 FTIR analysis

The FTIR method can provide broad and rapid information on the structural compositions of wood (Esteves et al. 2013). However, the method cannot directly allocate bands to every single component of wood (Owen & Thomas 1989). Hemicellulose ( $[C_5(H_2O)_4]_n$ ), cellulose ( $[C_6(H_2O)_5]_n$ ), and lignin ( $[C_{10}H_{12}O_3]$ ) are the main chemical components of wood. Nader et al. (1999) reported that wood surfaces cut with a  $CO_2$  laser are subjected to heating, oxidation and formation of a charcoal layer on the wood surface. The pyrolysis process of wood that occurred during laser-cutting was proven by Barcikowski et al. (2006) and Wang et al. 2013. The spectrum of the investigated laser-cut samples and reference samples is shown in Figure 16. The spectra showed O-H stretching at around  $3336\text{ cm}^{-1}$ . The intensity of the O-H bands was slightly higher in the laser-cut samples compared to that of the reference sample. This is due to the decomposition of various oxygen-containing groups (Yang et al. 2006) and the cleavage of aliphatic hydroxyl groups in the lateral chains (Liu et al. 2008). C-H stretching band methyl and methylene groups were observed in the range of  $2918\text{-}2928\text{ cm}^{-1}$  in the laser-cut samples and nearly in the same range of the reference sample,  $2922\text{ cm}^{-1}$ . The spectrum of the reference sample showed the presence of C=O carboxyl groups and acetyl groups in hemicellulose at around  $1735\text{ cm}^{-1}$ . However, the spectrum was removed or showed a slight curve in the laser-cut samples, indicating the absence of the C=O band. This result indicates that the laser power induces the deacetylation of hemicellulose by the cleavage of acetyl groups (Altgen et al. 2018a, b). The pick at around  $1237\text{ cm}^{-1}$  demonstrated an abundance of C-O, C-C, C-O, and C-O stretching in lignin and xylan in the reference sample, while the intensity of the bands is lower in the laser-cut samples at the same wavenumber. A significant change occurred during pyrolysis in the range of  $1900\text{-}1600\text{ cm}^{-1}$ , indicating the presence of organic compounds with the carbonyl group (C=O) belonging to numerous organic species, such as aldehydes, esters and ketones (Yang et al. 2006).

- Hunt, C. G., Frihart, C. R., Dunky, M., & Rohumaa, A. (2018). Understanding wood bonds—going beyond what meets the eye: a critical review. *Reviews of Adhesion and Adhesives*, 6(4), 369-440. <https://doi.org/10.7569/RAA.2018.097312>
- Powell, J. (1993). CO2 laser cutting (Vol. 214). London: Springer-Verlag.
- Belforte, D. A. (1998). Non-metal cutting. *Ind Laser Rev*, 13(9), 11-13.
- Barcikowski, S., Koch, G., & Odermatt, J. (2006). Characterisation and modification of the heat affected zone during laser material processing of wood and wood composites. *Holz als Roh- und Werkstoff*, 64(2), 94-103.
- Martínez-Conde, A., Krenke, T., Frybort, S., & Müller, U. (2017). Comparative analysis of CO2 laser and conventional sawing for cutting of lumber and wood-based materials. *Wood Science and Technology*, 51(4), 943-966.
- Badoniya, P. (2018). CO2 laser cutting of different materials—A review. *Int. Res. J. Eng. Technol*, 5, 1-12.
- Esteves, B., & Pereira, H. (2009). Wood modification by heat treatment: A review. *BioResources*, 4(1), 370-404.
- Kačík, F., & Kubovský, I. (2011). Chemical changes of beech wood due to CO2 laser irradiation. *Journal of Photochemistry and Photobiology A: Chemistry*, 222(1), 105-110.
- Piili, H., Hirvimäki, M., Salminen, A., & Lindell, H. (2009). Repeatability of laser cutting of uncoated and coated boards. *Proceedings of the NOLAMP, Copenhagen, Denmark*, 24-26.
- Riveiro, A., Quintero, F., Boutinguiza, M., Del Val, J., Comesaña, R., Lusquiños, F., & Pou, J. (2019). Laser cutting: A review on the influence of assist gas. *Materials*, 12(1), 157.
- Barnekov, V., Huber, H. A., & McMillin, C. W. (1989). Laser machining wood composites. *Forest Products Journal* 39 (10): 76-78.
- Quintero, F., Riveiro, A., Lusquiños, F., Comesaña, R., & Pou, J. (2011). Feasibility study on laser cutting of phenolic resin boards. *Physics Procedia*, 12, 578-583.
- Lum, K. C. P., Ng, S. L., & Black, I. (2000). CO2 laser cutting of MDF: 1. Determination of process parameter settings. *Optics & laser technology*, 32(1), 67-76.
- McMillin, C. W., & Harry, J. E. (1971). Laser machining of southern pine. *Forest Products Journal* 21 (10): 35-37.
- Hernandez-Castaneda, J. C., Sezer, H. K., & Li, L. (2011). The effect of moisture content in fibre laser cutting of pine wood. *Optics and Lasers in Engineering*, 49(9-10), 1139-1152.
- Gaff, M., Razaeei, F., Sikora, A., Hýsek, Š., Sedlecký, M., Ditommaso, G., ... & Řípa, K. (2020). Interactions of monitored factors upon tensile glue shear strength on laser cut wood. *Composite Structures*, 234, 111679.
- ISO 13061-1 (2014): Physical and mechanical properties of wood – Test methods for small clear wood specimens – Part 1: Determination of moisture content for physical and mechanical tests.
- EN. (2013). Adhesives for load-bearing timber structures-test methods-part 1: determination of longitudinal tensile shear strength. EN 302-1.2013.
- Nader, N., Legacey, S., & Chin, S. L. (1999). Preliminary investigations of ultrafast intense laser wood processing. *Forest products journal*, 49(6), 72.
- Wang, Y., Ando, K., & Hattori, N. (2013). Changes in the anatomy of surface and liquid uptake of wood after laser incising. *Wood science and technology*, 47(3), 447-455.
- Yang, J., Chen, H., Zhao, W., & Zhou, J. (2016). TG–FTIR–MS study of pyrolysis products evolving from peat. *Journal of Analytical and Applied Pyrolysis*, 117, 296-309
- Kamboj, G., Gaff, M., Smardzewski, J., Haviarová, E., Borůvka, V., Kumar Sethy, A., (2020). " Numerical and experimental investigation on the elastic stiffness of glued dovetail joints",

- 
- Construction and Building Materials, 263 (2020): 551-558, December 2020. DOI: 10.1016/j.conbuildmat.2020.120613
- Altgen, M., Willems, W., Hosseinpourpia, R., & Rautkari, L. (2018a). Hydroxyl accessibility and dimensional changes of Scots pine sapwood affected by alterations in the cell wall ultrastructure during heat-treatment. *Polymer Degradation and Stability*, 152, 244-252.
- Altgen, M., Uimonen, T., & Rautkari, L. (2018b). The effect of de- and re-polymerization during heat-treatment on the mechanical behavior of Scots pine sapwood under quasi-static load. *Polymer Degradation and Stability*, 147, 197-205.
- Esteves, B., Velez Marques, A., Domingos, I., & Pereira, H. (2013). Chemical changes of heat treated pine and eucalypt wood monitored by FTIR. *Maderas. Ciencia y tecnología*, 15(2), 245-258.
- Owen, N. L., & Thomas, D. W. (1989). Infrared studies of "hard" and "soft" woods. *Applied spectroscopy*, 43(3), 451-455.
- Liu, Q., Wang, S., Zheng, Y., Luo, Z., & Cen, K. (2008). Mechanism study of wood lignin pyrolysis by using TG-FTIR analysis. *Journal of analytical and applied pyrolysis*, 82(1), 170-177.
- Dolan, J. A. (2014). Characterization of laser modified surfaces for wood adhesion (Doctoral dissertation, Virginia Tech).
- Aicher, S., Ahmad, Z., & Hirsch, M. (2018). Bondline shear strength and wood failure of European and tropical hardwood glulams. *European Journal of Wood and Wood Products*, 76(4), 1205-1222.
- Xu, Y., Wang, B., Shen, Y., Wu, J., Feng, L., & Yu, H. (2017). Effect of softening treatment on cutting force during slicing the veneers of common fast-growing wood. *BioResources*, 12(4), 7205-7217.

---

## 6.5 The effect of alternating freezing and high temperatures on the tensile-shear strength of glued Norway spruce (*Picea abies* (L.) H. Karst.) and European larch (*Larix decidua* Mill.) wood

### Published as:

Gašparík, Miroslav, **Fatemeh Rezaei**, Elham Karami, Sumanta Das, Tomáš Kytka, Lukáš Vlk, Roberto Corleto, and Gianluca Ditommaso. "The effect of alternating freezing and high temperatures on the tensile-shear strength of glued Norway spruce (*Picea abies* (L.) H. Karst.) and European larch (*Larix decidua* Mill.) wood." *European Journal of Wood and Wood Products* (2022): 1-8



## The effect of alternating freezing and high temperatures on the tensile-shear strength of glued Norway spruce (*Picea abies* (L.) H. Karst.) and European larch (*Larix decidua* Mill.) wood

Miroslav Gašparík<sup>1</sup> · Fatemeh Rezaei<sup>1</sup> · Elham Karami<sup>1</sup> · Sumanta Das<sup>1</sup> · Tomáš Kytka<sup>1</sup> · Lukáš Vlk<sup>1</sup> · Roberto Corleto<sup>1</sup> · Gianluca Ditommaso<sup>1</sup>

Received: 7 October 2021 / Accepted: 13 June 2022  
© The Author(s), under exclusive licence to Springer-Verlag GmbH Germany, part of Springer Nature 2022

### Abstract

Wood bond strength and its durability under unstable climatic conditions is a critical factor for engineered wood products. This article aims to identify the effect of alternating freezing and high temperatures on the tensile-shear strength of adhesive-bonded wood. Emulsion polymer isocyanate and one-component polyurethane adhesives were used to bond European larch (*Larix decidua* Mill) and Norway spruce (*Picea abies* (L.) H. Karst.). The thermal loading of glued samples was carried out at temperatures of  $-15\text{ }^{\circ}\text{C}/70\text{ }^{\circ}\text{C}$  and  $-25\text{ }^{\circ}\text{C}/70\text{ }^{\circ}\text{C}$ . The tensile-shear strength was determined on the glued samples with a universal testing machine. The results showed that the tensile-shear strength of the glued wood exposed to  $-15\text{ }^{\circ}\text{C}/70\text{ }^{\circ}\text{C}$  and  $-25\text{ }^{\circ}\text{C}/70\text{ }^{\circ}\text{C}$  remained unchanged compared to that of reference samples. A negligible correlation was found between the thermal loading and the shear strength of glued samples.

### 1 Introduction

A satisfactory wood-adhesive bond is achievable by considering all bonding processes and its final application under varying environmental conditions. The wood-adhesive bond is highly affected by wood-related factors (wood species, moisture content, etc.), adhesive types (viscosity, molecular weight, etc.), loading and processing conditions (temperature, pressure, etc.), and the geometry of the bondline (thickness of adherent, overlap length, and type of joint, etc.) (Hunt et al. 2018). For example, the compression shear strength of European larch (*Larix decidua* Mill.) bonded with one-component polyurethane adhesive decreased by 32% when the moisture content of the larch samples, as an adherent, increased from 12 to 18%. Further increase in the moisture content (24%) led to zero compression shear strength of the glued larch samples (Pitzner et al. 2001). The wet condition combined with the arabinogalactan (larch specific extractive) and adhesive type (one-component

polyurethane) induces the weak bond strength (Künniger et al. 2006). Immediately after the formation of the bond and a long time after, the level of durability can be varied by environmental conditions and the load-bearing capacity. Stresses in wood and the wood-adhesive bond are generated by changes in moisture levels, varying temperatures, and relative humidity during the service life. If the stresses overcome the wood-bond strength, delamination occurs. (Niemz et al. 2005; Willem et al. 2013).

The mechanical properties of solid wood increase below normal temperatures and decrease when wood is heated (Green et al. 1999; Ozer 2002). At higher temperatures, 160–260 °C, thermal degradation of wood occurs, leading to inferior mechanical properties (Tjeerdma and Miltz 2005). Many scholars (Jiang et al. 2014; Niemz et al. 2014) emphasized a significant increase in the mechanical properties of wood as temperature decreased. Sznutku et al. (2013) only studied the effect of freezing temperatures on the mechanical properties of spruce wood. The mechanical properties of spruce wood were not changed at  $-10\text{ }^{\circ}\text{C}$ , while poor mechanical properties of spruce were observed at  $-1\text{ }^{\circ}\text{C}$ . Wang et al. (2015, 2016a) analyzed the tensile shear strength of spruce wood under freezing temperatures down to  $-60\text{ }^{\circ}\text{C}$  for 12 h. The shear strength of solid spruce wood decreased after it was exposed to the freezing temperatures, while the shear strength of pine species remained unchanged.

✉ Fatemeh Rezaei  
rezaei@fd.czu.cz

<sup>1</sup> Department of Wood Processing and Biomaterials, Faculty of Forestry and Wood Sciences, Czech University of Life Sciences Prague, Kamýcká 1176, Suchbátol, 165 00 Prague 6, Czech Republic

The behavior of wood-based materials under freezing or temperature rises above  $20 \pm 2$  °C was investigated by Ayrilmis et al. (2010). The bending strength of plywood and oriented strand board (bonded with phenol–formaldehyde) and medium-density fiberboard (bonded with urea–formaldehyde) increased when the temperature was decreased from 30 to  $-30$  °C.

Previous studies focused on the effect of high temperatures (Frangi et al. 2004; Falkner and Teutsch 2006; Clauss et al. 2011a, b, c) and cold temperatures (Kainz and Ritter 1998; Wacker 2003, 2009; Wang et al. 2015, 2016a, b) on the performance of a wood-adhesive bond. No previous study has investigated the effect of alternating low and high temperatures on wood adhesive bonds. This paper aims to show the tensile shear strength of a bondline made of spruce and larch species bonded with adhesives when first subjected to different freezing temperatures and subsequently to a constantly high temperature.

## 2 Materials and methods

### 2.1 Material

#### 2.1.1 Wood samples

Norway spruce (*Picea abies* (L.) H. Karst.) and European larch (*Larix decidua* Mill.) planks were obtained from a commercial supplier and kiln dried. Defect-free lamellae (no knots, cracks, etc.) with dimensions of  $5 \text{ mm} \times 45 \text{ mm} \times 500 \text{ mm}$  were air-conditioned in a humidity chamber HCP 108 (Memmert, Germany) at relative air humidity of  $65\% \pm 5\%$  and a temperature of  $20 \text{ °C} \pm 2 \text{ °C}$  to achieve an equilibrium moisture content of 12%. Table 1

**Table 1** Tensile shear strength of solid spruce and larch wood

Spruce ( <i>Picea abies</i> (L.) H. Karst.)	6–7.7 N/mm <sup>2</sup> (Konnerth et al. 2016)
	5–7.5 N/mm <sup>2</sup> (Richter et al. 2003)
Larch ( <i>Larix decidua</i> Mill.)	7–8.3 N/mm <sup>2</sup> (Konnerth et al. 2016)
	8, 8–11 N/mm <sup>2</sup> (Richter et al. 2003)

shows how strong the tensile shear strength of solid larch and spruce is.

#### 2.1.2 Adhesive

The two-component emulsion polymer isocyanate (EPI) adhesive Kestokol WR 11+ hardener WR (Kiilto Oy, Finland) and moisture-curing one-component polyurethane (PUR) adhesive Kestopur 1030 (Kiilto Oy, Finland) were used to glue the lamellas. According to ČSN EN 204 (2013) and ČSN EN 15425 (2017), these adhesives are in durability classes D4 (EPI) and I 70 GP 0.3 (PUR), respectively. The properties of the adhesives are shown in Table 2.

## 2.2 Methods

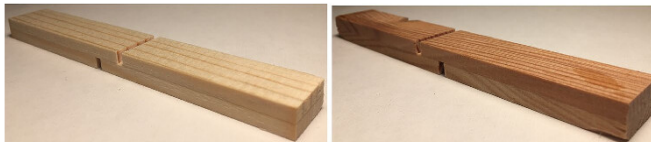
### 2.2.1 Adhesive application

A toothed spatula was used for the application of a thin layer with an adhesive spread of  $200 \text{ g/m}^2$  (for both EPI and PUR, on one side), according to the producer's recommendations. The growth ring angle (angle between growth rings and glued surface of the specimen) of the samples was  $30$  and  $85^\circ$ , according to ČSN EN 302-1 (2013). The 2-layered pieces were subsequently cold-pressed (ambient temperature  $20 \text{ °C}$ ) in an industrial press GS 6/90 (SCM GROUP S.p.A., Italy) under  $1 \text{ MPa}$  for  $20 \text{ min}$  (EPI) and  $90 \text{ min}$  (PUR), respectively. To allow complete curing of the EPI adhesive to final strength, the glued pieces were left in the room for 7 days depending on the producer's instructions. Finally, these glued pieces were cut into the final samples with dimensions of  $10 \text{ mm} \times 20 \text{ mm} \times 150 \text{ mm}$  according to standard ČSN EN 302-1 (2013). All samples were then air-conditioned in a humidity chamber HCP 108 (Memmert, Germany) under specific conditions (relative air humidity of  $65\% \pm 5\%$  and a temperature of  $20 \text{ °C} \pm 2 \text{ °C}$ ) to achieve an equilibrium moisture content of 12%. A total of 360 conditioned samples were obtained and separated into twelve groups for both wood species (30 samples per single group) according to thermal loading temperature and adhesive type (Fig. 1).

**Table 2** Properties of PUR and EPI adhesives

Adhesive type	Viscosity (mPa s)	Density (g/cm <sup>3</sup> )	Work-ing time (min)	Minimum pressing time (min)	Wood moisture content (%)
Kestokol WR 11 (EPI)	3500 (5000 with hardener)	1.15	7–12	20	6–15
Kestopur 1030 (PUR)	7000	1.2	Max. 30	90	6–20

Fig. 1 Glued sample of spruce (left) and larch (right) samples



### 2.2.2 Thermal loading

Thermal loading (freezing-high temperature) on the glued larch and spruce samples was carried out based on standard ČSN EN 321 (2002). To begin this process, first two freezing temperatures,  $-15\text{ }^{\circ}\text{C}$  and  $-25\text{ }^{\circ}\text{C}$ , were applied to the glued samples for 12 h in a laboratory freezer, MediLine LGT 3725 (Liebherr GmbH, Germany). The frozen samples were then moved to a thermal chamber SolidLine ED-S 115 (Binder GmbH, Germany) and subjected to a temperature of  $70 \pm 2\text{ }^{\circ}\text{C}$  for 12 h. When the heating process was finished, the heated samples were immediately tested.

### 2.2.3 Physical properties

To determine the effect of thermal loading on the wood samples, the moisture content and density of the glued samples were calculated according to ISO 13061-1 (2014) and ISO 13061-2 (2014). The weight and dimension of each glued sample before and after each condition (freezing/high temperature) were measured.

### 2.2.4 Tensile-shear strength

The tensile-shear strength ( $f_v$ ) was determined using a lap joint test according to EN 302-1 (2013) (Fig. 2). The universal testing machine UTS 50 (TIRA, Germany) was used to test the tensile-shear strength of the glued samples. The constant loading speed of the machine was set to  $5 \pm 0.5\text{ mm/min}$ . The time needed to reach failure was between 30 and 50 s. The computer software of the machine recorded the maximum loading force.

The tensile-shear strength  $\tau$  was calculated using Eq. 1,

$$f_v = \frac{F_{max}}{l_2 \times b} \quad (1)$$

where  $f_v$  is the tensile-shear strength at failure (MPa),  $F_{max}$  is the applied maximum loading force (N),  $l_2$  is the length of the bonded test surface (mm), and  $b$  is the width of the bonded test surface/sample (mm).

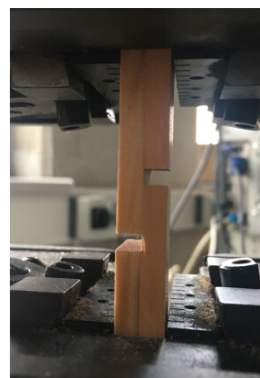


Fig. 2 Tensile-shear test

The obtained values of the tensile-shear strength were evaluated with Statistica 13 (TIBCO Software Inc., Palo Alto, USA) with an analysis of variance (ANOVA).

## 3 Results and discussion

The first set of statistical analyses (ANOVA) examined the impact of each factor, including thermal loading (freezing and subsequent high temperature), wood species, and types of adhesive on the tensile shear strength of the glued samples. The analyses also examined the effect of the interaction of all these factors on the shear strength of the glued samples. The shear strength of the glued samples was not significantly affected by all factors, except wood species, based on the given data in Table 3.

The results of the effect of the different wood species, larch and spruce, regardless of thermal loading and types of adhesives, on the shear strength of the glued samples are summarized in Fig. 3. The shear strength of the glued-larch samples was higher, roughly  $2.5\text{ N/mm}^2$ , than that of the glued-spruce samples. This result is significant at  $p=0.05$  (Table 3). A possible explanation for this result may be differences in density. Larch species in a range of

**Table 3** Statistical evaluation of tensile-shear strength of glued samples

Factors	Sum of squares	Degrees of freedom	Variance	Fisher's F test	Significance level P
Intercept	20,797.58	1	20,797.58	6709.321	***
Wood species	384.68	1	384.68	124.097	***
Thermal loading	3.68	2	1.84	0.594	NS
Adhesive type	6.82	1	6.82	2.201	NS
Wood species × thermal loading × adhesive type	3.43	2	1.71	0.553	NS
Error	1078.73	348	3.10		

NS not significant,  $P > 0.05$

\*\*\*Significant. The level of significance was accepted at  $P < 0.05$

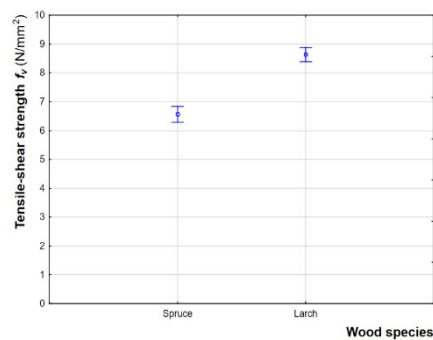


**Fig. 3** 95% confidence interval showing the influence of the wood species on the tensile-shear strength of glued wood (used both EPI and PUR adhesives, and both thermal loading temperatures,  $-15\text{ }^{\circ}\text{C}/70\text{ }^{\circ}\text{C}$  and  $-25\text{ }^{\circ}\text{C}/70\text{ }^{\circ}\text{C}$ )

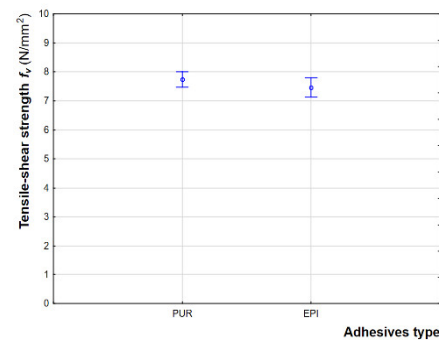


**Fig. 5** 95% confidence interval showing the influence of the adhesive type on the tensile-shear strength of glued wood (used both larch and spruce species, and both thermal loading temperatures,  $-15\text{ }^{\circ}\text{C}/70\text{ }^{\circ}\text{C}$  and  $-25\text{ }^{\circ}\text{C}/70\text{ }^{\circ}\text{C}$ )

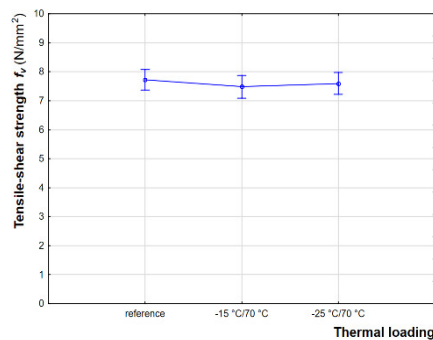


**Fig. 4** 95% confidence interval showing the influence of the thermal loading temperature on the tensile-shear strength of glued wood (used both EPI and PUR adhesives, larch and spruce species)

$535\text{ kg/m}^3$ — $670\text{ kg/m}^3$  is heavier than spruce wood with a range of  $370$ – $571\text{ kg/m}^3$ .

Figure 4 compares the effect of two ranges of freezing-high temperatures on the shear strength of the glued samples. The figure shows that by decreasing freezing temperatures from  $-15$  to  $-25\text{ }^{\circ}\text{C}$ , with a constant high temperature at  $70\text{ }^{\circ}\text{C}$ , the shear strength of the glued samples, irrespective of wood species and type of adhesive, remained the same, approximately  $7.5\text{ N/mm}^2$ . Closer inspection of the figure shows no significant differences between the shear strength of the glued samples with and without exposure to the freezing/high temperatures (Table 3).

The analyses of different adhesive systems, disregarding thermal loading and wood species, on the tensile shear strength of the glued samples are presented in Fig. 5. The shear strength of EPI adhesive, nearly  $7.5\text{ N/mm}^2$ , is slightly lower than that of PUR adhesive,  $7.8\text{ N/mm}^2$ . However, the difference is not statistically significant (Table 3). It is

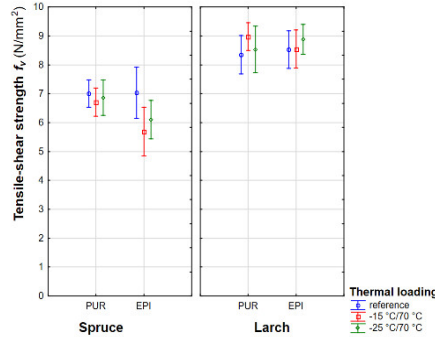


Fig. 6 Effect of wood species, adhesive type and temperature loading on the tensile-shear strength

almost evident that the performance of both PUR and EPI adhesives in the bondline is the same.

The effect of the cooperative interaction between all the factors on the shear strength of glued samples is shown in Fig. 6. In spruce samples bonded with PUR, the shear strength of the glued samples decreased slightly by 4.8% when exposed to a freezing temperature of  $-15\text{ }^{\circ}\text{C}$ . A further increase in the freezing temperature up to  $-25\text{ }^{\circ}\text{C}$  led to a minor decrease in the shear strength of the glued samples by 1.4%, compared to that of glued samples without thermal loading (reference). Similarly, the shear strength of spruce samples bonded with EPI decreased by 18.5% and 12.8% when exposed to freezing temperatures of  $-15\text{ }^{\circ}\text{C}$  and  $-25\text{ }^{\circ}\text{C}$ , respectively. The multi-factor ANOVA analysis did not show any significant differences between the shear strength of the glued spruce samples with and without exposure to the freezing/high temperatures (Table 3).

In larch samples bonded with PUR, the shear strength increased by 5.9% when exposed to a freezing temperature of  $-15\text{ }^{\circ}\text{C}$ . A slight increase of 1.1% in the shear strength of the glued samples exposed to a freezing temperature of  $-25\text{ }^{\circ}\text{C}$  was observed, compared to that of the reference samples. As far as EPI adhesive is concerned, an increase of 1.1% was achieved in the shear strength of the glued samples at  $-15\text{ }^{\circ}\text{C}$ . A more significant increase of 4.7% was

also observed in the shear strength of the glued samples at  $-25\text{ }^{\circ}\text{C}$ , compared to that of reference samples. No significant reduction in the tensile shear strength of the samples exposed to thermal loading was found compared to reference samples based on the multi-factorial ANOVA (Table 3).

The second set of analyses examined the correlation between the factors and the shear strength of the glued samples (Table 4). A positive correlation around 52% was found between the shear strength and wood species. A nearly 2% positive correlation between tensile shear strength and thermal loading was also found. A roughly 6% negative correlation was observed between the shear strength and the type of adhesive.

These findings are interesting and need to be discussed further. The formation of a wood adhesive bond is the result of the interaction between wood and adhesive. The strength formed in the bondline is under the influence of each bondline element, wood and adhesive subjected to environmental conditions. If wood dries at a temperature below  $150\text{ }^{\circ}\text{C}$ , both free (cell lumen) and bound water (cell wall) in wood evaporate. The mechanical properties of spruce wood remained unchanged under drying conditions between  $50$  and  $60\text{ }^{\circ}\text{C}$  (Teischinger 1992) and also between  $45$  and  $80\text{ }^{\circ}\text{C}$  (Oltean et al. 2010). Turning now to the experimental evidence on this paper, it seems that the shear strength of frozen spruce and larch samples was not reduced when exposed to elevated temperatures up to  $70\text{ }^{\circ}\text{C}$ , even though heating frozen wood differs fundamentally from unfrozen wood. This discrepancy can be attributed to the variability in the temperature field over time and in the conditions where the phase transformation of water occurs. Under freezing temperatures, Ayırlımis et al. (2010) argued that the improved bending strength of wood-based panels may partly be due to the formation of ice crystals in wood cell walls and cell lumens. Frozen water can stick to cellulose fiber, resulting in increased stiffness of the boards.

Several studies (Ayırlımis et al. 2010; Klement et al. 2021) have mentioned the possibility of freezable water within wood cell walls. However, this has not been documented by any experimental techniques. Several of the experimental techniques (e.g. DSC and low-field NMR) which are able to detect phase changes in water have failed to do so in wood. Biopolymeric materials like extracted cellulose and lignin have been found to contain water which freezes well below

Table 4 Spearman's correlation between factors and tensile-shear strength

Factors	Wood species	Thermal loading	Adhesive type	Tensile-shear strength $f_t$
Wood species	1.000	0.000	0.000	0.520
Thermal loading	0.000	1.000	0.000	0.026
Adhesive type	0.000	0.000	1.000	-0.064
Tensile-shear strength $f_t$	0.520	-0.026	-0.064	1.000

the normal freezing point of liquid water, this water is presumably found as clusters around strongly polar groups. No freezable cell wall water has been found within solid wood (Zelinka et al. 2012; Nopens et al. 2020). In the cell lumen, the formation of ice causes an expansion of liquid water in the lumen, leading to compressive stress in the cell wall (Ilic 1995). The elasticity of cell walls is reduced by lignin and induces a very low freezing temperature of free water.

When the frozen samples were exposed to a temperature of 70 °C, the moisture reduced and evaporated. This is quite obvious from Fig. 7. The moisture content of the samples was almost the same in reference samples and samples exposed to freezing temperatures of -15 °C and -20 °C (11.3–12.7%). As Klement et al. (2021) reported, the moisture level of the pine species before freezing did not have a remarkable effect on the loss of average moisture content during freezing.

After heating at 70 °C, there was a sharp decline, approximately 9%, in the level of moisture. With the onset of drying (loss of bound water), the moisture content evaporates in the upper layers, where tensile stresses develop, while compressive stresses develop in the middle layers. However, it should be considered that when the bonding area is subjected to a high temperature, the bonding area in the inner fibres is much less prone to shrinkage. This may be the reason why the shear strength of the glued samples under freezing and subsequent high temperatures was stable.

Apart from moisture content, another critical factor that significantly affects the tensile shear strength of the glued sample is density (Bodig and Jayne 1982). As depicted in Fig. 8, the density of solid larch and spruce wood samples remained approximately constant when exposed to freezing and subsequently high temperatures. This may be another reason for the consistent shear strength under freezing and subsequently high temperature.

The performance of these two adhesive systems, PUR and EPI, in the bondline of the glued samples under freezing and subsequently elevated temperatures is encouraging; the absorption of water in an adhesive system partially destroys the mechanical performance of a wood-adhesive bond, particularly in wood-based structural elements (Hunt et al. 2018). However, several studies (Kläusler and Claus 2013; Guo et al 2018; Grostad and Bredesen 2014) reported that PUR and EPI adhesives were quite stable under high humidity conditions.

The mechanical properties of a majority of PUR adhesives decline at a heating temperature of 70 °C. However, the sensitivity behavior to temperature is vastly dependent on the adhesive's formula (Claus et al. 2011a, b). A slight decrease in storage modulus of EPI adhesive from 20 to 70 °C was shown in a dynamic mechanical analysis by Umemura et al. (1998). It is clear from this paper that both PUR and EPI adhesives are quite stable at freezing temperatures up to -25 °C and subsequent high temperatures up to 70 °C.

**Fig. 7** Moisture variations of glued spruce and larch samples after each stage of freezing and subsequent high temperatures

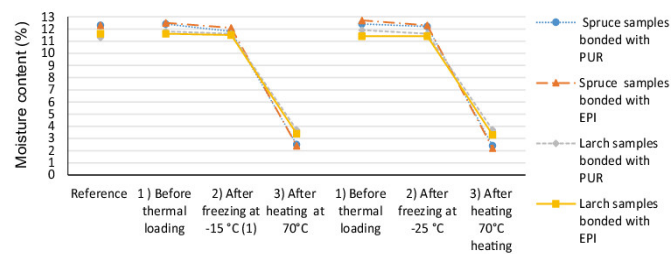
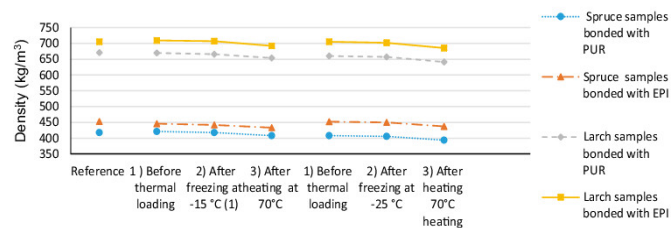


**Fig. 8** Density variations of glued larch and spruce samples under each stage of thermal loading



#### 4 Conclusion

The present study was designed to determine the behavior of the tensile shear strength of glued samples under alternating low and high temperatures. This study has found that the shear strength of the glued samples was not affected by different ranges of freezing temperatures followed by a constantly high temperature. The adhesive performance, emulsion polymer isocyanate and one-component polyurethane, subjected to alternating low and high temperatures was the same as that of the reference samples. Wood species played an essential role in the shear strength of the glued samples and showed a positive correlation with the shear strength of glued samples.

Wooden industrial structures and design can use spruce and larch wood glued with emulsion polymer isocyanate and one-component polyurethane adhesives under unstable climatic conditions (severe cold and relatively hot). Considerably more work will need to be done to determine the behavior of other wood species under relatively low/high temperatures. A further study could assess the long-term effects of exposure time and a higher range of low/high temperatures.

**Acknowledgements** This study was financially supported by the Advanced research supporting the forestry and wood-processing sector's adaptation to global change and the 4th industrial revolution [CZ.02.1.01/0.0/0.0/16\_019/000803] financed by OP RDE as well as the Internal Grant Agency (IGA) of the Faculty of Forestry and Wood Sciences [B-20\_04].

#### Declarations

**Conflict of interest** On behalf of all authors, the corresponding author states that there is no conflict of interest.

#### References

- Ayrilmis N, Ümit B, Nusret A (2010) Bending strength and modulus of elasticity of wood-based panels at cold and moderate temperatures. *Cold Reg Sci Technol* 63(1):40–43. <https://doi.org/10.1016/j.coldregions.2010.05.004>
- Bodig J, Jayne BA (1982) *Mechanics of wood and wood composites*. Van Nostrand Reinhold, New York
- Clauss S, Joscak M, Niemz P (2011a) Thermal stability of glued wood joints measured by shear tests. *Eur J Wood Prod* 69(1):101–111. <https://doi.org/10.1007/s00107-010-0411-4>
- Clauss S, Dijkstra DJ, Gabriel J, Kläusler O, Matner M, Meckel P, Niemz P (2011b) Influence of the chemical structure of PUR prepolymers on thermal stability. *Int J Adhes Adhes*. <https://doi.org/10.1016/j.ijadhadh.2011b.05.005>
- Clauss S, Gabriel J, Karbach A, Matner M, Niemz P (2011c) Influence of the adhesive formulation on the mechanical properties and bonding performance of polyurethane prepolymers. *Holzforchung* 65(6):835–844. <https://doi.org/10.1515/Hf.2011.095>
- ČSN EN 321 (2002) Wood-based panels—determination of moisture resistance under cyclic test conditions. Czech Standardization Agency, Prague
- ČSN EN 204 (2013) Classification of thermoplastic wood adhesives for non-structural applications. Czech Standardization Agency, Prague
- ČSN EN 302-1 (2013) Adhesives for load-bearing timber structures—test methods—part 1: determination of longitudinal tensile shear strength. Czech Standardization Agency, Prague
- ČSN EN 15425 (2017) Adhesives—one component polyurethane (PUR) for loadbearing timber structures—classification and performance requirements. Czech Standardization Agency, Prague
- Falkner H, Teutsch M (2006) Load-carrying capacity of glued laminated wood girders under temperature influence. *Bautechnik* 83(6):391–393. <https://doi.org/10.1002/bate.200610032>
- Frangi A, Fontana A, Mischler A (2004) Shear behavior of bond lines in glued laminated timber beams at high temperatures. *Wood Sci Technol* 38(2):119–126. <https://doi.org/10.1007/s00226-004-0223-y>
- Green DW, Evans JW, Logan JD, Nelson WJ (1999) Adjusting modulus of elasticity of lumber for changes in temperature. *For Prod J* 49(10):82–94
- Grostad K, Bredesen R (2014) EPI for glued laminated timber. In: *Materials and joints in timber structures recent developments of technology*, pp 355–364. [https://doi.org/10.1007/978-94-007-7811-5\\_32](https://doi.org/10.1007/978-94-007-7811-5_32)
- Guo J, Hu H, Zhang K, He Y, Guo X (2018) Revealing the mechanical properties of emulsion polymer isocyanate film in humid environments. *Polymers* 10(6):652. <https://doi.org/10.3390/polym10060652>
- Hunt CG, Frihart CR, Dunky M, Rohumaa A (2018) Understanding wood bonds—going beyond what meets the eye: a critical review. *Rev Adhes Adhes* 6(4):369–440. <https://doi.org/10.7569/RAA.2018.097312>
- Ilic J (1995) Advantages of prefreezing for reducing shrinkage-related degrade in eucalypts: general considerations and review of the literature. *Wood Sci Technol* 29(4):277–285
- ISO 13061-1 (2014) Physical and mechanical properties of wood—test methods for small clear wood specimens—part 1: determination of moisture content for physical and mechanical tests. International Organization for Standardization, Geneva
- ISO 13061-2 (2014) Physical and mechanical properties of wood—test methods for small clear wood specimens—part 2: determination of density for physical and mechanical tests. International Organization for Standardization, Geneva
- Jiang J, Lu J, Zhou Y, Zhao Y, Zhao L (2014) Compression strength and modulus of elasticity parallel to the grain of oak wood at ultra-low and high temperatures. *BioResources* 9(2):3571–3579. <https://doi.org/10.15376/biores.9.2.3571-3579>
- Kainz J, Ritter M (1998) Effect of cold temperatures on stress-laminated timber bridge deck. In: *Natterer J, Sandoz JL (eds) Proceedings of the 5th world conference on timber engineering*, vol 2. Swiss Federal Institute of Technology Lausanne, Montreux, pp 42–49
- Kläusler O, Clauss S (2013) Influence of moisture on stress-strain behavior of adhesives used for structural bonding of wood. *Int J Adhes Adhes* 44:57–65. <https://doi.org/10.1016/j.ijadhadh.2013.01.015>
- Klement I, Vilková P, Vilková T (2021) The influence of wood moisture content on the processes of freezing and heating. *Appl Sci* 11(13):6099. <https://doi.org/10.3390/app11136099>
- Konnerth J, Kluge M, Schweizer G, Miljković M, Gindl-Altmutter W (2016) Survey of selected adhesive bonding properties of nine European softwood and hardwood species. *Eur J Wood Prod* 74(6):809–819. <https://doi.org/10.1007/s00107-016-1087-1>

- Künninger T, Fischer A, Bordeanu NC, Richter K (2006) Water soluble larch extractive: impact on IP-PUR wood bonds. In: 5th UFRO symposium wood structures and properties, vol 6, pp 71–76
- Niemz P, Bärtschi H, Howald M (2005) "Untersuchungen zur Feuchteverteilung und Spannungsbildung in Holzbauteilen bei Wechselklimalagerung" ["Investigation of moisture distribution and stress formation in timber construction materials under changing climatic conditions"]. Schweiz Zeitsch Forstw 156:92–99. <https://doi.org/10.3188/szf.2005.0092>
- Niemz P, Hug S, Schneider T (2014) "Einfluss der Temperatur auf ausgewählte mechanische Eigenschaften von Esche, Buche, Ahorn und Fichte" ("Influence of temperature on selected mechanical properties of ash, beech, maple and spruce"). Forstarchiv 85(5):163–168
- Nopens M, Szama U, König S, Kaschuro S, Krause A, Fröba M (2020) Determination of mesopores in the wood cell wall at dry and wet state. Sci Rep 10(1):1–11
- Oltean L, Teischinger A, Hansmann C (2010) Influence of low and moderate temperature kiln drying schedules on specific mechanical properties of Norway spruce wood. Eur J Wood Prod 69(3):451–457. <https://doi.org/10.1007/s00107-010-0467-1>
- Ozer I (2002) Some mechanical properties of frozen juvenile and mature wood of *Pinus nigra* var *pallasiana* Anal. and *Pinus brutia* Ten. Institute of Natural Sciences, Istanbul University, Istanbul, p 75
- Pitzner B, Bernasconi A, Frühwald A (2001) Arbeitsbericht aus dem Institut für Holzphysik und mechanische Technologie des Holzes Nr. 2001/5: Verklebung einheimischer dauerhafter Holzarten zur Sicherung von Marktsegmenten im Außenbau [Work report of the institute for wood physics and mechanical technology of wood No 2001/5: bonding of domestic wood species with natural durability to secure market segments for exterior solutions]. Bundesforschungsanstalt für Forst- und Holzwirtschaft, Hamburg
- Richter HG, Oelker M, Koch G (2003) macroHOLZdata: descriptions, illustrations, identification, and information retrieval. In English and German. Version: 06-2019
- Szmutku MB, Campean M, Porojan M (2013) Strength reduction of spruce wood through slow freezing. Eur J Wood Prod 71:205–210. <https://doi.org/10.1007/s00107-013-0667-6>
- Teischinger A (1992) Effect of different drying temperatures on selected physical wood properties. In: Proc. 3rd IUFRO int wood drying conference, Vienna, pp 211–216
- Tjeerdsmas BF, Militz H (2005) Chemical changes in hydrothermal treated wood: FTIR analysis of combined hydrothermal and dry heat-treated wood. Eur J Wood Prod 63(2):102–111. <https://doi.org/10.1007/s00107-004-0532-8>
- Umemura K, Takahashi A, Kawai S (1998) Durability of isocyanate resin adhesives for wood-I: thermal properties of isocyanate resin cured with water. J Wood Sci 44(3):204–210. <https://doi.org/10.1007/BF00521964>
- Wacker JP (2003) Cold temperature effects on stress-laminated timber bridges—a laboratory study. Res. Pap. FPL-RP-605, U.S. Department of Agriculture, Forest Service, Forest Products Laboratory, Madison
- Wacker JP (2009) Performance of stress-laminated timber highway bridges in cold climates. In: Proceedings of the 14th conference on cold regions engineering, August 31–September 2, Duluth, pp 637–649
- Wang X, Hagman O, Sundqvist B, Ormarsson S, Wan H, Niemz P (2015) Impact of cold temperatures on the shear strength of Norway spruce joints glued with different adhesives. Eur J Wood Prod 73:225–233. <https://doi.org/10.1007/s00107-015-0882-4>
- Wang X, Hagman O, Sundqvist B, Ormarsson S, Wan H, Niemz P (2016a) Shear strength of Scots pine wood and glued joints in a cold climate. Bioresource 11(1):944–956. <https://doi.org/10.15376/biores.11.1.944-956>
- Wang X, Björnberg J, Hagman O, Ahmed SA, Wan H, Niemz P (2016b) Effect of low temperatures on the block shear strength of Norway spruce glulam joints. Bioresource 11(4):9638–9648. <https://doi.org/10.15376/biores.11.4.9638-9648>
- Willem GJ, Kuilen VD, Gard W (2013) Damage assessment and residual service life estimation of cracked timber beams. Adv Mater Res 778:402–409. <https://doi.org/10.4028/www.scientific.net/AMR.778.402>
- Zelinka SL, Lambrecht MJ, Glass SV, Wiedenhoeft AC, Yelle DJ (2012) Examination of water phase transitions in Loblolly pine and cell wall components by differential scanning calorimetry. Thermochim Acta 533:39–45. <https://doi.org/10.1016/j.tca.2012.01.015>

**Publisher's Note** Springer Nature remains neutral with regard to jurisdictional claims in published maps and institutional affiliations.